

1. INTRODUCTION

Today nanomedicine is proving their efficacy in many diseases. These technologies are new but quickly increasing day by day. In this science materials the nanoscale range are utilized for the drug delivery purpose¹. In disease contrast the major challenge is large sized drugs, there delivery and concentration at targeted site that includes the poor bioavailability, in vivo unsteadiness, and insufficient solubility that affects the absorption of drug in the body. The issue through targeted delivery not only reflects efficiency but adverse effects too. In these consequences recent approaches of targeted delivery may be a good option^{2,3}.

1.1 Nanomedicine

is a promising field employing the usage of scientific information's through methods of nanoscience in disease management. Applicability of nanoscience is increasing day by day that is in nanorobots, nanosensors in dignostical kits which are not only providing treatment but health awareness too amongst the global population. Applicability of nanoparticle-based method reported which is having combined approach i.e. disease management and imaging modes for diagnosis puposes⁴, this increases the applicability of mineral nanoparticles focused on specific delivery of drug. Nanoparticles seemingly give support to drugs from the destruction of gastrointestinal acid secretions and show usefulness in drug delivery of frugally water-soluble drugs.

The available research data suggest that Nanodrugs have higher oral bioavailability due to uptake method of absorptive endocytosis.

The Nanoparticles reside in systemic circulation for longer duration which enables release of complex drugs as per specific doses. These findings reduce the adverse effects and fewer plasma fluctuations⁵.

The nanosized particles enter the tissues and provide the drug uptake through cells which give an effective delivery of drug with targeted therapeutic achievement. The drug acceptance through cells from nanoparticles is greatly than large particles with various sizes between 1 and 10 μm ^{6,7}. More ever, the targeted action of nanoparticles assures therapeutic efficacy with lesser toxicities.

The applicability of nanoparticles in drug delivery is related to physicochemical features of drugs therefore the natural bioactive compounds with nanoscience are growing quickly. It gives advantages and specificities to deliver the drug at targeted sites.

It is applicable for those drugs which are having poor solubility, lesser absorption can be targeted with these nanoparticles⁸.

1.2 targeted drug delivery system

The basic rule that is applicable in the optimization is the therapeutic goals of drug with minimization of toxicities due to target related to dosages, molecular bases and concentrations at different sites⁹.

The receptor targeting by drugs all the way through optimized drug delivery techniques is not the only way to achieve or enhance the therapeutic goals, however it's also important to decrease the toxicities related to low therapeutic index and elevated doses¹⁰.

The applications of targeted drug delivery in many treatments and diagnostic procedures such as cancer , ocular and brain delivery, vaccines, radio imaging, transdermal delivery and many more.

1.2.1 Carriers used commonly for Targeted Drug Delivery

- **Colloidal Carrier drug delivery system**

These are nano scaled targeting vesicular dosage form, which includes noisome, multiple emulsions, liposomes, and nanospheres. They are helpful in improving the of drug efficacy also decreasing its toxicity. They are very important and promising entities basically essential for effective passage of drugs. It is the drug vectors, which appropriately deliver and hold the active drug to route of administration, although they deliver it within the area of targeted site¹¹.

- **Vesicular Carrier Systems**

Nanosomes are one of the recent advancements in these carrier systems. The different forms of nanosomes are ethosomes, liposomes, transferosomes, niosomes. These all are vesicular carriers nanosome according to modifications in their structure, however their individuality and concentration throughout preparation and storage proposed for therapeutic applications^{12, 13}.

- **Microparticulate Systems**

The microparticulate systems are based on minute sizes such as micro liter and millimeter on scale. The role of micro-particulate system is the enhancement in bioavailability of predictable medicines and to reduce the toxicities. The examples of micro-particulate systems are NPs, magnetic microspheres, and microparticles¹⁴.

Polymeric Carriers

In formulation development polymer is one of important parameter as polymers have unique properties which have not accomplished by other ingredients. The advancement in polymer technology leads the progression of numerous NDDS, with specificity of surface and bulk properties that contribute the dosage form more effective with lesser toxicities. The Polymer technology is an important tool in advancement of drug delivery, as they give direction in delivery of excipients that allows controlled and targeted delivery of medicament¹⁵.

Polymeric micelles

Polymeric micelles are nanosized structures which are having hydrophobic center and a hydrophilic covering, in which encapsulation of drugs are in the central part. The polymeric nanovesicles structure suggests bilayer in aqueous center which facilitates dividing the center from the exterior middle. The encapsulation also prevents the interaction between hydrophilic drugs and hydrophobic molecules inside the membrane; as a result these vesicles have the potential for delivering the incompatible drugs like proteins, anticancer drugs, and genes¹⁶.

- **Dendrimers**

Other types of polymeric carriers are dendrimers which is used for drug targeting purposes. The dendrimers are mono-dispersed macromolecules which are having fit expressed and multi-branched structures with bulbous units. They contain three parts on functional basis that is central point, functional groups on external surface, and interior branching units.

The polar and non polar drugs targeted in dendrimers through electrostatic interface in addition to hydrophobic division. In dendrimers active medicaments are bounded with inner shell by covalent linking to outer groups. Nucleic acids and Gene plasmids are illustration which can link during electrostatic interactions. The release of drug is firm by the character linkage¹⁷. The essential parameters for dendrimers are particle size, rigidity, surface, shape, flexibility, structural design and rudimentary composition should be considered¹⁸.

- **Monoclonal Antibodies**

They are showing good results as beneficial agents in targeting delivery for various diseases, like cancer and viral/bacterial infections. The monoclonal antibodies are helpful in the disease management through conjugation among anti cancer drugs, bacterial toxins, enzymes radioisotopes, cytokines, and for targeting of tumors. Today human monoclonal antibodies are being formulated as anticancer drugs. The first human monoclonal antibodies adalimumab is convincingly approved for clinical use¹⁹.

1.2.2 Drug targeting types

- **Active Targeting**

The challenge with active targeting is to determine the suitable targeting agent, selectivity and transport nanoparticle systems to cancerous tissue site. The strategies are based on the targeting agents' or ligands' ability to attach to the cancer cell. The interactions lead to beneficial delivery the therapeutic on the tumor-specific regions²⁰.

- **Passive Targeting**

In passive targeting the drug targets are available in systemic circulation and they work through the systemic physiology based on physic-chemical distinctiveness of drug which will depend on the concentration of drugs at targeted location, like in tumor tissue for anticancer drugs²¹. Nanoparticles are mostly used in passive targeting as a carrier for the targeted delivery which strengthen noteworthy concentration of the drug in targeted level the process is through slow lymphatic drainage the EPR effect²².

- **Inverse Targeting**

This drug targeting is based on passive uptake of the colloidal carrier through reticulo-endothelial systems.

Dual Targeting

This targeting is based on carrier mediated delivery of molecule by means of its own beneficial activity and therefore escalating the curative effect of the drug²³.

- **Double Targeting**

The targeting is based on combination of sequential and spatial methods i.e. structural position to precise location and sequential delivery at a restricted rate.

- **Combination targeting**

This method is facilitated by delivery on targeted sites by means of carriers and other devices of molecular specific which provide direction to reach at target^{19, 24}.

- **Physical, Biological and Chemical Targeting**

In Physical targeting is based on various parameters like size, composition, or other characters not especially intended for the direction of a natural receptor.

Chemical targeting includes delivery of drugs on targeted sites at all the method through the utilization of prodrugs at specific site. Mediator agent can be bound for the region through enzymes or chemical reactions with the aim to guide them for the targeted delivery of drug and vehicle.

Biological targeting permits the delivery of antibodies, peptides and proteins, other bio-molecule in a precise way. Gene appearance is able to mark to zones for the cellular level explicit supporters in body systems²⁵.

- **Specific and systemic Targeting**

In systemic targeting the drug delivery is through curative systems based on a persistent route like i.e. administration of nano-technological structures. Local targeted approaches are aim to deliver the drug at the local site. These systems transport the drug through blood circulation after

the completion of distribution but main restrictions of this system take place in toxicities of drug in specific tissue²⁶.

- **Targeting based on Location and Disease**

Targeting the drug in intracellular is the best method i.e. gastrointestinal, brain, and respiratory tract targeting are a number of model of site specific targeting. The Intracellular drug distribution of proteins, nanocarriers, and Abs, permits the efficacy through nucleus or specific organelles. Various drug release systems have been employed with target specificity to the gastro-intestinal system. For treating tumors and other infectious diseases, disease-based targeted delivery is preferable to polymer based drug delivery like dopamine-liposome conjugates. It is possible to treat infections with nano-DDSs as an alternative to antibiotics. Designing of nano vaccines for accomplish superior targeting and enhanced cellular reaction is a new vision. Some important pathogens are targeted with specific and specialized approaches to prevent their persistence inside cells; that can be seen in the structures of antimicrobial agent's nanoparticles^{26, 9, 27, and 28}.

- **Carrier Systems, Vehicle for Targeted Drug Delivery**

In addition to specific carrier systems, TDDSs require specific targeting mechanisms by encapsulating or bonding with a spacer moiety. These drug-delivery vehicles are utilized as carriers for example lipoprotein-based carriers micelles, liposomes, and NP-based carriers^{29,30}.

The unique characteristics requires for carriers in delivery of drugs i.e. should be steady, biodegradable, biocompatible, and released out of the body and should not affect homeostatic parameters. The release of drug and biodegradation of polymer are vital steps in formulating the

nano-sized system. Other parameters such as diffusion, and solubility are necessary for drug release procedure³¹.

1.3 Cancer

Cancer is the growing concern as it causes fatality across the globe, in the times past, many researches showed their interest in finding novel therapeutics to decrease the adverse effects related to available treatments. During the disease progression, tumor proliferates that creates a varied inhabitant cells distinguished by dissimilar structures and the various responsivity to treatments³². The Identification of important genes involves in tumor genesis and spread of cancer is key parameters for understanding pathophysiology of disease and finding therapeutic goals. Various researchers worked for identification of cancer biomarkers³³.

The most common cancers in males are in respiratory, excretory and urinary system related; however in women, respiratory, endocrine and reproductive system related are reported³⁴.

1.3.1 Pathogenesis of cancer

The disease pathogenesis based on the different forms of cancer i.e. primary cancer and secondary cancer³⁵. Tumor means growth of unusual cell that is neoplasms, can be malignant, according to the findings the benign tumors are specific to small area but the malignant tumor can move and metastasize to other parts of body.

The findings suggest that proteinase an enzyme secerated by metastatic cancer cell, degrade proteins and help in the movement of these cells to other locations³⁶.

The angiogenesis process leads the removal of cellular waste from the blood and oxygen. In disease hypoxic conditions cause the induction of some proteins such as HIF-1(hypoxia

inducible factor-1alpha) which results in the increase expression of vascular endothelial growth factor^{37, 38}.

1.3.2 Role of immune system in cancer

Our immune system is enriched with different compounds and molecules like amino acid, cytokines which forms a network for biochemical progression to identify and show defense against the foreign Antigens. Our homeostasis play an important role in the maintenance for immune system through adaptive and innate responses that helps in first line of defense³⁹.

In the case of microbes and allergic antigens our nonspecific responses are mediated by innate this is so quick as far as time is concern because of immediate responses its short and hence not able to store in immunological memory. Inborn immunity system is not very strong to produce an immunological retention, but it is capable to distinguish within “self” and “non self” or dissimilar collections of pathogens and the threat related to pathogen⁴⁰. On the basis of another theory the inborn (inert) immunity system conveys rapid defense to the host cell by involving signaling bioactive protein like cytokines. The cytokines protein has numerous persistence liable on the situation they were released in the cells and the site of the receptor it binds to⁴¹. The significant cell which is used in phagocytosis are usual killer cells called phagocytes which provides rapid host defense by engulfing cells⁴². In the case of adaptive immunity growth of immunological retention is related to definite kind of immune responses which targets the foreign antigens. Acquired immunity includes specific antibody and immune cells which attacks and abolish foreign antigens and is capable to protect from diseases by remembering in the future

of that substances impression and rising a new immune response. Such kind of immunity develops through the lymphocytes, called the T and B cells⁴³.

Some T cells can identify as “non self” organic molecules which do not require mediated antigen presentation.^{44, 45}

According to the immunological reactions the binding of specific genes contributes the inhibition of T cell activation. Some researchers reported that some cancer cells also having the induction property which leads suppression of immune system⁴⁶.

In the maturation process of white blood cells are important because they activate the other helper cells that are having antibodies specific for the individual immunologic responses and they are known as immunoglobulins⁴⁷.

The functions of all antibodies are different in terms of their functions though the antibodies functions remain same that is to deactivate the antigen^{48, 49}.

1.3.3 Some common types of cancer

Cancer can be classified according to their presence in specific body part. It can be classified as⁵⁰:

Carcinoma- That starts from skin and tissues, the different types of carcinomas are adenocarcinoma, carcinoma of basal, squamous and transitional cell carcinoma. As epithelial tissues find in the outer coverings of organs so carcinoma starts from these tissues and further progress tacks place inside the part.

- **Sarcoma-** the connective tissues support in the attachment of various parts of the body i.e. cartilage, bone muscles the sarcoma affects them and disease aggravation can be seen at these site specifically.
- **Lymphoma** – It is the important systems of our body and useful in immunity of the body through the network of capillaries which help in filtration of body fluid. The lymphoma starts from the lymph glands and further progress in this our white blood cell are dividing in atypical manner.
- **Myeloma-** Such type of cancer develops in plasma cell. Plasma cells are nothing but a kind of white blood cell, situated in the bone marrow. They are able to prepare antibodies known as immunoglobulins, very helpful to fight infections. It can be out of control by multiplying itself.
- **Leukemia-** This cancer is related to white blood cell⁵⁰. This cancer is one of the commonest blood cancers among kids and teenagers, every one out of three cancers is leukemia. Leukemia is of two types, ALL and CLL. ALL is very common in children. Chronic lymphocytic leukemias are infrequent in children.
a) Acute lymphocytic leukaemia (ALL)- This is a cancer of white blood cells. This cancer develops, once bone marrow cell grows mistakes in its DNA assembly. Common symptoms are enflamed lymph nodes, frequent fever without proper cause, pale skin, fatigue, bleeding gums due to frequent infections. Chemotherapy and targeted drug delivery is mostly used in the treatment.

b) Chronic lymphocytic leukemia (CLL)- This kind of cancer develops in blood as well as bone marrow. Its progress is slower as compared to other type of cancer. Generally, it affects older adults. CLL symptoms cannot be seen for a year. When it starts showing symptoms it may cause fatigue, swelling of (but painless) lymph nodes, fever, weight loss, bruising etc. Treatment includes chemotherapy, bone marrow transplantation is the final treatment in the case of aggressive stage. Survival rate of patients now exceeded to 7- 8 years⁵¹.

1.3.4 Blood cancer scenario in India

Studies recommend that in India, blood cancer is most communal reasons of death and around one lakh people identified every year with a type of blood cancer for example lymphoma, leukaemia and multiple myeloma. Lymphomas and leukemia influence adults as well as children but Myeloma is comparatively common disorder in adults⁵². Blood cancer scenario is shown in the figure.1.1.

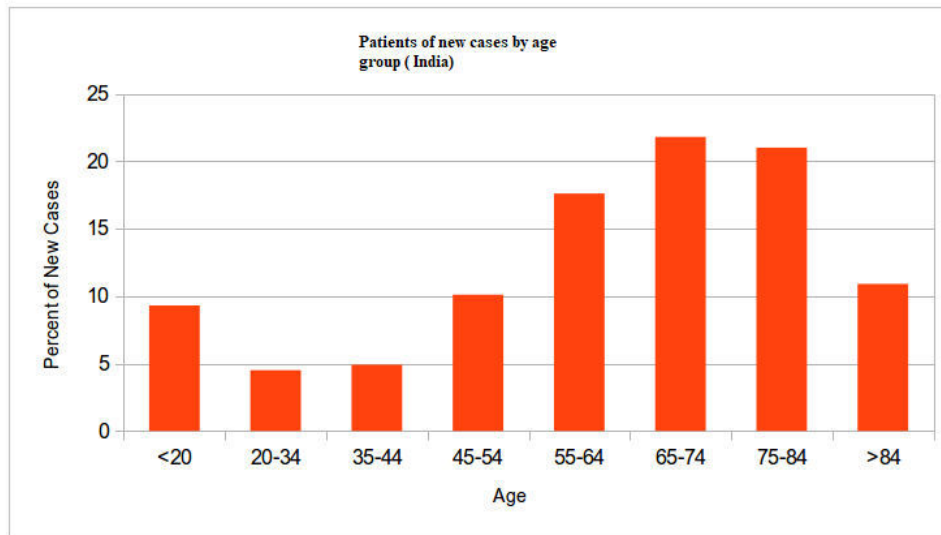


Figure 1.1. Blood cancer scenario in India

1.3.5 Disadvantages of anticancer drug

- Most of the drugs are poorly water soluble/hydrophobic in nature which promotes their precipitation in aqueous medium.
- Anticancer drugs are much weak in the selection of their targeted tissues.
- The anticancer drugs experience a huge distribution in a bulky body volume with chronic adverse effects in non-target tissues.
- Their unintentional eruption can cause harm of healthy tissues.

1.4 Types of nanoparticles:

A) Lipid based nanoparticles- This kind of nanoparticle is made up of minimum one lipid bilayer surrounding an internal water compartment.

a) Solid lipid nanoparticle: SLN mostly composed lipids and phospholipids that remain in solid segment and a surfactant is required for emulsification process. The size ranges from 50 to 1000 nm. SLNs includes inimitable character like minor size, big surface area, great drug loading efficiency, and having better ability to advance the performance of nanoparticles⁵³.

b) Liposomes: They are the most discovered nanoparticles used in site specific delivery systems. It is the sphere-shaped lipid vesicles (generally 50–500 nm in diameter made up of one or more than one lipid bilayers, because of emulsifying synthetic or natural lipids in an aqueous medium.

c) Nanostructured lipid carrier (NLC): They are having aqueous medium as core matrix already containing surfactants. Lipids are multipurpose particles that can produce inversely structured solid matrices. NLC may represent an inadequate loading efficiency because of drug removal next to polymorphic changes throughout the storage, mainly if the lipid matrix contains alike molecules.

B) Polymeric nanoparticles

a) Nano capsules – It is the systems of drug delivery in which active the drug is solubilized in a core material which is kept into a cavity enclosed by thin polymeric wall. Nanocapsules is used as nano sized drug carriers to achieve controlled release and effective drug targeting.

b) Nanospheres- Nanospheres are solid polymers in which have entrapped drug in the polymer medium. It is available in spherical shape and the particles size ranges between 10-200 nm⁵⁴.

c) Polymeric vesicles: It is also known as polymersomes made up of hollow spherical nanoparticles containing aqueous cavity surrounded by polymeric membrane. Polymeric vesicles having great abilities in drug delivery, gene therapy, theranostics, because of its exceptional cell membrane-like assembly.

d) Polymeric Micelles: Micelles characterize a significant drug delivery arrangement used for poorly water-soluble or hydrophobic anticancer drugs. Due to its nano size (10–100 nm), biocompatibility, high degree of stability and extended flow time period in the blood it is used as versatile carrier drug delivery⁵⁵.

e) Dendrimers- They are small-sized, outwardly symmetrical particles containing definite assembly with a characteristically balanced core, an internal shell, and an external shell.

A) Inorganic nanoparticles-

a) Nanoshells: They are sphere-shaped molecules containing a dielectric (poor conductor of electricity) core (silica) surrounded by a thin metallic cover (usually gold) most commonly gold. For its optical and chemical belongings, these nanoparticles are very useful in cancer treatment.

b) Quantum dots: They are nanocrystals of semiconductor material available in less than 10nm in size⁵⁶.

1.4.1 Method of preparation of polymeric nanoparticles- Polymeric nanoparticles can be prepared by following method:

- Solvent evaporation method
- Ionic gelation method
- Solvent diffusion method
- Salting out method
- Supercritical fluid technology

Solvent evaporation technique

This method comprises, dissolution of polymer in an organic (volatile) solvent (dichloromethane, acetone, chloroform) followed by dispersion of drug in polymer containing organic solvent to form dispersion. This dispersion solution should be added to large volume aqueous solution already containing some emulsifier. Finally, o/w emulsion is prepared by allowing the evaporation of volatile solvent at suitable temperature with continuous stirring followed by sonication and drying. It is very much useful in the formulation of hydrophobic drug.

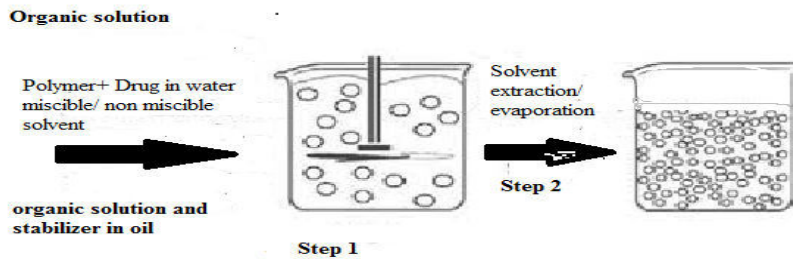


Figure 1.2. Solvent evaporation method

Ionic or inotropic gelation method

This technique includes a combination of two liquids (aqueous phases) here, first solution is the polymeric solution of chitosan polymer, and the second one is polyanionic tripolyphosphate. The method involves interaction of positively charged and negative charge of tripolyphosphate for the preparation of nanosized particle.

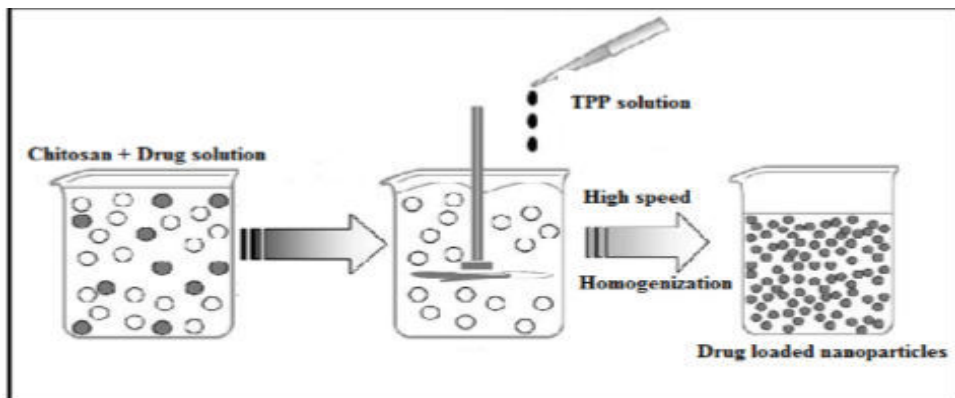


Figure 1.3. Ionic gelation technique

Solvent diffusion method

This method is the commonest method employed for miscible solvent depicted in figure no. 1.4.

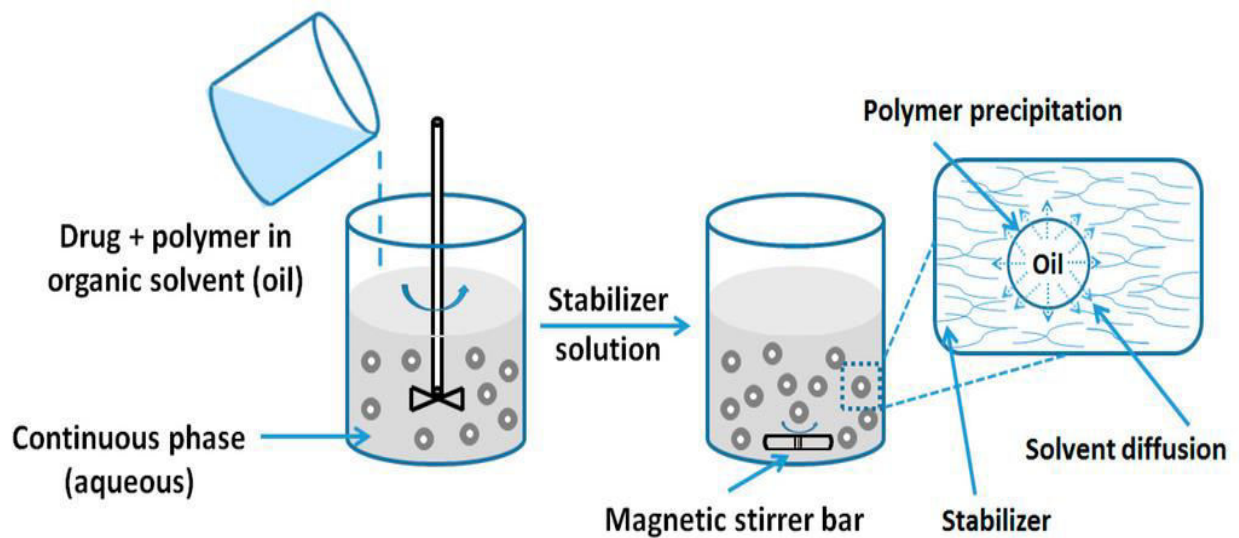


Figure.1.4. Solvent diffusion technique

Salting out method

This method is used for good solubility properties ease of separation from the aqueous medium, acetone is used as water miscible solvent. Generally drugs and polymer are mixed followed by emulsification by continuous stirring into the aqueous gel solution containing stabilizer and salting out agent. Finally, the diffusion of drugs and polymer will form nanoparticles. This method is appropriate for those drugs and polymers which are soluble in glacial solvents like acetone or ethanol.

1.5 Prospects of Nanoparticle drug delivery:

Nano-technology and concept of nanomedicine is growing day by day. In many diseases nanomedicine has played a vital role with target specific action. The uses of nanomedicine in targeted delivery not only reduce the dosage but toxicities too. In disease contrast the toxicities of anticancer drugs is already well known, many clinical trial is going on which will prove the efficacy and safety of anticancer nano formulations. The need of the hour is to develop the nano formulation with specific targeted delivery.

2. RESEARCH ENVISAGED & PLAN OF WORK

Cancer is growing concern amongst global population. Anti- cancer drugs are available but their toxicities is well known, so for that need is to develop the effective formulation which should be effective and safe.

However, no advancement can be observed in the earlier period against cancer with least toxicities.

Objectives of the current research work were to develop the nanosized particles of anticancer drug for CLL disease which can minimize the dosages as well as the toxicities of current available treatment for the disease.

2.1 EXPECTED OUTCOME OF THE PROPOSED WORK

The proposed research work was thought to be a beginning step in the development of-(D) glucosamine based novel delivery system of preferred anticancer drugs. (D) glucosamine complexation is anticipated to conquer the difficulty of poor drug solubility and nanocarrier will help to attain desired release. These nano-platforms based on amalgamation of strategy are one amongst the current novel approaches and can assist in enhancing the efficiency of drugs. In addition, the delivery system with desired delivery features will lead to a better therapeutic potential in order to meet the needs of the patients at the required time and level.

The present study is an approach for the development, optimization and evaluation of nanosized particles containing anticancer drugs. In order to fulfill this following studies have been undertaken:

1. Review of literature

2. Selection of drug, Poly-(D) glucosamine Chitosan based polymers and delivery system based on physiochemical properties.
3. Drug - anticancer category
4. Poly-(D)glucosamine based polymers Chitosan
5. Preformulation studies
 - Physiochemical characterization of drugs
 - Identification of drug
6. Preparation of Nano-sized particles of selected drugs with Poly-(D)glucosamine based polymers and PLGA polymers
8. In vitro characterization of prepared nanocarrier
 - Particle size and particle size distribution
 - Shape and morphology (SEM and TEM)
 - zeta potential
 - Percentage yield
 - Entrapment efficiency
9. Optimization of various parameters: (by Factorial design using design expert software)
 - Formulation parameters
 - Processing parameters
10. Preparation and evaluation of suitable dosage form
11. Stability studies as per ICH guidelines
12. Compilation and presentation of data

3. BRIEF REVIEW OF THE WORK ALREADY DONE IN THE FIELD

The comprehensive literature review carried for the cancer and nanocarriers used in the treatment, various nanocarriers and polymer used in the treatment including targeted site. The nanocarriers are the unique delivery system for drugs like cancer. Till date, few work focused on anticancer nanoparticles, so our work can give a new aspect in this area. A detail of the important work that has been carried out is summarized below:

1. Disease

2. Nano particles

3. bandamustine

4. anti-cancer drugs

- **Kyung Hyun Min et al., (2008)** reported the work based on chitosan nanoparticles-encapsulated camptothecin for cancer treatment ⁵⁷.
- **Jae Hyung Park et al., (2010)** reported the role of low molecular drugs in targeted delivery ⁵⁸.
- **Wang et al., (2011)** formulated chitosan-cyclodextrin nanospheres of doxorubicin hydrochloride by in situ formation to achieve sustained release ⁵⁹.
- **Rajashree Nanda et al., (2011)** prepared and performed characterization of chitosan–polylactide composites blended with Cloisite 30B ⁶⁰.

- **Joung-Pyo Nam et al., (2013)** formulated paclitaxel and lauric acid-*O*- carboxymethyl chitosan-transferrin micelles ⁶¹.

- **Chao Feng et al., (2014)** reported oral bioavailability of chitosan and doxorubicin hydrochloride ⁶².
- **David Lucio et al., (2014)** reported role of polymorphism of chitosan and carboxymethyl chitosan and its solubilisation ⁶³.
- **Khan et al., (2016)** formulated Bendamustine nanoparticles by using different polymers i.e. PLGA, PEG) and evaluated that these nanoparticles have anticancer activity against various cells ⁶⁴.
- **Gidwani and Vyas (2016)** reported through research work based on stability studies of bendamustine PLGA nanospheres for three months that showed the slight variations in zeta potential and particle size ⁶⁵.
- **Franiak et al., (2017)** reported through his research work Glycodendrimer PPI which showed that the dendrimer have significant action on gene protein with lesser harmful effects in CLL cells ⁶⁶.
- **Bhandari et al., (2017)** revealed by research work based on aerogels of cellulose nanofibre and its applicability in oral drug delivery ⁶⁷.
- **Taylor et al., (2017)** reviewed the genetics bases, diagnosis and types of hematological cancer. They elaborated that genetic changes affects TP53 which can be used for therapeutic site for disease management and BRAFV600E mutations can be for the diagnosis of chronic lymphocytic leukemia ⁶⁸.
- **Vinhas et al., (2017)** reviewed the utilization of nano particles for the leukemia treatment management. They discussed about the novel approaches and types of constructs of nanomedicines in liquid tumors ⁶⁹.
- **Hallek et al., (2018)** reported the current progression in the lane of treatment and management of CLL with the challenges ahead ⁷⁰.
- **Thomas et al., (2018)** studied the optimized and fabricated Bendamustine loaded hydroxyapatite nanoparticles through in vitro, in vivo, and analytical studies ⁷¹.

- **Ziemba B et al., (2020)** revealed through his research work in-vitro studies in xenograft model by Glycodendrimer Nanoparticles. The reported results showed inhibition in extend of CLL ⁷².
- **Franiak et al., (2020)** formulated the dendrimers and explained that Cationic PPI-G4-M3 has maximum anti cancer activity and elevated toxicities as compare to neutral dendrimers, fludarabine in CLL ⁷³.
- **Shakeran et al., (2021)** Designed chitosen based biodegradable nanocarriers for methotrexate drug delivery in breast cancer. The result showed that significant decrement in viability of cells achieved at low concentrations ⁷⁴.
- **Cavalcante et al., (2021)** reported through their research work based on the methotrexate and PLGA nanoparticles in which they targeted the STAT3/NF-κB signaling ⁷⁵.
- **Li et al., (2021)** reported that PLGA based nanocarrier of Paclitaxel have precise targeting capability in colorectal cancer ⁷⁶.
- **Ghilardi et al., (2022)** revealed that Bendamustine have similar efficacy and lesser toxicities as compare to fludarabine and cyclophosphamide in lymphodepletion ⁷⁷.
- **Ghaz-Jahanian et al., (2022)** reviewed the chitosan nanocarriers application in tumor targeted drug delivery system ⁷⁸.
- **Resen et al., (2022)** reported the usefulness of fluorouracil and gemcitabine hydrochloride based citosan coated nanoparticles in breast cancer ⁷⁹.
- **Priya et al., (2022)** reviewed the pharmaceutical applications of nanofibres based on polysaccharides ⁸⁰.
- **Rinaldi et al., (2022)** Prepared nanostructures of oleic acid (pH-sensitive). That suggests the combining drug delivery in pH-dependent show the anti cancer effect for fatty acid and is the key feature for future based treatment for melanoma disease ⁸¹.
- **Zhang et al., (2022)** reported the role of lipid polymer nanocomplexes in disease management ⁸².
- **Xiong et al., (2022)** confirmed the DTIC-NPs-Apt as active target for anticancer drugs in the treatment with no side effects in melanoma ⁸³.

- **Singh et al., (2022)** designed the micelles of PLGA and (soya) lecithin for improved efficacy of methotrexate in cancerous cells ⁸⁴.

4. DRUG AND EXCIPIENT PROFILE

4.1 Bendamustine:

Bendamustine is an anticancer drug and is derivative of mechlorethamine with a purine-like benzimidazole ring belongs to electrophilic alkyl groups⁸⁵.

4.1.1 Brand Name:

It is available in different brand names across different countries examples are Bendeka, Belrapzo, Treanda®, Vivimusta.). In India, it is available commercially with different brand names as lyophilized powder for injection⁸⁶. The brand name and marketed preparation of bendamustine in India are highlighted in table 1.1.

Table.1.1 Bendamustine brands in India:

Sr No.	Brand Name	Strength	volume	Dosage form
1	Bendit	Bendit 100x20 ml	2ml	Bendit Injection
2	Bimode	Bimode 100mg	1ml	Bimode Injection
3	Maxtorin	Maxtorin 100mg	20ml	Maxtorin Injection
4	Mustin	Mustin 100 mg	1 ml	Mustin Injection
5	Purplz	Purplz 100mg	1 ml	Purplz Injection
6	Rolanda	Rolanda 100 mg	1 ml	Rolanda Injection

4.2 Drug category:

Antineoplastic agent, Alkylating agent

4.3 Physicochemical property:

Bendamustine is off-white coloured powder with molecular formula $C_{16}H_{22}Cl_3N_3O_2$. The drug is higher in organic solvents. It's melting point ranges from 150-154°C. Its molecular Weight is 394.72 g/mol with partition coefficient of 4.23 It is photosensitive in nature.

4.4 Chemical structure:

Chemically, it is 5- [Bis (2-chloroethyl)-amino]-1-methyl-1H-benzimidazole-2-butanoic acid.

The structure of bendamustine is shown in figure.1.5.

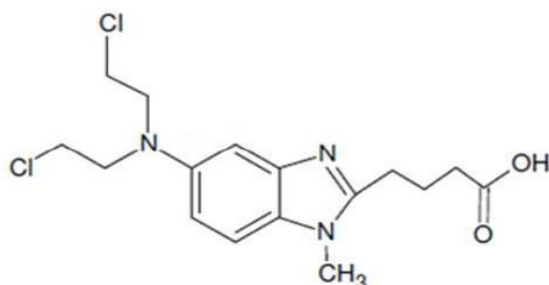


Figure.1.5: Structure of bendamustine

4.5 Pharmacology and mechanism of action:

It is mechlorethamine derivative able to form electrophilic alkyl groups which can covalently bond to another molecule.

4.5.1 Dosage and route of administration

It is administered parenterally as Injection (i.v. infusion) and for adult dose in Chronic Lymphocytic Leukemia is 100mg.

4.5.2 Pharmacokinetics:

Absorption

Bendamustine is administered through intravenous infusion. After a single IV dose of bendamustine, C_{max} occurs at the end of infusion with value of 11.5µg/ml⁸⁷.

Distribution

About 95 % bendamustine is bounded to protein (generally to albumin). Data says that it is not probable to dislocate or be dislocated by extremely protein-binding drugs. BM is not extensively distributed in tissues. The volume of distribution (V_s) is around 25 L. It is having short half-life causes the rapid metabolism and excretion.

Metabolism

Bendamustine is mostly hydrolysed to active HP₁ and HP₂ and also metabolised CYP1A₂ enzymes to active M₃ and M₄, which effect their extreme concentrations close to the same time just like the main drug.

Elimination

The findings suggest the half of administered drug excreted through urine and faecal. Bendamustine clearance from plasma is quick and the half life is 40 minutes.

4.5.3 Drug Interactions:

Bendamustine is not approved yet in combination form, but it may enhance inclusive response rates when combined with rituximab⁸⁸.

4.5.4 Adverse effects/Side effects:

Adverse effects including signs of an allergic reaction, hypersensitive reactions is very common and anaemia, neutropenia, thrombocytopenia, anorexia, diarrhoea, dyspepsia, nausea, pyrexia, constipation, herpes simplex, herpes zoster, pneumonia, fatigue, hypersensitivity, headache, hypokalemia, tumor lysis syndrome, myelosuppression, vomiting, cardiac failure, infusion reactions has also seen in patients.

4.6 EXCIPIENT PROFILE:

4.6.1 Chitosan

Chitosan is a sugar used and has linear polysaccharide made up of β -linked D-glucosamine as well as N-acetyl-D-glucosamine⁸⁹. Chitosan is widely used in pharma manufacturing.

Synonyms-Chitosan, Poliglusam, Chicco, Flonac C, Flonac N, Sea Cure Plus, Kytex H.

Structure-

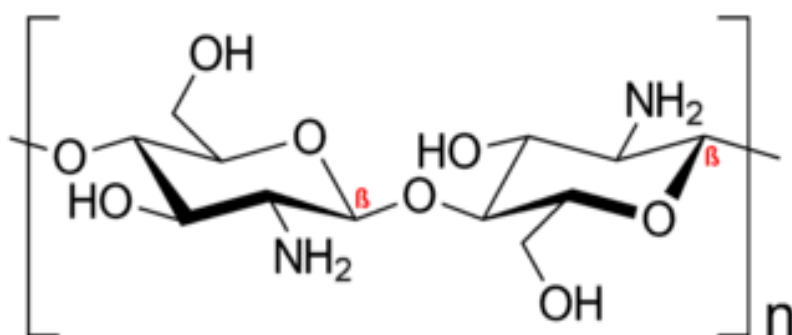


Fig. 1.6 Chemical structure of Chitosan

4.6.2 Properties

Physical Properties- Chitosan is off white free flowing powder. However, it has a unique fishy odor, and when added to pharmaceutical preparation, significantly impair the aroma of the preparation.

Molecular Formula- $\text{C}_{56}\text{H}_{103}\text{N}_9\text{O}_{39}$

Molecular weight- 1526.5

Solubility- the solubility depends on solvents more ever chitosan is sparingly soluble in water. The solubility is higher in organic solvents.

Acidity/Alkalinity (pH)- Its pH is between 6-6.5.

Density- in the range of 0.20- 0.38 g/mL.

Melting point- The melting point of chitosan is between 214.77 - 216.69°C.

4.7 Application:

Development, Optimization And Evaluation of Nanosized Particles Containing Anticancer Drug

Chitosan having an excellent property and that is why used in various formulation manufacturing⁹⁰.

4.8 Sodium Tripolyphosphate (SYP):

Sodium triphosphate is an inorganic compound having formula $\text{Na}_5\text{P}_3\text{O}_{10}$.

Structure-

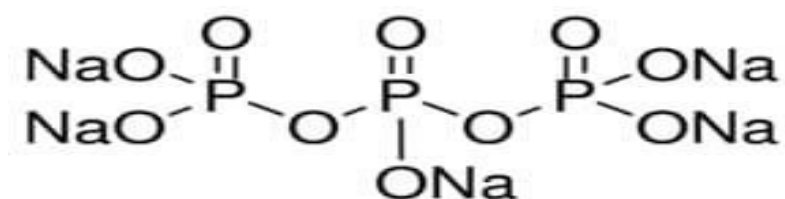


Fig. 1.7: Chemical structure of Tripolyphosphate

4.8.1 Physicochemical properties- It is white, freeflowing and odourless powder without any contamination. TPP is Incompatible with strong oxidizing agents and strong acids and Hygroscopic in nature.

Molar mass- 367.864 g/mol

Density- 2.52 g/cm³

Melting point- 622 °C

Solubility -It is easily soluble in water, and its aqueous solution is alkaline. Sodium Tripolyphosphate is accessible in white crystalline and powder form. It easily dilutes in water and is insoluble in ethanol. The solubility in water is 14.5 g/100 mL (25 °C).

Acidity/Alkalinity (pH)- pH range 5.0–6.5.

4.9 Application:

TPP acts as a stabilizer in the preparation of nanoparticles⁹¹.

4.10. PLGA (Poly lactic-co- glycolic acid):

PLGA or poly is used in the formulations of many nanocarrier systems, due to its biodegradability and biocompatibility. It belongs to the category of polyesters. These polymers are classified on the origin of different substituent (R₁, R₂) on the support with a primary ester linkage.

4.11 Structure:

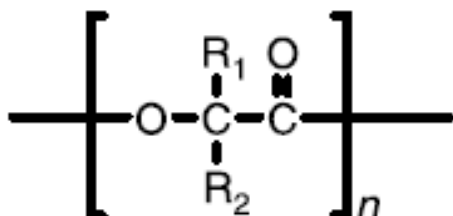


Fig1.8: Chemical structure of PLGA

4.12 Molecular formula-C₅H₈O₅

4.13 IUPAC name: 2-(2-hydroxyacetyl)oxypropanoic acid

4.14 Synthesis:

PLGA is prepared by different ratios of monomers, lactic and glycolic acid at 120 °C temperatures.

4.15 Physicochemical properties:

Appearance- Available in white to off- white powder.

Molecular weight-148.11

Density-Pure PLGA powder should have a density of 1.25 g/cm³.

Melting Point-240°C-280°C

Solubility- It is freely soluble in organic compounds like methylene chloride and others.

Acidity/Alkalinity (pH)-It is basic in nature. pH ranges between 5.5-7.4

4.16 PVA (Polyvinyl alcohol):

PVA is biodegradable and highly flexible, nontoxic polymer used as an emulsifying agent for lowering the solutions interfacial tensions⁹².

4.17 Structure:

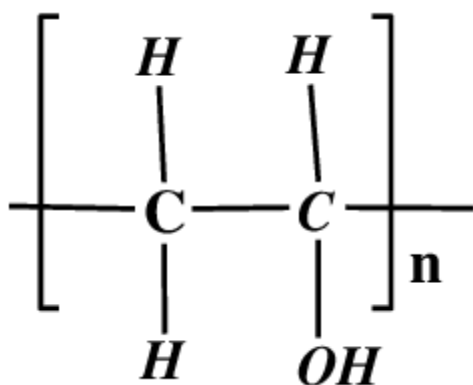


Fig.1.9: Chemical structure of PVA

4.18 Molecular formula- $(C_2H_4O)_x$

4.19 IUPAC name- poly (1-acetyloxiethylene)

4.20 Physicochemical properties:

Appearance- Polyvinyl alcohol appears as odourless white to cream-colored granules or powder.

Molecular weight- 44.5

Melting point- 200°C

Flash Point- 79.44°C

Density- 1.19–1.31 g/cm³

Solubility- solubility of PVA depends on hydrolysis and molecular weight⁹³. It is Insoluble in most organic solvents. Its slightly soluble in ethanol and other organic compounds.

4.21 Application:

It's generally used as surfactant in various pharmaceutical industries.

5 MATERIAL AND METHODS

5.1 Material

The drug sample was received from the pharma industry as a gift sample on request and all the chemicals were analytical grade.

5.2 Method:

5.2.1 Introduction

Preformulation is the study that emphasis on the physic-chemical characteristics of a newly discovered drug that may influence the drug function, behavior and the advancement of a dosage form. The study will offer significant material for formulation, strategy and the necessity for molecular variation. These studies are intended basically to discover the conditions in which the molecule will be more stable^{94, 95}. It is required to progress a well-designed, stable, effective and safe dosage form by founding the compatibility with added excipients and by determining the physical and chemical parameter of newly discovered drug materials.

Before starting a preformulation study following points are required:

- The study of existing physical and chemical data with chemical structure, potency of the new products and the dosage form are required⁹⁶.
- Probable dosage quantity and the planned route of drug administration is necessary.
- It provides condition and progress schedule of newly discovered dosage form.

The present research work, is based on selected drug bendamustine (BM) tested for its recognition by melting point, solubility studies, partition coefficient, UV absorption maxima study and FTIR spectroscopy.

5.2.2 Physical and morphological evaluation of drug

In physical and morphological evaluation of Bendamustine, color, odor and texture were examined visually.

Procedure: Melting Point determination is the necessary parameter to determine the purity of active drug. The melting point of (BM) is examined with the help of capillary tube technique. A minor amount of powdered sample was located into a capillary tube. The drug filled tube was then positioned in the melting point apparatus. The temperature at which powder started to melt as well as the temperature when the powder melted completely, was noted ⁹⁷.

5.2.3 Solubility study

Procedure: Finding out the solubility of bendamustine at various temperatures for three different solutions was taken, both solutions tested, for the equilibrium solubility 10 ml of each solvent was taken in different test tubes. Then exactly weighed quantity of each drug (BM) (approx.10 mg) was added in small increment and shaken for 5 minutes every time till precipitation occurs ⁹⁸.

5.2.4 Determination of absorption maxima (λ max):

Development, Optimization and Evaluation of Nanosized Particles Containing Anticancer Drug

Procedure: The maximum absorbance of (BM) was determined by UV-Spectrophotometer (double beam) consuming methanol as solvent and scanning the solution (100 μ g/ml) between 200-400nm⁹⁹.

5.2.5 Preparation of standard solution:

Procedure: For the analysis purpose standard solution of Bendamustine prepared in 1mg/ml by dissolving the 100mg of drug in 100ml of methanol . Furthermore the solution was diluted by methanol to obtain standard solutions of 100 μ g/ml¹⁰⁰.

5.2.6 Determination of calibration curve of Bendamustine:

Procedure: From the prepared standard solution 20ml of solution withdrawn in 100 ml of volumetric flask to obtain 40 μ g/ml solution. From this stock solution of 40 μ g/ml aliquots of 0.5,1,2,3,4,5-----10 ml was withdrawn and further diluted with 10ml of methanol to achieve dilutions of 4, 8, 12, 16, 20, 24, 28, 32, 36 and 40 μ g/ml. The absorbance of resultant dilutions was determined at 329 nm¹⁰¹.

5.2.7 FTIR Spectroscopy of pure drug

Procedure: The active drug spectrum was determined with the help of (FTIR Shimadzu –DRS-8000). In which no need to make KBr pellets, just directly 1-2mg of drug was located in the sample holder after that the spectrum was recorded¹⁰².

5.2.8 Drug –Excipient Compatibility by FTIR

Drug-Excipient compatibility study is important for maximizing stability of dosage form and to get good quality of product by avoid the incompatibilities during production. The drug and excipient compatibility characterizes a significant stage in the study of preformulation part for the development of all dosage kind forms. Drug particles having several sensitive and reactive functional groups¹⁰³.

Procedure:

For the compatibility study drug and excipients were prepared in 1:1 ratio i.e., 10 mg of pure drug, polymer and drug plus polymer samples taken and directly assessed by FTIR (Shimadzu – DRS-8000).

5.2.9 Determination of Partition coefficient:

This is described as the equal parts of unionized drug that is dispersed in the organic as well as aqueous phase till the equilibrium achieved.

$$P_o/w = (C_{oil}/C_{water}) \text{ at equilibrium}$$

Procedure: For the Assessment of degree of lipophilicity i.e. partition coefficient for BM was completed separately by shaking flask process. Firstly, 10mg of pure BM was mixed with 25 ml of distilled water and 25 ml of n- octanol too. Then the blend was shaken separately up to half an hour duration. After that both the phases (oil and water) were mixed together in a separating funnel and shaken for 4 hrs on a mechanical shaker. After shaking the mixtures, allow them to stand till the phase separation process ended. The total quantity of substance present in both

phases was determined by UV analysis and related with the amount of the substance initially used¹⁰⁴.

5.3 Preparation and characterization of nanoparticle¹⁰⁵

5.3.1 Ionic gelation technique: In ionotropic or ionic gelation technique the polymeric nanoparticles can be assessed by the cross-linking process of biodegradable hydrophilic polymer (chitosan) with drug Bendamustine.

Chitosan nanoparticles have grown more reflection as carriers' system due to its enhanced stability, very less toxicity, easy preparation method and providing versatile routes of administration¹⁰⁵.

5.3.2 Emulsion solvent Diffusion technique:

In this method initially, nano emulsion was formulated. The Polymer (PLGA) was dissolved in organic solvent dichloromethane. After that the desired quantity of bandmustine was dispersed in polymeric solution. Then the sample was added gently in aqueous solution of PVA (surfactant) under continuous magnetic stirring followed by sonication process (Prob sonicator, meco Ultrasonics, India) for 5-7 minutes. For the smooth conduction of emulsification process, magnetic stirring (Remi, India) was continued for 5-6 hours. After that Oil in water emulsion was formed and in this step dichloromethane diffused in the aqueous phase and therefore, nanoparticles formed by polymer precipitation. For the whole diffusion of DCM the extra amount of water was added. Finally, the nanoparticles were obtained by centrifugation method¹⁰⁶.

5.3.3 Freeze drying

Development, Optimization and Evaluation of Nanosized Particles Containing Anticancer Drug

This process involves the total exclusion of water and other solvents of the given sample by sublimation process. This method is also known as lyophilization. It keeps the temperature of the sample very low as much as essential throughout the procedure to skip the variations of the dried sample appearance and characteristics¹⁰⁷.

- **Preparation of Bendamustine loaded Chitosan Nanoparticles by ionic gelation technique:**

In this technique, different concentration of chitosan polymer ranging from 1-5mg/ml was dissolved in 1% v/v solution of acetic acid. The chitosan solution pH was adjusted to 4.5-4.6 with 0.1 N NaOH. Then the calculated amount of 2 mg/mL Bendamustine in methanol mixed with chitosan solution (5ml). In the next step cross linking agent or surfactant tripolyphosphate was also mixed in deionized water. Finally, magnetic stirring was done in that the surfactant solution was added in the chitosan solution by carefully adding drop by drop at room temperature for some period of time followed by sonication for 5-7 minutes, until an opalescent suspension was obtained. Then centrifugation process for 30 minutes at 15,000 rpm also water was used for washing of nanoparticles. After that they were kept for freeze drying and treated by 3% of mannitol used as protecting agent in lyophilization process.

- **Preparation of nanoparticle through solvent diffusion technique:**

The second method was emulsion solvent diffusion technique adopted for the for Bendamustine nanoparticles. The precisely weighed quantity of PLGA and drug was mixed in (10 ml) of dichloromethane. After that the obtained polymeric drug solution added to aqueous solution of PVA (4%w/v) with continuous stirring for 4 hours, until the oil in water emulsion was formed. 30 ml of deionized water was also added for complete diffusion of organic phase into water. The finally Nanoparticles separated by centrifugation technique at 10,000rpm for 30min afterward separation of the supernatant from precipitants was completed. This precipitant containing nanoparticles was freeze dried and evaluation studies were performed.

5.4 Optimization of Chitosan based nanoparticles prepared by ionic gelation technique

The study was designed to assess persuade of process variables on characteristics parameters that is particle size and entrapment efficiency of nanoparticles. The variables chosen through preliminary studies, single variable always changed at that time while keeping all others constant. Optimization was done in three steps. In step one preliminary studies done experimentally using the process parameters which was Polymer concentration (0.5%-0.75%), concentration of surfactant (0.5-1%) and sonication time (5-7min) for nanoparticles.

These factors are very much important in to control size, size distribution and other physiochemical parameters of nanoparticles. In the next step process parameter based on pre study was selected once again and optimized. Total 8 batches of formulations were selected and characterized. In last step the suitable nanoparticle formulation obtained through drug entrapment efficiency with minimum particle size. With the help of this method the best

experimental formulation with same concentration ingredient was prepared and percentage bias was determined ¹⁰⁸.

5.4.1 Process and formulation parameter of Chitosan Nanoparticles

Procedure

The prepared nanoparticles were optimized for selected variables based on the preliminary study applying the Box-Behnken design in which 8 batches were selected using 3 factors and 2 levels and data was generated for each batch. Amount of polymer A, Amount of Surfactant B and sonication time C called the independent variables (three factors) which would affect the dependent variable. The optimization was done by Design expert (version 10) software. Through the optimization process a formulation with greatest desirability factor was carefully chosen and data was studied ¹⁰⁹.

Table1.2: Process and formulation parameter of Chitosan Nanoparticles prepared by Ionic gelation technique⁸:

1) Preliminary studies for the formation of CS nanoparticles		
Variables	Range	Selection Parameter
Concentration of chitosan	0.1-1.0%w/v	Formation of nanoparticle
Concentration of Surfactant	0.5-1.0%	
2) Selection and optimization of key variables		
Key variable	Range	Selected parameter
Polymer Concentration	0.5-0.75%w/v	Particle size and Drug entrapment efficiency
Surfactant Concentration	0.5-1.0%	

Sonication time	5-7 min	
-----------------	---------	--

Table1.3: Process and formulation parameters for PLGA Nanoparticle prepared by emulsion solvent Diffusion technique:

1) Preliminary studies for formation of nanoparticles		
Variable(s)	Range	Selection parameter
Conc. of PLGA (Polymer)	1.0–4.0 %w/v	Formation of Nanoparticle
Conc. of PVA (surfactant)	1.0-5.0 % w/v	
2) Selection and optimization of key variables		
Key variable	Range	Selection parameter
Conc. of PLGA (Polymer)	0.5-3.0% w/w	Particle size and drug entrapment efficiency
Conc. Of PVA (Surfactant)	1.0-4.0 %	
Sonication time	5-7 min	

In the next step prepared nanoparticle were optimized for selected variables based on the initial study through with Box-Behnken design. The quadratic model produced by the design was:

$$Y = A_0 + A_1X_1 + A_2X_2 + A_3X_3 + A_4X_1X_2 + A_5X_2X_3 + A_6X_1X_3 + A_7X_1^2 + A_8X_2^2 + A_9X_3^2 \dots \dots \text{equ. 1}$$

Where Y is a kind of measured response also known as dependent variable related individually to factor level combination; A₀ to A₉ are called regression coefficients of particular variables. X₁, X₂ and X₃ are the respective codes of independent variables. The independent variables were denoted by -1, and +1 level related to the maximum and minimum (low and high)

separately. The independent variables Y_1 and Y_2 were denoted as PS which is particle size and %EE for drug entrapment efficiency. To represent the measured responses; 3D graph was plotted to describe the connection among independent variables as well as dependent variables. The value of % bias expressed the reliability of the model. The value of bias was determined by using equation

$$\%Bias = \frac{\text{Predicted value} - \text{Experimental value}}{\text{Predicted value}} \times 100 \dots\dots \text{equation.2}$$

The independent parameters also selected from preliminary studies were also used for optimization through design expert software. The range of parameters selected for Chitosan nanoparticle were based on various parameter i.e.

- a) Amount of polymer (0.5% - 0.75%) and
- b) Amount of surfactant (0.5% - 1.0%)
- c) Sonication time (5-7min)

The coded values for variables (independent, dependent) in experimental plan in table 1.4.

Table.1.4: Highest and lowest range of selected independent variable for ionic gelation technique.

Independent variables	Levels		Dependent Variables
	Low (-)	High (+)	
Polymer Concentration (A)	0.5	0.75	(Y1) Particle size and (Y2) drug Entrapment Efficiency
Concentration of Surfactant (B)	0.5	1.0	

Sonication time (C)	5	7	
---------------------	---	---	--

Table 1.5: The independent variables with their coded and actual values of 8 batches of Chitosan Nanoparticle

Nanoparticles Formulation	Independent variables Coded values			Independent variables Actual values		
	A	B	C	A	B	C
NPF1	1	1	1	0.75	1	7
NPF2	-1	1	1	0.5	1	7
NPF3	1	1	-1	0.75	1	5
NPF4	-1	1	-1	0.5	1	5
NPF5	1	-1	1	0.75	0.5	7
NPF6	-1	-1	1	0.5	0.5	7
NPF7	1	-1	-1	0.75	0.5	5
NPF8	-1	-1	-1	0.5	0.5	5
Dependent variables						Limits
Y1 - Particle size (nm)						Minimize
Y2 – Drug Entrapment efficiency (%)						Maximize

where, A = polymer concentration , B = surfactant concentration , C= sonication time and (-1), and (+1) low and high level individually for independent variables

The formulation parameters of PLGA prepared nanoparticles through solvent diffusion technique were optimized meant for minimum particle size and maximum entrapment efficiency using response surface quadratic model. Created on the preliminary study, PLGA (polymer) and PVA (surfactant) were optimized by design expert software respectively. For the outcome of dissimilar variables on formulation parameters such as particle size (PS), (Y1) and Entrapment % EE (Y2) of the already prepared nanoparticles factorial design response was used. The independent variables were as follows:

- a) Concentration of polymer (A) [0.5%-3%]
- b) Concentration of surfactant (B) [1.0%-4%] and
- c) Sonication time (C) [5-7 MIN]

The coded values for independent and dependent variables in experimental design models are given in table 6T-5.

Table 1.6: Highest and lowest range of selected independent variables for solvent diffusion technique.

Independent variables	Levels		Dependent Variables
	Low (-)	High (+)	
Polymer Concentration (A)	0.5	3	Y1 (Particle size), Y2 (Entrapment Efficiency)
Surfactant Concentration (B)	1	4	
Sonication time (C)	5	7	

The chosen independent variables considerably affect the detected responses for the particle size, % EE. The key effect and interaction factors were obtained by Design-Expert software by Polynomial equations. ANOVA was used for the numerical justification of the equations. The design engaged for optimization process for 8 batches of Nanoparticle formulation, has been shown along with the results in table.1.7.

Table 1.7: Independent variables with their coded and actual value of 8 batches of Bendamustine loaded PLGA Nanoparticle

Nanoparticles Formulation	Independent variables [Coded values]			Independent variables [Actual values]		
	A	B	C	A	B	C
NPF1	-1	1	-1	0.1	4	5
NPF2	1	1	-1	3	4	5
NPF3	-1	1	-1	0.1	1	5
NPF4	1	1	1	3	4	7
NPF5	-1	1	1	0.1	4	7
NPF6	1	-1	-1	3	1	5
NPF7	-1	-1	1	0.1	1	7
NPF8	1	-1	1	3	1	7
Dependent variables						Limits
Y₁ = Particle size (PS)						Minimize
Y₂ = Entrapment efficiency (%EE)						Maximize

5.5

Characterization of prepared nanoparticles¹¹⁰:

To get maximum optimized formulation along with least particle size, greatest drug entrapment efficiency, the 8 unlike groups of each Chitosan and PLGA nanoparticles were characterized for parameters written below:

5.5.1 Particle size distribution, PDI and Zeta potential:

The particle size distribution, PDI and zeta potential of chitosan and Poly lactic co glycolic acid based nanoparticles were calculated by dynamic light scattering using Malvern Instruments. The analysis was performed in a triplicate manner at an angle of 90⁰ at the temperature of 25⁰C. Both the testing samples were dispersed in the adequate quantity of ultra-pure water (pH-7) before starting the experimentation. The polydispersity index can be described by particle size distribution which is defined as width or broadness of molecular mass. The zeta potential was calculated by using Helmholtz–Smoluchowski equation ¹¹¹:

$$\xi = EM \times \frac{4\pi\eta}{\varepsilon} \dots\dots\text{equ.no.3}$$

Here

ξ for zeta potential (mv)

A for electrophoretic mobility

η for viscosity of dispersion medium

ε for dielectric constant

5.5.2 Percentage yield ¹¹²:

Development, Optimization and Evaluation of Nanosized Particles Containing Anticancer Drug

The nanocarriers of Chitosan and PLGA were estranged from aqueous medium by centrifugation at about 15,000-20,000 rpm and dried up at room temperature then weighed and percentage yield of the formulation was calculated using equations.no.4.

Percentage yield =Weight of nanoparticles /weight of polymer + weight of drug x 100...equation.4

5.5.3 Drug loading, entrapment efficiency:

For the calculation of drug loading and entrapment efficiency, initially both chitosan and PLGA nanoparticles were mixed in 10 ml methanol followed by centrifugation with high-Speed cooling Centrifuge for 30 minutes at 14,000 rpm and after that it was filtered with membrane filter. Then the filtrate was diluted with methanol again later scanned with UV Spectrophotometer at 330 nm¹¹³. The percentage of drug entrapment efficiency and drug loading was obtained by the resulting formula.

$$\% \text{ Entrapment Efficiency} = \frac{\text{Weight of drug in nanoparticle} - \text{Weight of drug in supernatant}}{\text{Weight o f drug in nanoparticle}} \times 100$$

$$\% \text{ of Drug loading} = \frac{\text{Total weight of drug entrapped/ Total weight of nanoparticle} \times 100$$

5.5.4 Transmission electron microscopy:

Surface methodology and contour of nanoparticles were assessed by TEM. In Transmission electron microscopy a beam of electrons is passed on all the way through a sample to create an representation. For the study, initially diluted sample was positioned as drop on a carbon coated copper grid and then marked with a drop of aqueous solution of phosphotungstic acid 2 %. Extra staining was cleaned through filter paper. Samples were dried at room temperature and finally the transmission electron microscopy image was captured ¹¹⁴.

5.5.5 Differential scanning calorimetry

DSC was done for the determination of physical nature of the drug Bendamustine and polymer interaction in nano carrier system. The DSC curves were recorded for pure drug BM with chitosan and PLGA, along with the lyophilized drug laden nanocarriers. The calibration was done by using alumina powder as the standard. For the DSC examination a slight amount of test sample was kept in hermetically sealed aluminum pans and was heated at 50–300 °C under the continuous flow of dry nitrogen with heating rate of 10 to 11 °C/min ¹¹⁵.

5.5.6 X-ray diffractions study (XRD)

This was executed for the examination of crystalline or unstructured nature of prepared nanoparticles. The lyophilized powder test samples (BM loaded chitosan and PLGA nanoparticle) were kept in the stage and scanned in the range of 2^θ to 60^θ with a specified voltage current ¹¹⁶.

5.5.7 In-vitro drug release

The in-vitro drug release of BM loaded chitosan as well as PLGA nanoparticles and pure drug suspension was assessed by dialysis membrane. Initially the dialysis membrane was put into

distilled water for 24 hours. After that the accurately weighed nanoparticle samples were placed in the donor section of dialysis membrane and was in 10 ml of dissolution medium (phosphate buffer, pH7.4 for BM) at the temperature of $37^{\circ}\text{C} \pm 0.5^{\circ}\text{C}$ by continuous stirring with 100 rpm. Aliquots were withdrawn in a regular interval of time and exactly the similar amount of dissolution medium added during the analysis. All these withdrawn test samples were properly weakened by adding methanol, examined by UV-visible spectroscopy at 329nm. The percent of cumulative release of drug was calculated ¹¹⁷.

5.5.8 Kinetics of Drug release ¹¹⁸

The drug released data is very much useful in concluding the kinetics of drug release and its methodology. To obtain different mathematical models normally one or two circumstances arisen. In the first case, the drug movement method will be Fickian diffusion and case II will be non-Fickian. The models studied given below in a tabulation form:

Table.1.8. Interpretation of Drug release mechanism

Release exponent (n)	Drug release mechanism	Order of release
0.5	Fickian diffusion	$t^{-0.5}$
$0.45 < n = 0.89$	Non-Fickian diffusion	t^{n-1}
0.89	Case II transport	Zero order release
More then 0.89	Super case II transport	T^{n-1}

- a) **Zero order drug release kinetics** – in this study concentration did not affect the drug release rate. Here, the graph was designed among the cumulative percent drug released and time.

- b) **First order drug release kinetics** – this kinetics depends on concentration.
- c) **Higuchi's kinetics** – It is also known as the Higuchi's classical diffusion equation/Higuchi matrix. In this system, the drug release is related to Fickian diffusion through insoluble matrix.
- d) **Korsmeyer Peppas exponential kinetics** – This model is very valuable once the release mechanism is unidentified or when additional type of drug release mechanism is involved.

5.6 Formulation and evaluation of dosage form ¹¹⁹:

5.6.1 Introduction:

Pharmaceutical dosage form is a type of physical form in which a drug has administered. Here the active drug is mixed with excipients considering the parameters like particle size, solubility, polymorphism, pH to form the final drug product. It is a carrier system for drug to reach in the site of action². In the current study and research, the best optimized formulation (NPF-4) and (NPF-8) of bendamustine loaded chitosan and PLGA nanoparticle was formulated as dry lyophilized powder and evaluated. Bendamustine causes hydrolysis, so it is formulated as lyophilized powder. The conventional marketed formulation of Bendamustine is marketed as lyophilized powder which is very much suitable for intravenous administration.

Based on the outcomes of in-vitro experiment, entrapment efficiency and cumulative percentage drug release, chitosan and PLGA nanoparticles were formulated into lyophilized powder. These prepared nanoparticles were additionally estimated for in-vitro and experimentation.

5.6.2 lyophilized Powder

Lyophilization technique was used for get rid of water from test sample by freezing it, then the ice form was changed directly from solid to vapor by skipping the liquid phase. It was found that the injection routes have significant influence on pharmacokinetics of drug. The lyophilized powder is best for parenteral preparation as it is easily reconstituted with water for injection.

Advantages of Lyophilized powder:

- Lyophilization is required when bulk drug ingredient is not stable in liquid or frozen form.
- Processing a liquid with ease so it is compatible with aseptic operation
- It is necessary to enhance the stability of dry powder dosage form.
- Dissolution of final product is very rapid,

5.6.3 Formulation of lyophilized powder of bendamustine loaded chitosan and PLGA nanoparticle:

Both the nanocarrier system (NPS-4, NPS-8) was formulated into dry lyophilized powder by (Heto Power Dry LL 3000 freeze dryer, Stuttgart, Germany) lyophilizer at temperature -40°C and pressure 0.10 mbar for 48 hours for BM- PLGA nanoparticle and -35°C for 60 hours. The lyophilized powder was prepared and stored for further study.

5.7 Evaluation of prepared lyophilized formulations:

The prepared lyophilized powder formulations were estimated for following parameter:

- Drug Content
- Mean particle size and Zeta Potential

- Entrapment efficiency
- In-vitro drug release

5.7.1 Drug Content ¹²⁰:

The drug content was calculated by 10ml of each formulation was dissolved in 10ml water and set aside for 24 hours. The sample was diluted about 10µg/ml with methanol and scanned by using UV-Spectrophotometer. The absorbance was noted at 329 for BM.

5.7.2 Drug entrapment efficacy ¹²¹:

Percentage of entrapment efficacy of each formulation was based on this formula

Percentage of entrapment efficacy= total drug added-free non-entrapped/total drug added

5.7.3 Particle size Distribution and Zeta Potential ¹²²:

The particle size distribution, and zeta potential of chitosan, PLGA-based formulations were calculated by DLS using Malvern Instruments. Analysis was performed in a triplicate manner at an angle of 90⁰ at the temperature of 25⁰C. Both the testing samples were dispersed in the adequate quantity of pure water before experimentation.

5.7.4 In-vitro drug release ¹²³:

In-vitro release of BM loaded chitosan as well as PLGA lyophilized formulations and pure drug suspension was assessed through dialysis membrane using modified Franz diffusion cell, was already discussed in the preparation of nanoparticles.

5.7.5 In-vitro Cytotoxic study ¹²⁴

Cytotoxicity study has chosen as a trial model and an significant pointer for cell toxicity assessment because it is very simple, rapid and highly sensitive as it can protect experimental animals from toxicity.

The cytotoxic study of lyophilized powder of both the formulation loading bendamustine was determined using the cell line, Z-138 Lymphocytic Leukemia. After 48 hours of contact with the drug and cell line, cell viability was calculated with the help of MTT assay and IC₅₀ (Inhibitory concentration) values. The results were compared with pure drug suspension.

5.7.6 MTT Assay ¹²⁵

Now a days the most normally used technique for the examination of cell growth rate and toxicity. In this method, cells were seeded in 96 well microtiter plates with in minimum vital medium and incubated during the night. Serial dilution was done in triplicate and again incubated for another 48 hours in specified conditions. After that the cells were treated with MTT then after 4.5 hours the complete medium was drawn out from the wells. The absorbance was measured at 570 nm through 96 well microplate readers. The percentage of cell viability was estimated through the following formula:

$$\text{Cell Viability \%} = \frac{\text{Absorbance of Sample}}{\text{Absorbance of control}} \times 100$$

5.7.7 IC₅₀ calculation ¹²⁶

IC₅₀ was calculated according to the drug concentration at which the cell viability reduced to 50 %.

5.7.8 Stability study ¹²⁷

Pharmaceutical stability testing and study is very much significantly used in the determination of drug product's shelf life, ideal storage environments, retest time duration, and declaring its general quality for patients. In this study product should be monitored, whether any physical, chemical, biological, and microbiological changes is occurring or not in a fixed interval of time. The formulations of bendamustine were studied as per the ICH guidelines for formulations at room temperature $25^{\circ}\text{C} \pm 2^{\circ}\text{C}$ and for accelerated conditions $40^{\circ}\text{C} \pm 2^{\circ}\text{C}$ in stability chamber. Both the formulations were stored for 6 months time period and checked, for any changes in the content of drug at intervals of one, three and six months.

6. RESULT AND DISCUSSION:**6.1 Preformulation study data of Bendamustine loaded Chitosan and PLGA nanoparticle:****6.1.1 Physical and morphological Evaluation**

The pure drug bendamustine was appeared as off-white colored microcrystalline powder with amphoteric properties. The melting point was found to be 150⁰C. The official range stated in literature is 150-154⁰C. Results are given in table.no 1.8.

Table.1.9: Physical and morphological properties of Bendamustine:

Sr.no	Property	Observation
1	State	Microcrystalline powder
2	Color	Off- white
3	Odor	Odorless
4	Melting Point	152 ⁰ C

6.1.2 Solubility study

The bendamustine is freely soluble in methanol and partially soluble in water. The result of solubility is depicted in table1.10

Table.1.10: solubility study of bendamustine

Solvent	Solubility	Inference
Distilled water	1 part of solute is soluble in 30 parts of solvent.	Sparingly soluble
Chloroform	1 part of solute in more than 10000 parts of solvent.	Insoluble
Dichloromethane	1 part of solute in 20 parts of solvent.	Soluble
Acetone	1 part of solute in more than 10000 parts of solvent.	Insoluble
Ethanol	1 part of solute in 20 parts of solvent.	Soluble
Methanol	1 part of solute in 10 parts of solvent.	Freely soluble
Iso- propanol	1 part of solute in 20 parts of solvent	Soluble

6.1.3UV-Visible Spectroscopy study

6.1.3.1 Absorption maxima and standard curve

A UV absorption maximum of BM in methanol was calculated by scanning the solution (40µg/ml) of BM from 200 nm to 430 nm by UV-Spectrophotometer. The maximum absorbance of BM solution was recorded 329 nm in methanol. The standard calibration curve of BM was prepared in solvent methanol in the concentration of 4-40 µg/ml with good correctness for methanol. The absorption maximum of BM in methanol is shown in figure.1.10

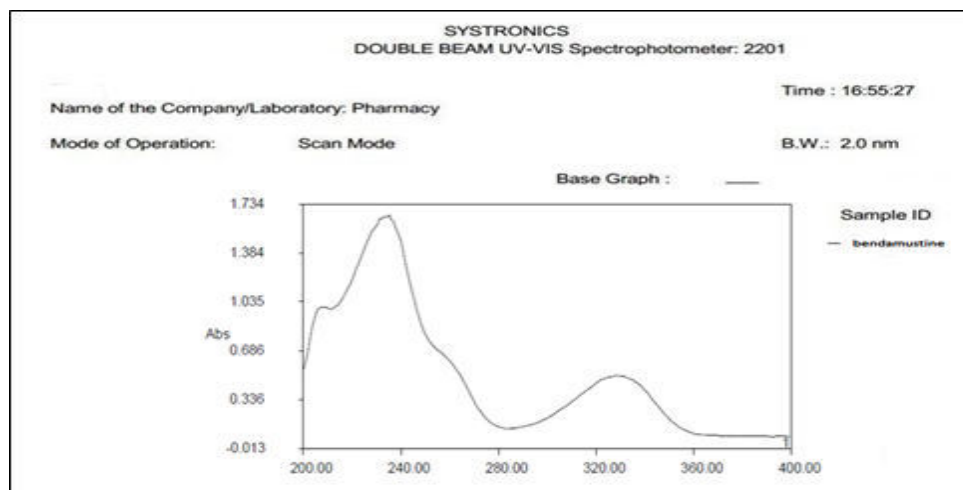


Figure.1.10: Standard calibration curve of bendamustine

6.1.3.2 Calibration curve of BM

The calibration curve of bendamustine was accessed in methanol by using UV-spectrophotometer. The prepared drug solutions of concentration ranging 4-40 $\mu\text{g/ml}$ were scanned at λ_{max} (absorbance maxima) 329 nm and the absorbance was determined. The data are shown in Table 1.10. The calibration curve of BM is shown in figure.1.11

Table.1.11: Absorbance of bendamustine solution at 329nm:

S. No.	Concentration (µg/ml)	Absorbance
1.	4	0.136
2.	8	0.236
3.	12	0.332
4.	16	0.426
5.	20	0.534
6.	24	0.639
7.	28	0.728
8.	32	0.832
9.	36	0.924
10.	40	1.028

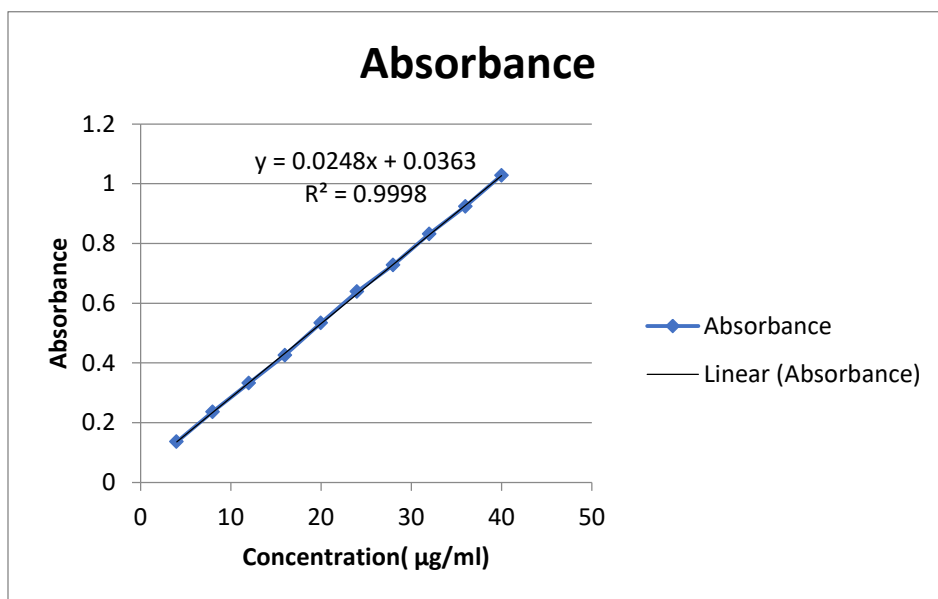


Figure 1.11: Calibration curve of Bendamustine

6.1.4 FTIR Spectra of pure drug and Excipients (for chitosan bendamustine nanoparticle):

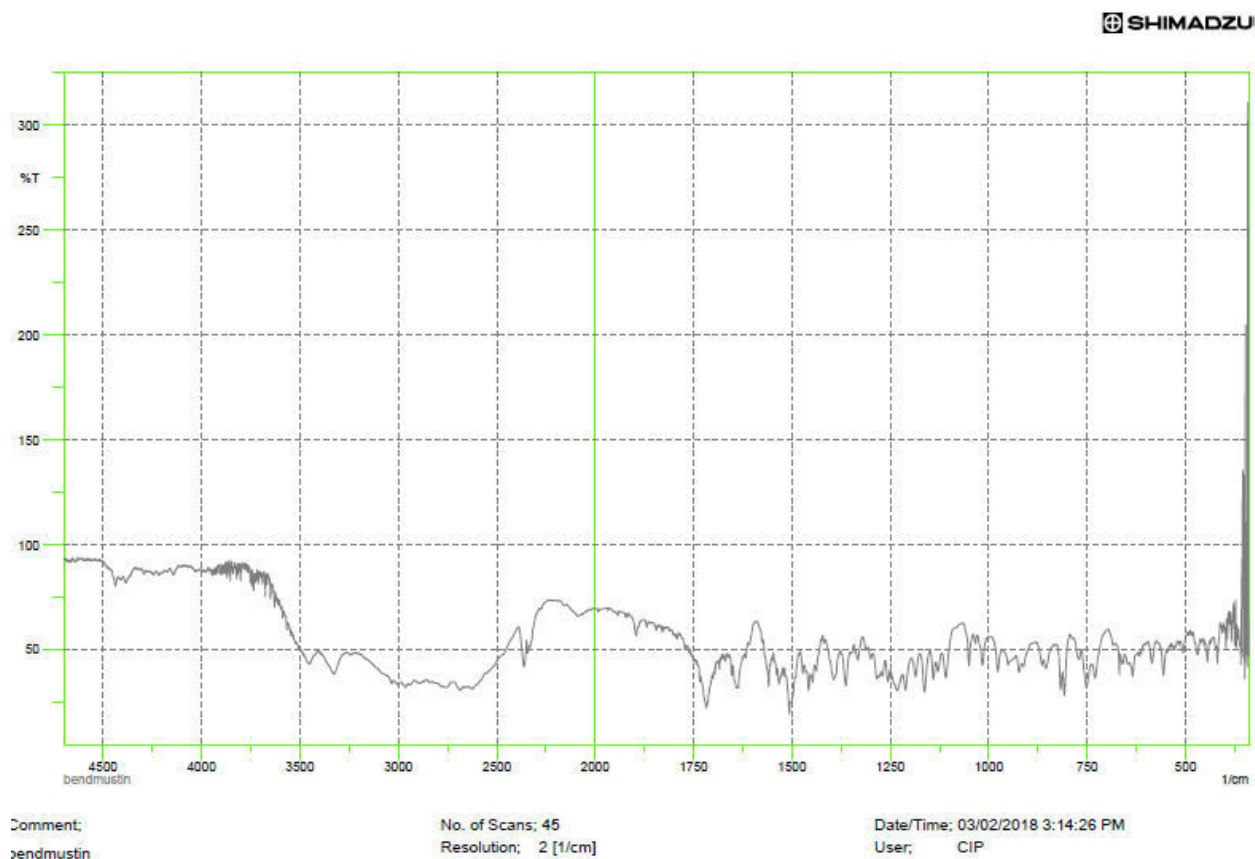


Figure 1.12: FTIR Spectra of Bendamustine

The FTIR spectra of BM explained which show distinguishing peaks at 3315 cm⁻¹ due to O-H stretching bond, at 2715.01 cm⁻¹ C-H stretching, 1502.60 cm⁻¹, N-CH₃ stretching and 1634.06 cm⁻¹ C=C stretching. The peaks are as shown in Figure 1.12 and Table 1.11, which gives the distinguishing absorption of different functional groups of drugs.

Table. 1.12: Important absorptionpeaks of bendamustine

Functional group	Observed wave number (cm ⁻¹)
-OH stretching	3315
-C-H stretching	2715 .01
C=C stretching	1650.06
-N-CH3 stretching	1502.60

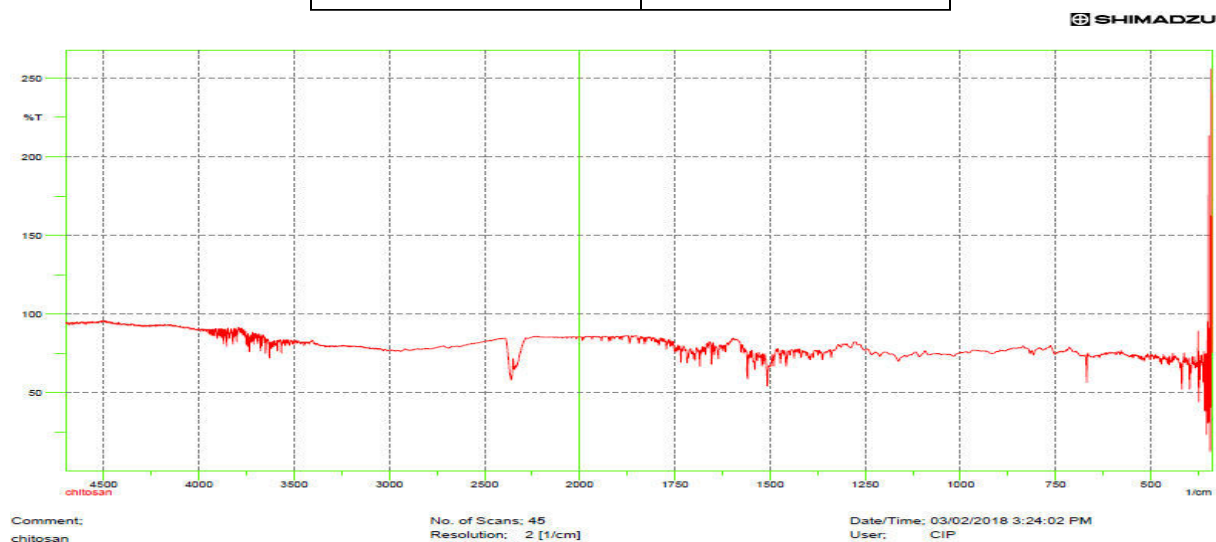


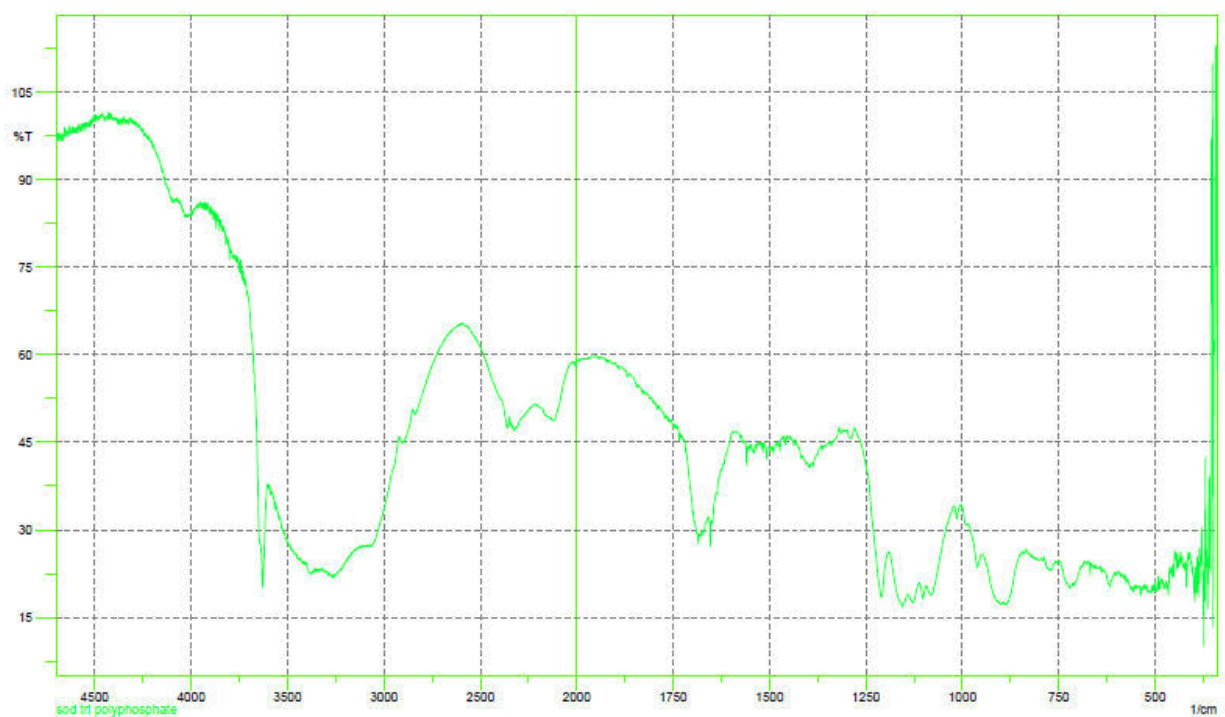
Figure 1.13: FTIR Spectra of Chitosan

An FTIR spectrum of chitosan was characterized by typical absorption band at about 3478.68cm⁻¹ (-OH stretching). The absorption peaks at about 1656.80cm⁻¹, 1571 and 1422.53cm⁻¹ were related to occurrence of C=O stretching of the amide I band with bending vibrations of N-H amide II band, C-H bending, OH bending respectively.

Table.1.13: Important peaks of Chitosan

Functional group	Observed wave number (cm ⁻¹)
-OH stretching	3478.68
C=O stretching	1656.80
N-H bending	1571
C-H bending	1422
OH bending	1376.18

SHIMADZU



Comment:
sod tri polyphosphate

No. of Scans; 45
Resolution: 2 [1/cm]

Date/Time: 03/02/2018 2:47:30 PM
User: CIP

Figure 1.14: FTIR Spectra of TPP

In the FTIR spectra of TPP distinguishing bands were observed at 1211 cm^{-1} (P = O stretching), 1145 cm^{-1} symmetric and asymmetric stretching vibrations in PO_2 group, 1087 cm^{-1} and 865 cm^{-1} stretching of P-O-P bridge.

6.1.5 Drug Excipient compatibility study by FTIR:

In order to find out the interaction/compatibility between BM, selected polymer (Chitosan), selected surfactant (TPP), FTIR spectra were recorded and the major peaks were determined. The spectra of mixtures of BM with chitosan, TPP showed the occurrence of typical peaks of the drug (BM) at 3414.8 cm^{-1} O-H group stretching, 2953.01 cm^{-1} C-H group stretching, 1502.60 cm^{-1} N- CH_3 stretching and 1634.06 cm^{-1} C=C stretching of aromatic with slight variation or shifting in the peaks.

The spectrum of bendamustine with the selected excipients (Chitosan, TPP) respectively showed all the characteristic peaks of BM with no additional or new peaks other than peaks of individual components. This indicates the compatibility of BM with selected excipients.

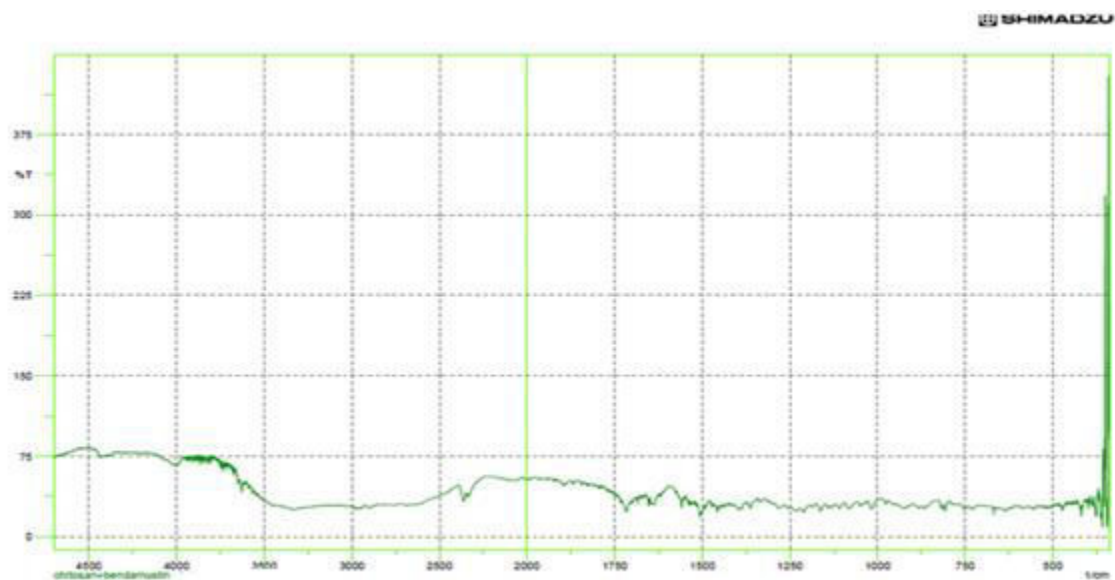


Figure 1.16: FTIR Spectra of Bendamustine with Chitosan

FTIR Spectra of drug and Excipients (for bendamustine loaded PLGA nanoparticle):

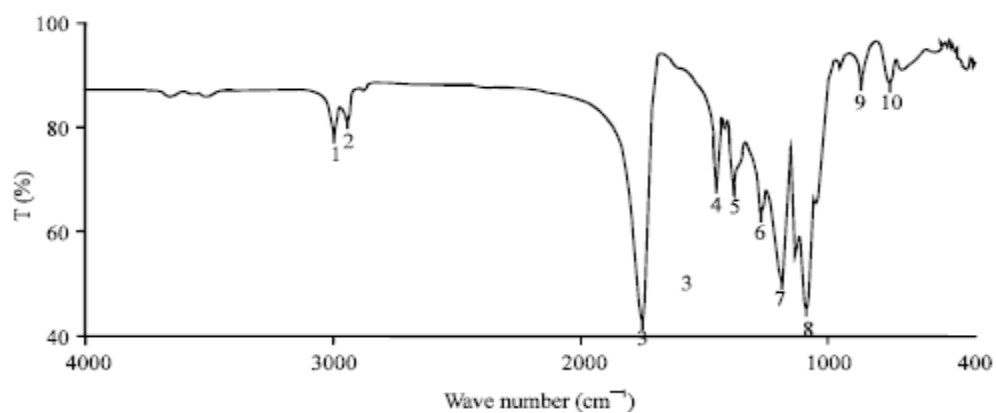


Figure 1.17: FTIR Spectra of PLGA

The FTIR spectra of PLGA showed the typical absorption peaks of -CH , -CH_2 , -CH_3 stretching at approximate range of $2850\text{-}3050\text{ cm}^{-1}$, C-O stretching at $1020\text{-}1270\text{ cm}^{-1}$, and carbonyl group C=O stretching in the range between $1700\text{-}1800\text{ cm}^{-1}$. The figure 1.17 shows the FTIR spectra of PLGA.

Table.1.14: Important peaks of PLGA

Functional group	wave number(cm^{-1})
OH- stretch	3512
-CH- stretch	2995
C=O stretch	1757
C-O stretch	1368
C-C stretch	868

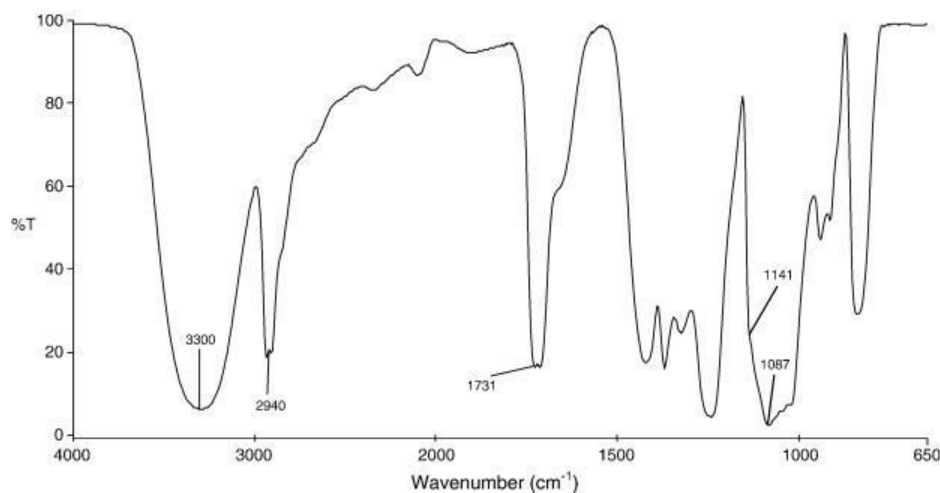
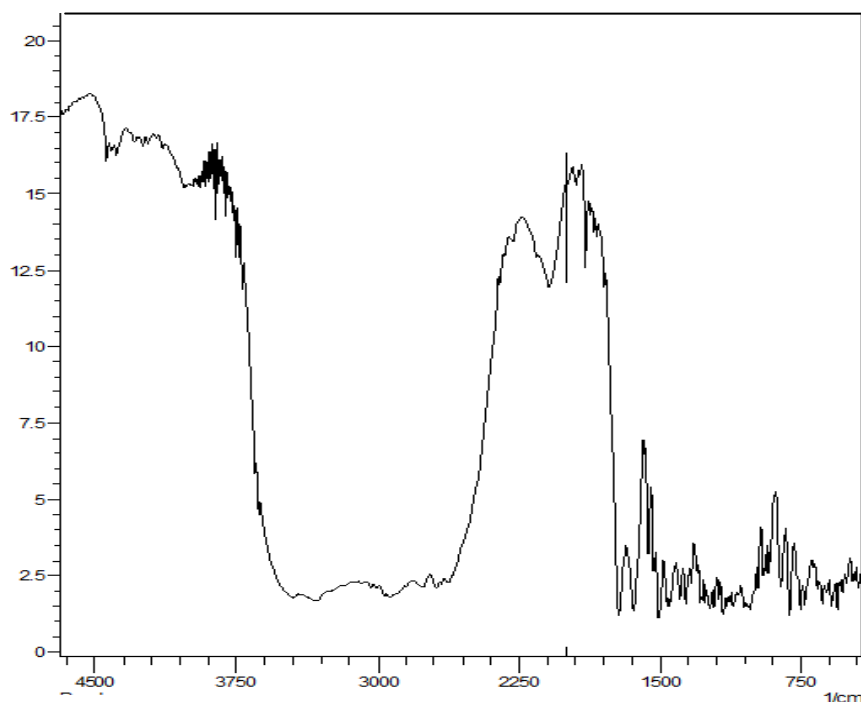


Figure 1.18: FTIR Spectra of PVA

The FTIR spectra of PVA showed peaks related to hydroxyl and acetate groups. The many bands observed inside 3550 and 3200 cm^{-1} are correlated to stretching of O-H group and the intra-molecular and intermolecular hydrogen bonds. Findings suggest between $2840\text{-}3000\text{ cm}^{-1}$ the

stretching of C-H group (alkyl group) and at 1750-1735 cm^{-1} is due to the stretching of C=O, C-O (acetate group).

In order to study the compatibility between BM, selected polymer PLGA and other excipients like PVA, acetone, dichloromethane the spectra was recorded and the main peaks were determined. The spectra of mixtures of BM with PLGA, PVA, acetone and dichloromethane showed the occurrence of typical peaks of the drug peaks (BM) at 3414.8 cm^{-1} due to O-H group stretching, at 2953.01 cm^{-1} C-H group stretching of aliphatic, 1502.60 cm^{-1} N-CH₃ functional group stretching and 1634.06 cm^{-1} C=C stretching of aromatic with slight shifting or variation in the peaks. Though, no additional or new peaks were observed that clarifies the pure drug was completely compatible with all the selected excipients. The IR spectra of BM with PLGA, PVA are depicted in figure no. 1.19 to 1.20.



Some important characteristic absorption peak of compatibility between BM and PLGA

Table.1.15: Important peaks obtained from BM and PLGA interaction

Functional group	wave number (cm ⁻¹)
OH- stretching	3415.8
C-H stretching	2952.01
C=C stretching	1631.06
N-CH ₃ stretching	1502.6
CH ₂ stretching	2840
CH ₃ stretching	3050
C-O stretching	1135
C=O stretching	1765

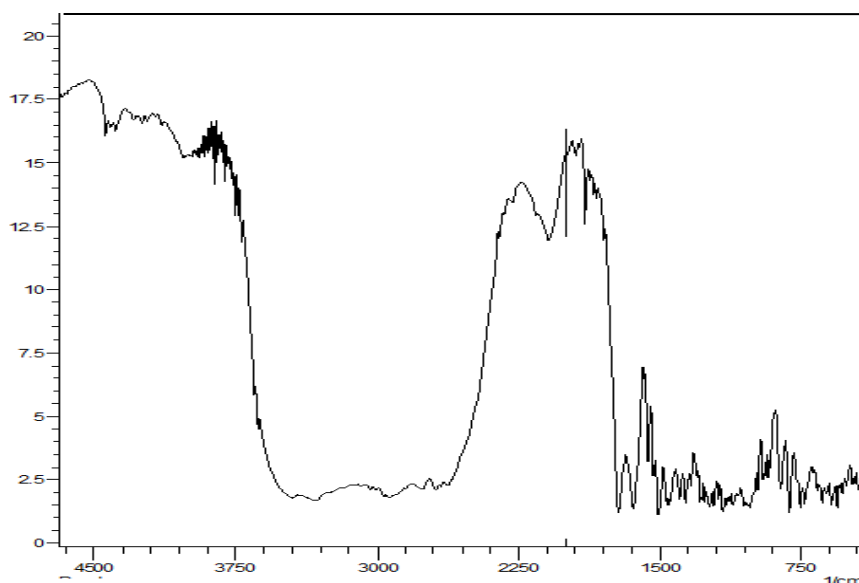


Table.1.16: Some characteristic peaks obtained from BM and PVA interaction:

Functional group	Wave number (cm⁻¹)
OH- stretching	3415.8
C-H stretching	2952.01
C=C stretching	1631.06
N-CH ₃ stretching	1502.6
CH ₂ stretching	2840
C-O stretching	1135
C=O stretching	1764

6.1.6 Partition Coefficient:

The partition coefficient of bendamustine was estimated 4.2. The observed results are depicted in table 1.16 Results of partition coefficient value of BM confirmed its lipophilic nature.

Table.1.17: Partition coefficient of Bendamustine

S. No.	Medium	Partition coefficient(n-octanol/aq. Phase)
1.	n-Octanol: Water	4.2
2.	n-Octanol: PBS pH (7.4)	3.8

6.2 Preparation of Chitosan Nanoparticles:

Chitosan nanoparticle was successfully prepared through ionic gelation method. The master formula for the preparation depicted in the table. 1.17.

Table.1.18: The formula for the preparation of chitosan nanoparticles

Sr. No	Name of Ingredient	Quantity
1.	Chitosan	5mg/ml
2.	Sodium Tripolyphosphate	1%w/v
3	Methanol	5ml
4.	Mannitol	1%
5.	Water	10ml
Conditions		
Sonication time	5-7 min	
Sonication time	5 minutes	
Temperature	Room temperature	

6.3 Optimization of Chitosan nanoparticle:

In the Optimization process firstly, Preliminary studies were done to determine the suitable range of polymer and surfactant for the formation of nanoparticles with the drug. Different concentrations of polymer i.e. 0.1-0.75% w/v of chitosan and surfactant 0.5-1.0% w/v were taken for the preparation of chitosan nanoparticles through ionic gelation method. The results revealed that within selected range of polymer and surfactant concentration demonstrated three kinds of phenomena i.e. solution, with low and high concentration of polymer and surfactant were further observed for formation of optimum nanocarriers through design expert software. So, the result of key variables of particle size and other physiochemical parameters of nano sized particles were studied primarily for finding the correct ratio that result in nanoparticle of small

size of nano range by means of constricted size distribution. Table 1.18 shows selected formulations of chitosan nanoparticles particle size and their entrapment efficiency.

Table.1.19: Formulations of Chitosan Nanoparticles Particle Size And Their Entrapment Efficiency

Nanoparticle formulation no.	Particle size (nm)	Entrapment efficiency %
NPS1	140.12±4.2	60.18±0.16
NPS2	110.51±6.2	50.01±0.21
NPS3	124.12±2.3	53.05±0.19
NPS4	130.27±3.4	64.11±0.13
NPS5	145.09±3.5	61.15±0.17
NPS6	151.15±4.1	63.16±0.23
NPS7	137.19±3.6	57.12±0.20
NPS8	160.09±5.1	63.18±0.12

6.3.1 Effects on Particle Size of Chitosan Nanoparticle

The particle size of 8 batches of Chitosan nanoparticle ranged from 110.51±6.2 nm to 169±5.1 nm for three factors, two level combinations. The following quadratic equation described the influence of independent variables on particle size:

$$Y_1 \text{ (Particle size)} = 130.70 + 9.22A + 7.34B - 6.12C + 1.67AB - 0.65AC - 0.48BC + 22.43A^2 + 27.11B^2 + 17.18C^2$$

From this equation that was clear through increased concentration of polymer particle size quickly increased where as it also implicates that increased polymer concentration gave positive effect on particle size. The considerable enhancement of polymer concentration may be attributed to the increase in the quantity of chitosan chains for the dispensation of bigger particles once stimulated by TPP a cross linking agent. It is also notable that decreased cross linking density between chitosan and TPP, resulted particle accumulation and formation of large particles. Similarly, it also implicated that elevated concentration level of TPP encourages a quicker cross linking observable fact that may be the reason for particle size improvement. The negative value before coefficient C shows increased sonication time would decrease the particle size. Increased sonication time delivers more energy therefore, creating smaller size of nanoparticle.

3D plot showing the effect between PC-SC, PC-ST and SC-ST have been given away in figure.1.21, 1.22 and 1.23 respectively, where ST is the sonication time, SC is concentration of surfactant and PC is concentration of polymer

Design-Expert® Software

Factor Coding: Actual
particle size (nm)



X1 = A: polymer concentration
X2 = B: surfactant concentration.

Actual Factor
C: Sonication time = 6

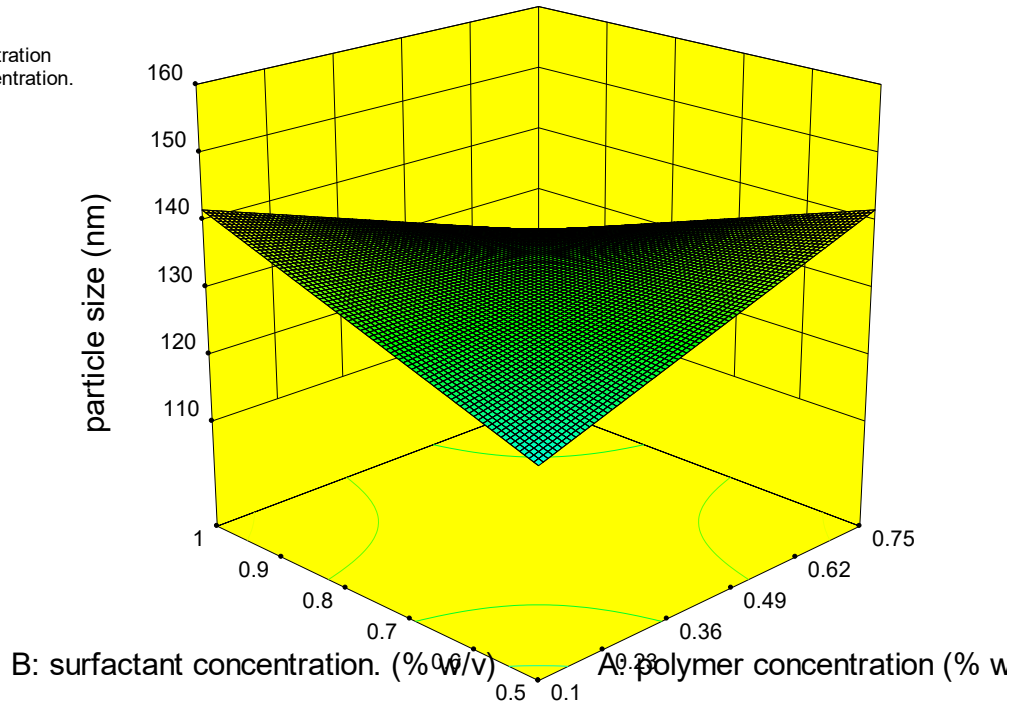


Figure 1.21: 3D response surface plot PC and SC

Design-Expert® Software

Factor Coding: Actual
particle size (nm)



X1 = A: polymer concentration
X2 = C: sonication time

Actual Factor
B: surfactant concentration. = 0.75

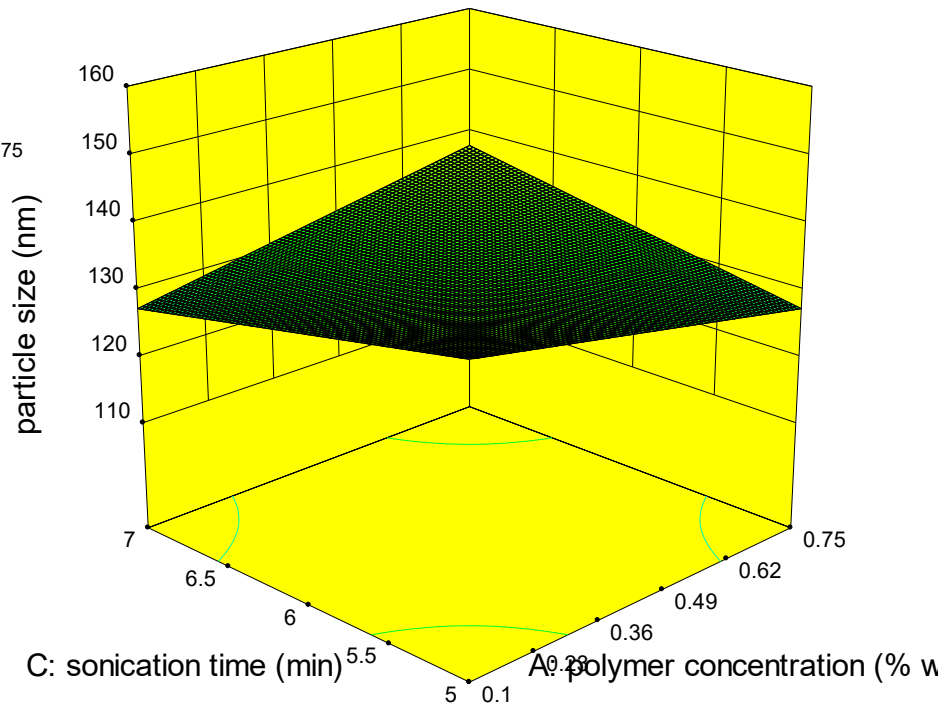


Figure 1.22: 3D response plot between PC and ST

Design-Expert® Software

Factor Coding: Actual
particle size (nm)



X1 = B: surfactant concentration.
X2 = C: sonication time

Actual Factor
A: polymer concentration = 0.425

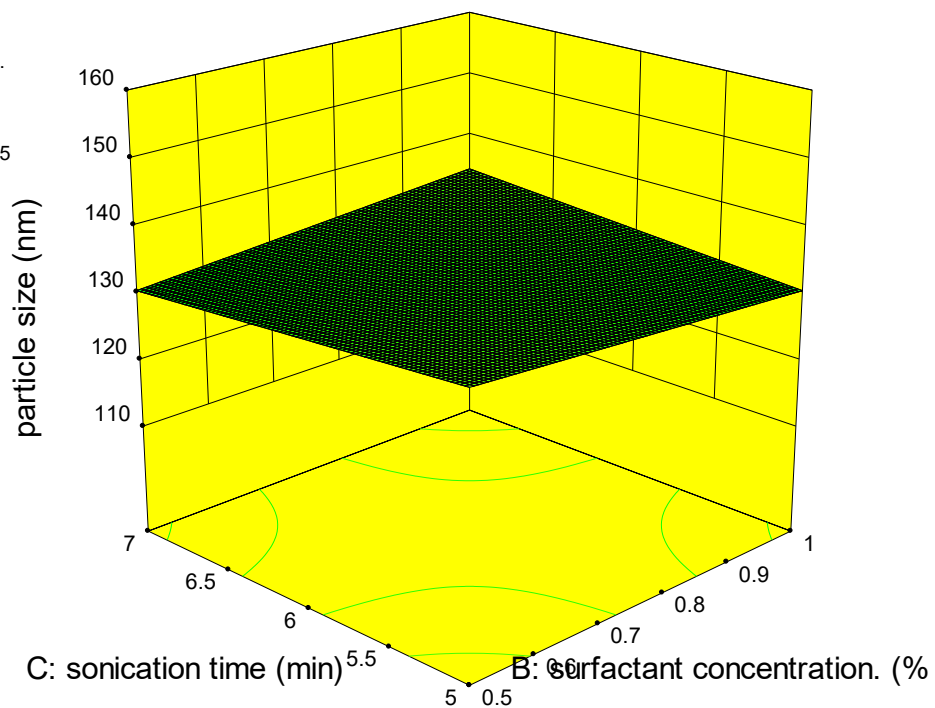


Figure 1.23: 3D surface plot between SC and ST

6.3.2 Result on Entrapment Efficiency:

The entrapment efficiency of 8 batches of BM chitosan nanoparticle ranged from 50.01%±2.1 to 64.11±3.1 % for two level three factor combination. The following quadratic equation described the influence of independent variables on entrapment efficiency.

$$Y_2(\text{EE})\% = 59.57 + 0.11A - 1.99B - 0.35C + 0.98AB - 1.23AC - 1.99BC + 0.70A^2 - 4.38B^2 - 3.40C^2$$

From the equation no.8 it was clear that the coefficient A had a positive effect on Y2 (entrapment efficiency) which clarifies EE% increases with increase in polymer concentration. All the results were significant at $p \leq 0.05$. 3D surface plot on behalf of the influence between PC-SC, PC-ST and SC-ST have been given in figure 6F-17 to 6F-19 for EE% respectively.

Design-Expert® Software
Factor Coding: Actual
Entrapment efficiency (%)



X1 = A: polymer concentration
X2 = B: surfactant concentration.

Actual Factor
C: sonication time = 6

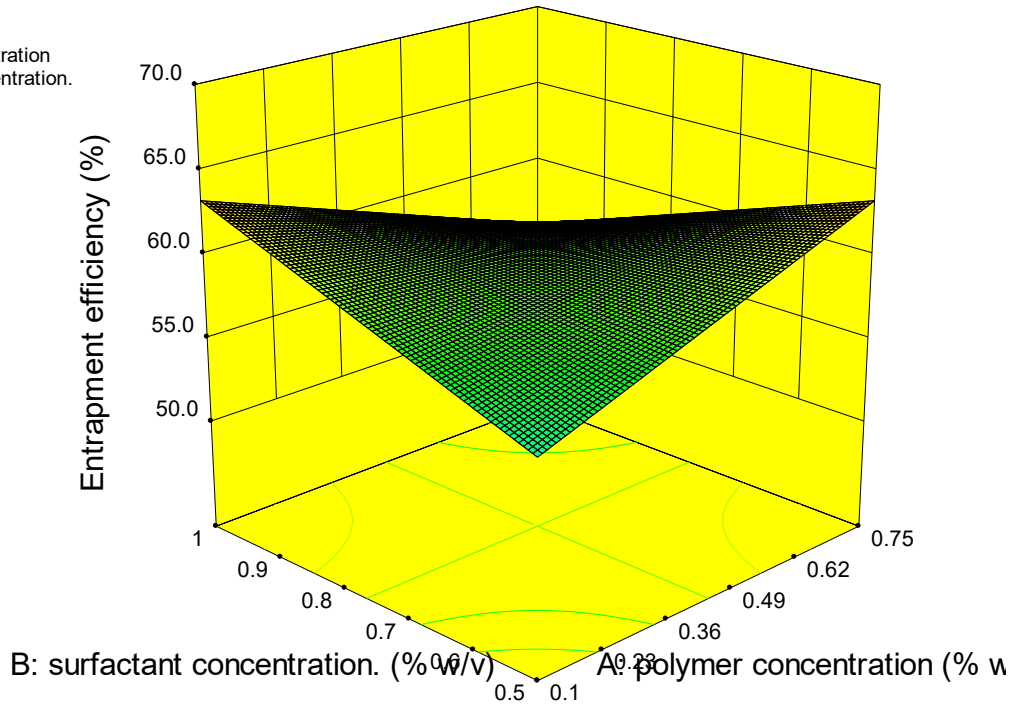


Figure 1.24: 3D surface plot between PC and SC

Design-Expert® Software
Factor Coding: Actual
Entrapment efficiency (%)



X1 = A: polymer concentration
X2 = C: sonication time

Actual Factor
B: surfactant concentration. = 0.75

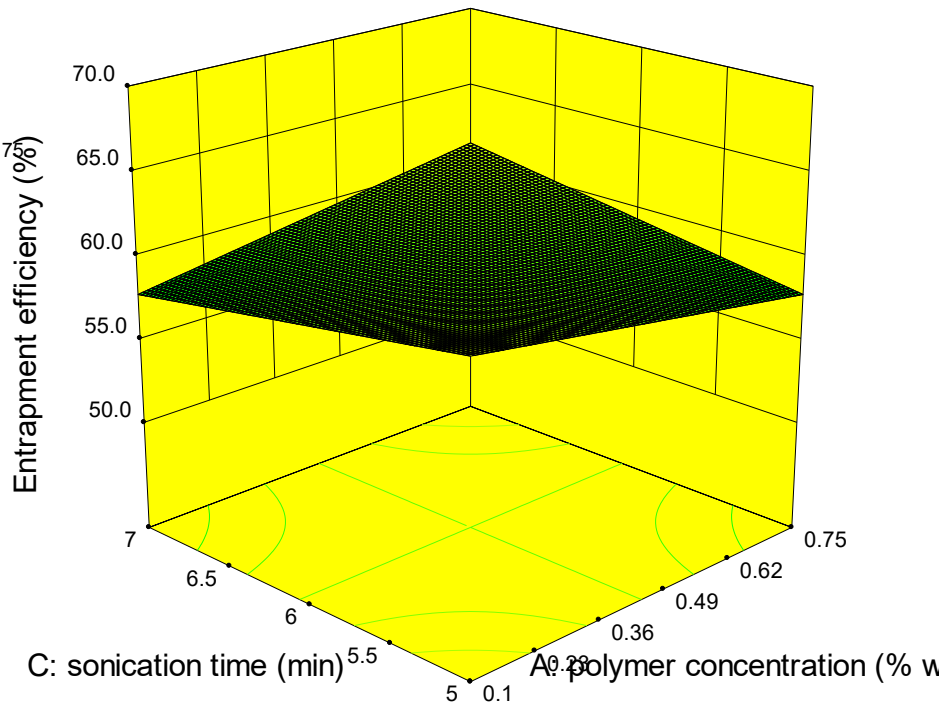


Figure 1.25: 3D surface plot between PC and ST

Design-Expert® Software
 Factor Coding: Actual
 Entrapment efficiency (%)
 66.05
 50.12

X1 = B: surfactant concentration.
 X2 = C: sonication time

Actual Factor
 A: polymer concentration = 0.425

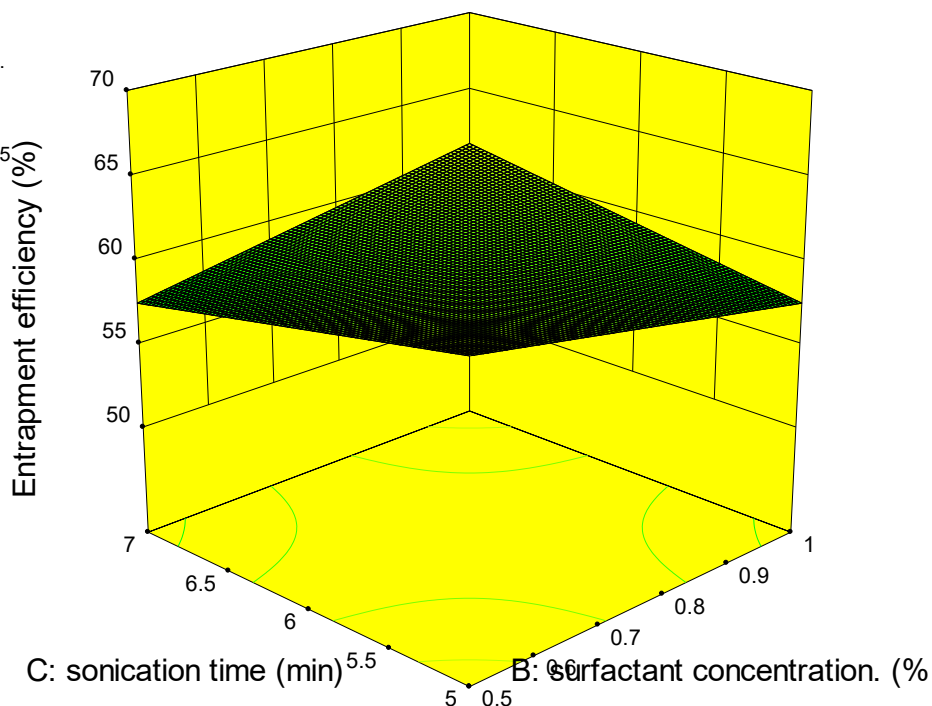


Figure 1.26: 3D surface plot between SC and ST

The design expert version 10 software was used to evaluate the required process for getting best optimized formulation. The optimization results were based on predetermined principle of highest entrapment efficiency and smallest particle size.

It is clear from results obtained in table.1.18 the nanoparticle formulations (NPF-4) prepared with polymer (0.75%) and surfactant (0.5%) concentration respectively, were in desired nano size range (130.27 ± 3.4) and good entrapment efficiency (64.11 ± 3.1) and 6 min sonication time. So, the formulations NPS-4 was considered as optimum formulations and were designated for further studies.

The results of ANOVA model depicted in table 1.20 summary and results of analysis of variance for PS and EE (for BM-CH nanoparticle). The significance of determination coefficient (R^2) and adjusting coefficient were greater than 90% which proves that the model is exceedingly significant.

Table.1.20: Summary and results of analysis of variance for PS and EE (for BM-CH nanoparticle)

Response	Sum of squares	Degree of freedom	Mean square	F value	R^2	Adj. R^2	Perp. R^2
Particle size	1176.23	7	680.62	10.60	0.9972	0.9824	0.9723
Entrapment efficiency	221.52	7	111.23	6.05	0.9921	0.9812	0.9608

6.4 Characterization of Bendamustine loaded chitosan nanoparticle:

6.4.1 Result of Mean Particle Size, Polydispersity Index

The average particle size of blank chitosan nanoparticle 128.24 ± 1.06 and the size of optimized chitosan nanoparticles was $130.27 \text{ nm} \pm 3.4$ with Polydispersity Index (PDI) i.e. 0.245. It is remarkable that particle size of blank nanoparticle is smaller than that of drug loaded nanoparticle. Zeta potential of blank nanoparticle was found around $-19 \pm 0.22 \text{ mV}$ and the drug loaded nanoparticle was around $-21.3 \pm 0.02 \text{ mV}$ with slight increase. The rise in zeta potential may be because of the charge absorbed by Bendamustine particle surface. The negative or positive charge is required for particle repulsion and to make stable nanoparticle as they do not form any aggregates. Figure.1.27 and 1.28 illustrates the narrow particle size range and zeta potential of Chitosan loaded nanoparticle.

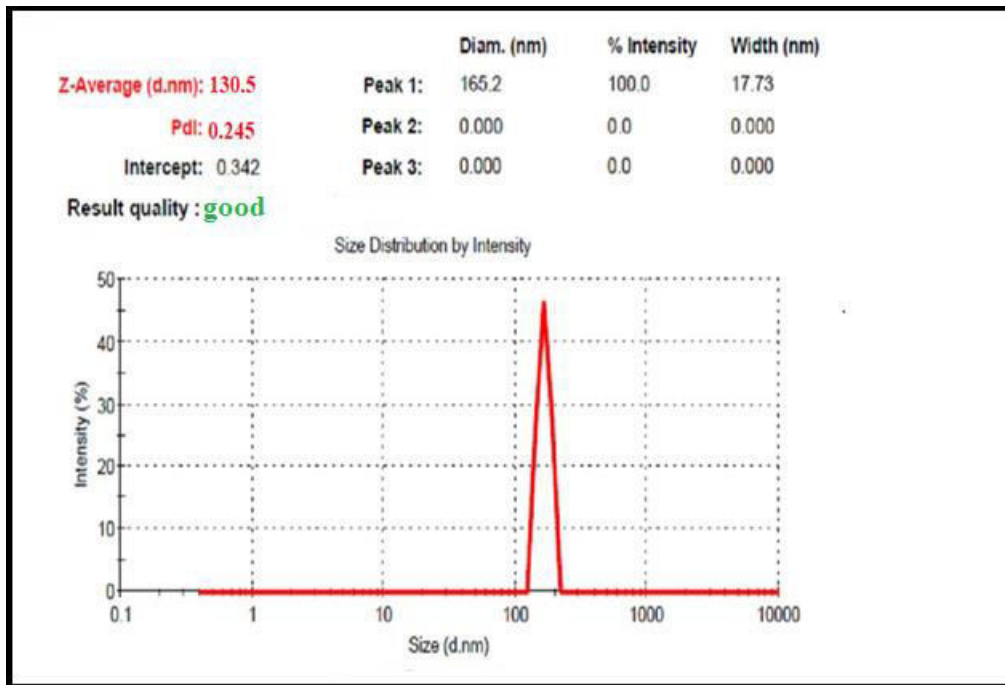


Figure 1.27: Result of Mean Particle Size, Polydispersity Index formulation.no.4

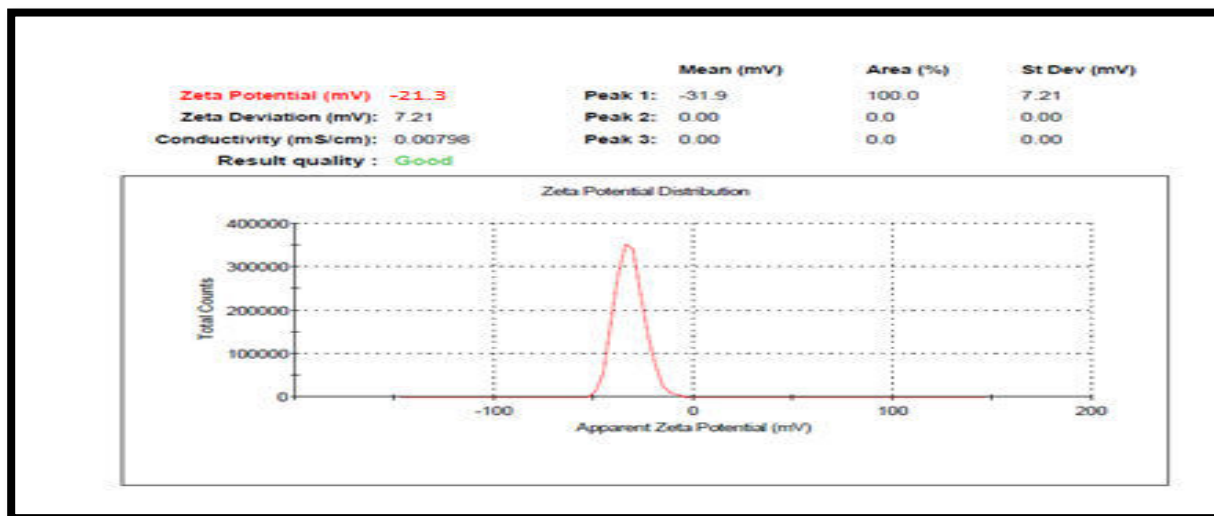


Figure1.28: Zeta potential of preferred formulation.no.4(Chitosan nanoparticle)

6.4.2 Result of Entrapment Efficiency, Process Yield and Drug Loading Percentage of Optimized Chitosan Nanoparticle

Result of percentage yield of optimized chitosan nanoparticle formulation was $66.20 \pm 0.20\%$, where as the % drug loading of preferred formulation was 25.20% with entrapment efficiency found to be $64.11 \pm 0.13\%$.

6.4.3 Result of Transmission Electron Microscopy of Chitosan Nanoparticle

The TEM was used to determine the particle size, shape, and distribution. Transmission electron microscopy examine images displays the image of nanoparticles that is in spherical shape. Scanned images also confirmed that particles uniform size and polydispersity index with distribution in within the range. All the particles were non-accumulated. The Transmission electron microscopy images are depicted in figure 1.29.

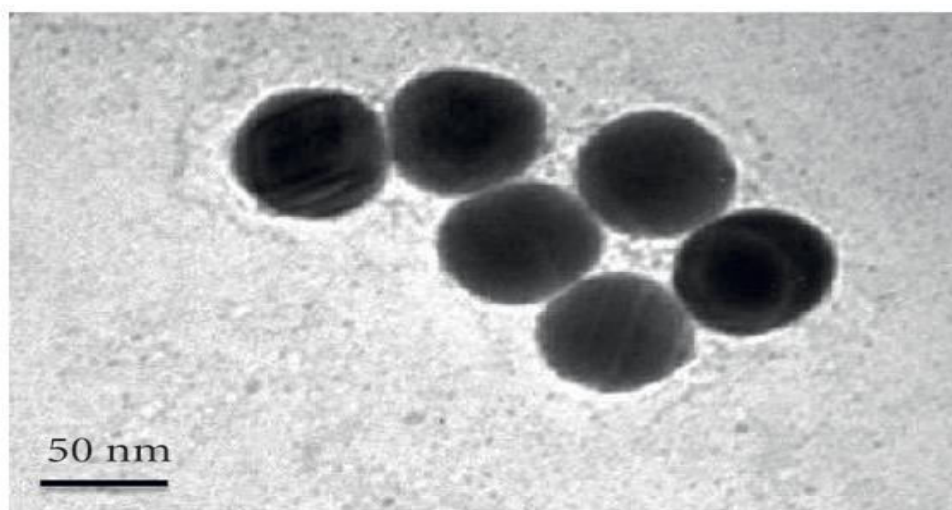


Figure1.29: TEM image of chitosan nanoparticle

6.4.4 Result of Differential Scanning Calorimetry of Chitosan Nanoparticles

The thermograms of differential scanning calorimetry for chitosan, bendamustine and optimized chitosan nanoparticle (NPS -4) are given in figure 1.30. The active drug bendamustine displayed a narrow peak which resembled its melting point at 155°C , representing that the drug is crystalline in nature. Because of the thermal decomposition of drug, a broad peak was observed with high temperature at around 400°C .

The results of Chitosan polymer showed a broad endothermic peak around 91.26°C . After that exothermic peak started at 270°C . The drug was not showing any endothermic peak in nanoparticle formulation which confirms the amorphous phase and presence of drug in the polymeric nanoparticles.

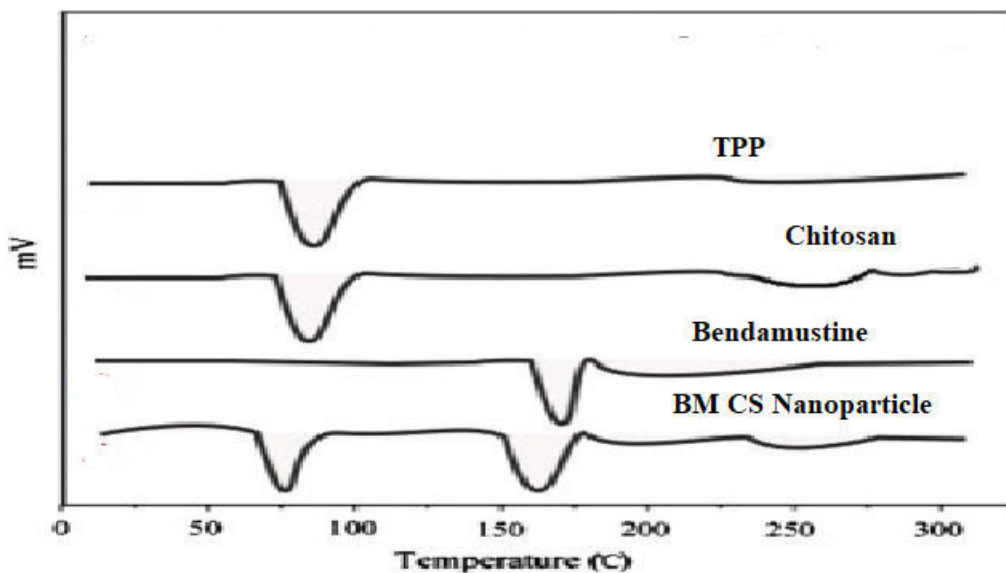
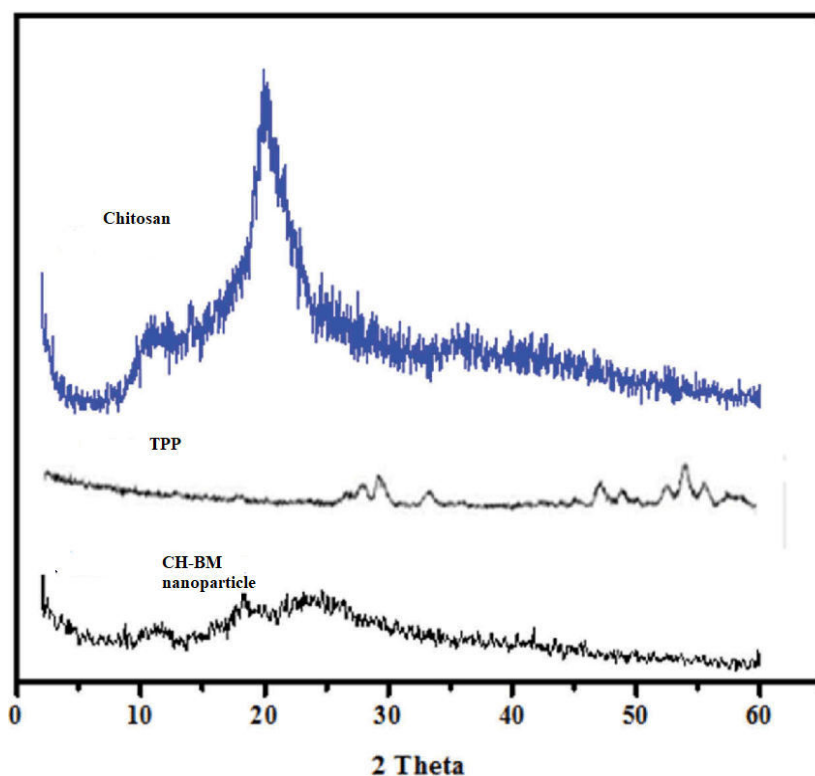


Figure 1.30: DSC Thermogram of TPP, Chitosan, Bendamustine and Chitosan Bendamustine nanoparticle

6.4.5 Result of X-Ray Diffraction Studies

The x-ray diffraction patterns of chitosan, TPP and chitosan nanoparticle were recorded in the fig. 1.32. The pattern of chitosan shows two peaks at $2\theta=10^\circ$ and 20° indicating the crystalline structure of chitosan. Though these peaks become weak as formation of new peaks were observed at $2\theta=11.6, 16.5, 18.2$ and 22.1° . Subsequently, crosslinking with TPP throughout the preparation of chitosan nanoparticles, the crystalline structure of inherent chitosan was demolished and shifting of small peak was observed at $2\theta = 18.85^\circ$.



6.4.6 Result of In-Vitro Drug Release Studies:

The In vitro studies on drug release of bendamustine and chitosan nanoparticles were calculated on the basis of phosphate buffer pH 7.4 and compared through pure suspension of drug for 48 hours and it was observed that BM drug suspension released nearly 99.3% of its pure drug towards the end of 6th hours, though 80.3 % of release was detected at the end of 48th hour from chitosan nanoparticle which displayed steady and sustained release throughout the complete cycle of study. The drug release pattern of chitosan nanoparticle arisen in biphasic way, with an early eruption and rapid release proceeded by sustained release of drug. The result can be seen in table.1.21: results of in vitro drug release of optimized bendamustine and chitosan nanoparticles

Table.1.21: results of In Vitro drug release of optimized bendamustine and chitosan nanoparticles

Time (hrs)	Cumulative percent of drug release of pure BM suspension	Cumulative % drug release (Bendamustine chitosan nanoparticle)
0	0	0
0.5	30.9 ±1.23	20.6± 0.22
1	41.8 ±0.69	47.6± 0.27
2	60.4± 0.11	49.3± 0.18
4	71.1± 0.31	54.6± 0.21
6	99.1± 0.40	58.4± 0.16
8	-	62.6± 0.16
10	-	70.9± 0.20

12	-	72.7± 0.11
18	-	76.9± 0.29
24	-	78.19± 0.24
48	-	80.3± 0.25

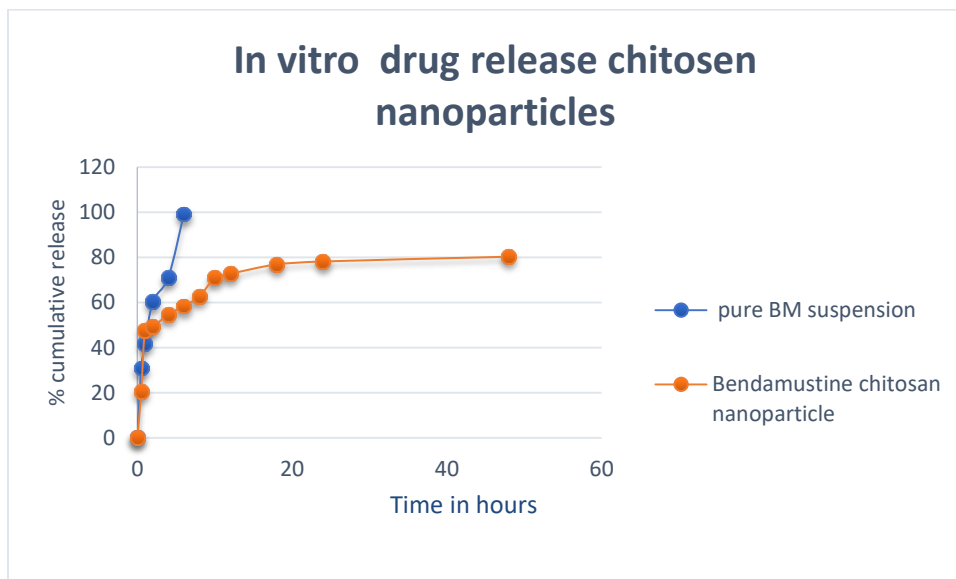


Figure1.32: Drug release study of pure drug suspension and Bendamustine loaded chitosan nanoparticle

6.4.6.1 Result of Drug release kinetics

According to the best fit of ANOVA model and with the uppermost correlation R² value (0.96) and the degree of drug release proponent n=0.78 that specifies the pattern of drug release is non-fickian and also followed the standard korsmeyer-peppas model. The drug release kinetics result can be seen in table 1.22 drug release behavior of BM from optimized chitosan nanoparticle.

Table.1.22: Drug release behavior of BM from optimized Chitosan nanoparticle

Optimized nanoparticle formulation no.	Zero order		First Order		Higuchi model		Korsmeyer-peppas		
	K	R ²	K	R ²	K	R ²	K	n	R ²
NPF 4	1.3160x10 ⁻¹	0.8195	1.7463x10 ⁻³	0.945	2.178	0.932	5.868x10 ⁻³	0.78	0.96

6.5. Results of Preparation of PLGA Nanoparticles by Solvent Diffusion Technique:

The PLGA nanoparticles were finally prepared by solvent diffusion method were prepared by were successfully prepared by emulsion- solvent diffusion method. The master formula was given in table.1.23.

Table.1.23: The formula for the PLGA Nanoparticles by Solvent Diffusion Technique

	Name of Ingredient	Quantity
1.	Polylactic glycolic acid (Polymer)	3mg/ml
2.	Polyvinyl alcohol (Surfactant)	2% w/v
3.	Dichloromethane	10ml
4.	Acetone	10ml
5.	Water	50ml
Conditions		
Stirring speed	500 RPM	
Sonication time	5-7 minutes	
Temperature	Room temperature	

6.6 Optimization of PLGA nanoparticle:

In the Optimization process of PLGA nanoparticle firstly, Preliminary studies were done to determine the suitable range of polymer and surfactant for the formation of nanoparticles (just like chitosan nanoparticle) in the presence of drug. The different concentration of polymer (0.5-3.0 % w/v of PLGA) and surfactant (1.0-2.0 % w/v) were selected for preliminary study for

preparation of PLGA nanoparticles by solvent diffusion technique. Outcomes of preliminary studies within selected range of polymer and surfactant concentration demonstrated two kinds of phenomena i.e., solution, PLGA initial low concentration was 0.5% w/v with surfactants 1% w/v, and the higher concentration of PLGA 3% w/v with surfactant 2 % w/v aggregates or precipitates were obtained.

As founded on the results of preliminary studies, ranges of opalescent parameters were selected as key variables (concentration of Polymer and surfactant) were further examined for formation of optimum PLGA nanoparticle nanoparticles. Table 1.24 The particle size and entrapment efficiency of 8 formulations of nanoparticles were shown in table.1.23 results of PLGA formulated nanoparticles on particle size and entrapment efficiency.

Table1.24: Results of PLGA formulated nanoparticles on Particle size and entrapment efficiency

NSF	Particle size in (nano meter)	Entrapment efficiency in (%)
NPF1	150.9±0.51	81.20±0.04
NPF2	145.2±0.17	80.09±0.07
NPF3	135.6±0.02	79.11±1.03
NPF4	128.2±1.05	76.20±2.31
NPF5	121.3±1.23	74.15±1.12

NPF6	111.2±0.22	70.10±1.03
NPF7	107.6±0.6	60.23± 3.12
NPF8	103.5±0.04	78.13±4.16

6.6.1 Results of BM-PLGA Nanoparticle on Particle Size

The particle size of 8 formulations of BM-PLGA nanoparticle ranged from 103.5±0.04 nm to 150.9±0.51 nm for 3 factor- 2 levels combinations. The influence of independent variables dependent variable i.e. the quadratic equation was designed to describe the particle size.

$$Y_1 \text{ (particle size)} = 115 + 2.165A + 0.740B - 0.672C + 0.94AB - 4.17AC - 6.22BC + 11.30A^2 + 27.06B^2 + 16.12C^2$$

The positive values of factor in the equation show the response factor in the equation specifies that increase in the response variable with the factor. In this A is a polymer concentration which is independent variable had a noteworthy plus positive effect on equation. It also emphasizes that increase in the concentration of polymer raised particle size instantly that is because of during

the emulsification process increase in polymer concentration will increase the viscosity of organic phase which may promote the development of larger size of nanodroplets.

The positive sign of the equation indicates that increased concentration of surfactant may increase the particlesize. Surfactant helps to provide the stability to emulsion nanodroplets and protect them from coalescence with each other. Thus, a smallest quantity of surfactant is essential to get optimum range of nanoparticle².

The 3D response plot was plotted for the effect among ST&SC, PC & S, and SC& PC have depicted in figure 1.33,1.34 and 1.35 respectively; where ST is the sonication time, SC Surfactant concentration and PC is polymer concentration.

Design-Expert® Software
Factor Coding: Actual
particle size (nm)



X1 = A: polymer concentration
X2 = B: surfactant concentration

Actual Factor
C: sonication time = 6

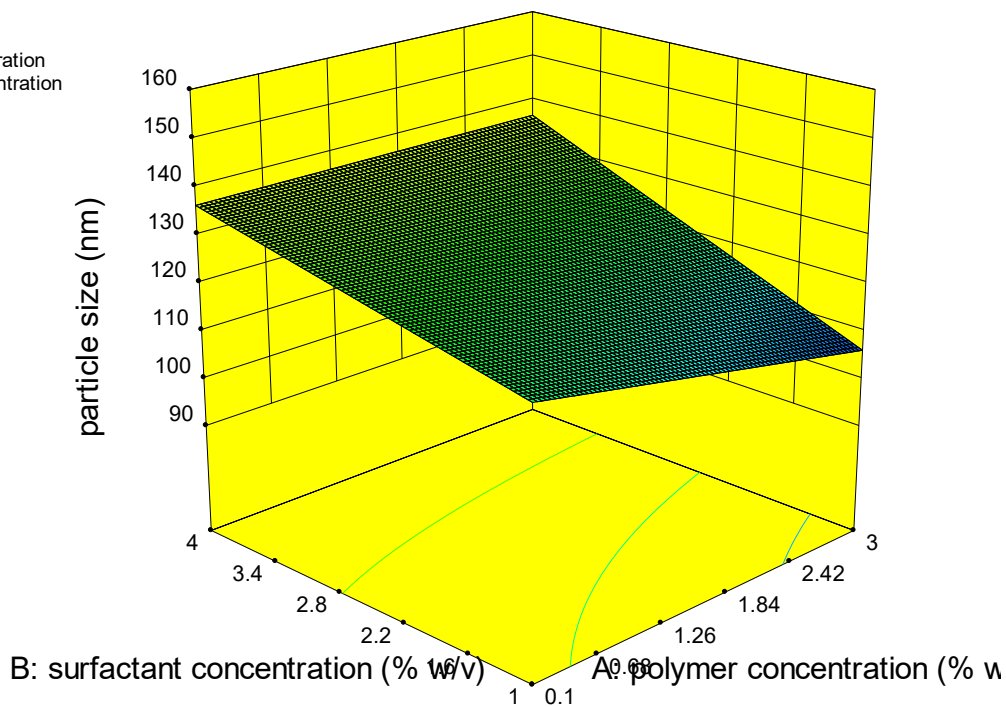


Figure 1.33: 3D surface plot between PC and SC (For BM-PLGA nanoparticle)

Design-Expert® Software

Factor Coding: Actual
particle size (nm)



X1 = A: polymer concentration
X2 = C: sonication time

Actual Factor
B: surfactant concentration = 2.5

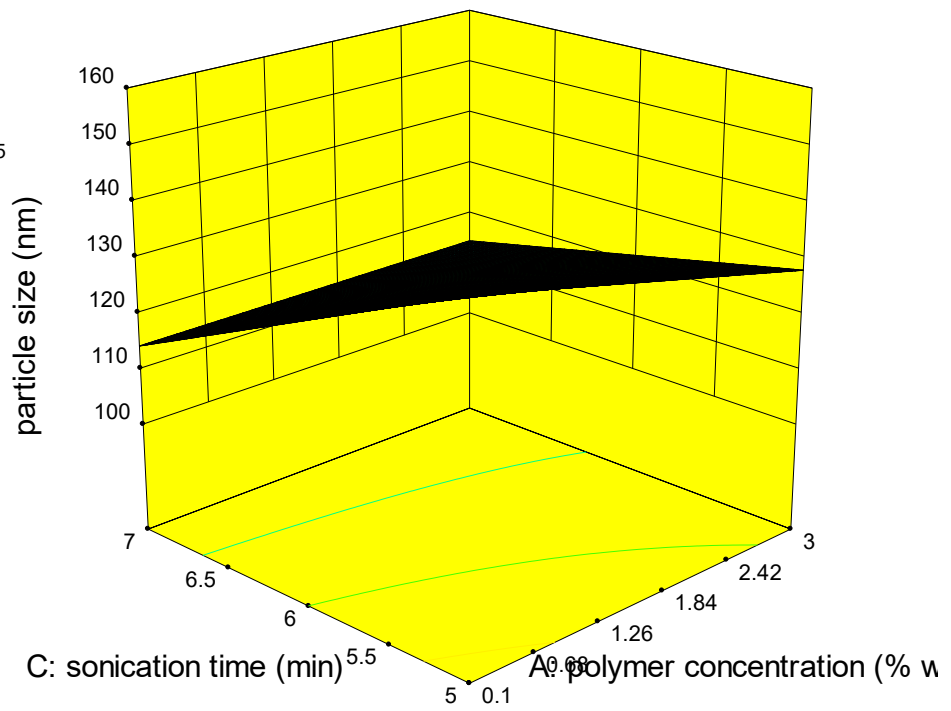


Figure 1.34: 3D surface plot between PC and ST

Design-Expert® Software

Factor Coding: Actual

particle size (nm)

151.9

101.3

X1 = B: surfactant concentration

X2 = C: sonication time

Actual Factor

A: polymer concentration = 1.55

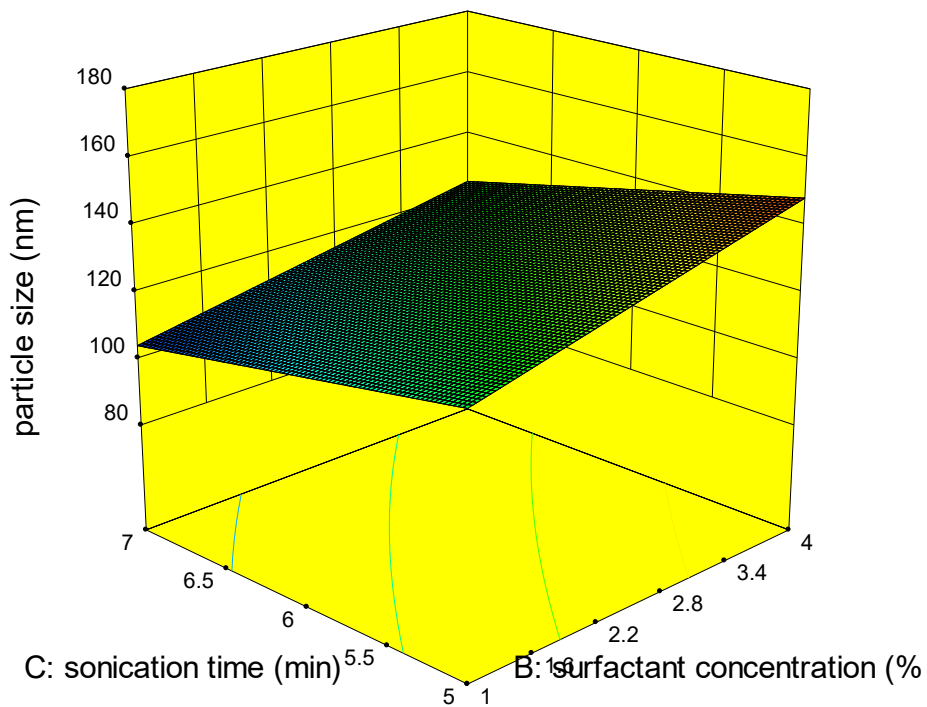


Figure 1.35: 3D surface plot between SC and ST

6.6.2 Results of Entrapment Efficiency of PLGA Nanoparticle

The result on entrapment efficiency of 8 batches was ranged between 58% to 82%. Result was validated through the equation based on independent variable and dependent variables which can be described by following reaction:

$$Y_2 (EE\%) = 75.67 + 3.14A - 1.41B - 1.07C - 0.98AB + 1.26AC - 1.35BC + 0.70A^2 - 4.28B^2 - 3.50C^2$$

Positive sign before A indicates that the entrapment efficiency increases as polymer concentration raised. The negative value before B and C signifies that entrapment efficiency decreases when surfactant concentration and sonication time increases.

All the results were significant at $p \leq 0.05$.

Design-Expert® Software
Factor Coding: Actual
entrapment efficiency (%)



X1 = A: polymer concentration
X2 = B: surfactant concentration

Actual Factor
C: sonication time = 6

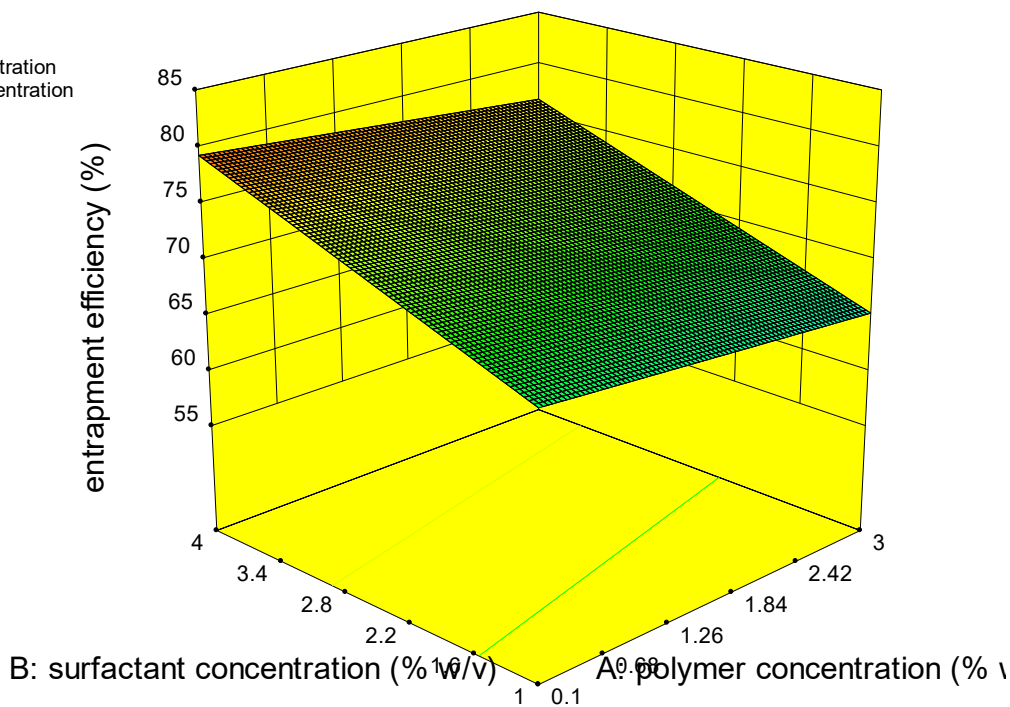


Figure 1.36: 3D surface plot between PC and SC

Design-Expert® Software
 Factor Coding: Actual
 entrapment efficiency (%)
 82
 58

X1 = A: polymer concentration
 X2 = C: sonication time

Actual Factor
 B: surfactant concentration = 2.5%

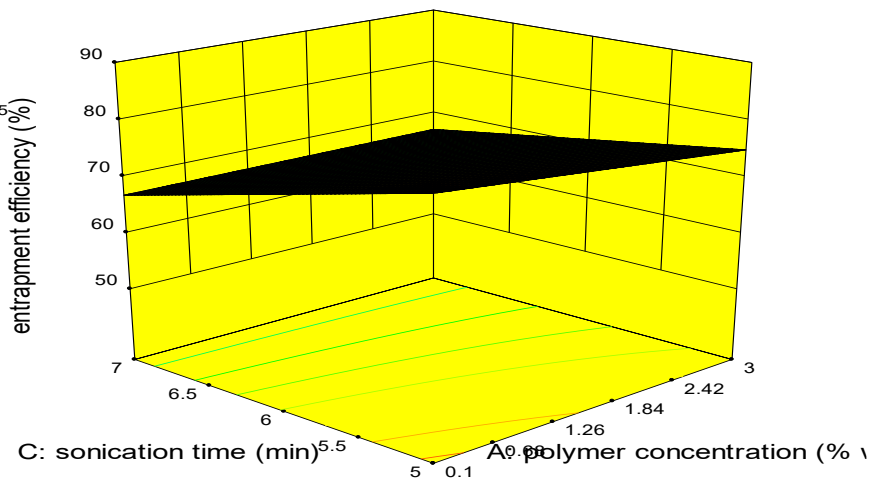


Figure 1.37: 3D surface plot between PC and SC

Design-Expert® Software
 Factor Coding: Actual
 entrapment efficiency (%)
 82
 58

X1 = B: surfactant concentration
 X2 = C: sonication time

Actual Factor
 A: polymer concentration = 1.55%

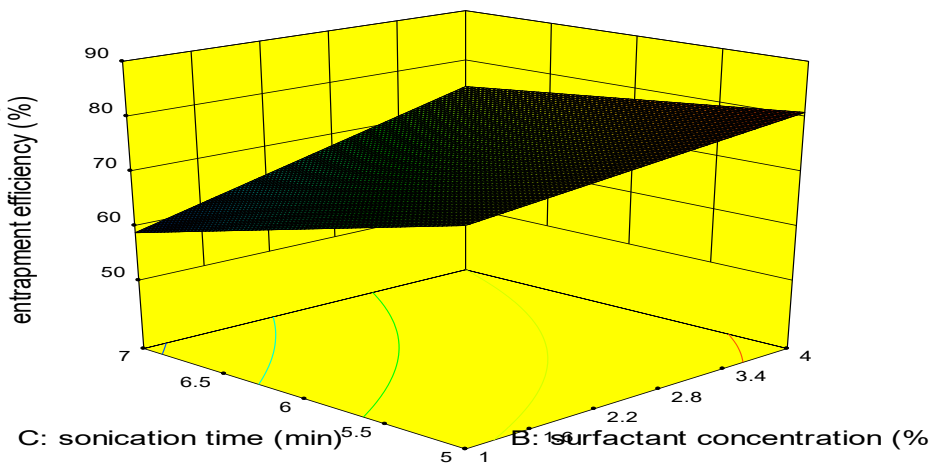


Figure 1.38: 3D surface plot between SC and ST

The particle size and entrapment efficiency for optimized formulations NPF-8 obtained with sonication time 6 minutes were found to be suitable. According to these results, formulation NPF-8 was the optimized formulation with particle size 103.5 nm and 79 % entrapment efficiency. Table 1.25 Summary and results of analysis of variance for PS and EE (for BM-PLGA nanoparticle) based on ANOVA model with significant values. The value of determination coefficient (R^2) and adjusting coefficient were greater than 90% which proves that the model is significant.

Table.1.25: Summary and results of analysis of variance for PS and EE (for BM-PLGA nanoparticle)

Response	Sum of square	Degree of freedom	Mean square	F value	R^2	Adjs. R^2	Perp. R^2
Particle size	2321.46	7	687.38	10.60	0.9948	0.9845	0.9723
Entrapment efficiency	575.88	7	19.01	8.70	0.9807	0.9756	0.9678

6.7 Characterization of PLGA nanoparticles

Results of mean particle size and zeta potential

The particle size of blank PLGA nanoparticle was 101.23 ± 0.04 nm, and the size of preferred formulation loaded with BM was calculated 103.50 ± 0.04 nm with the 0.307 poly dispersity index. It was observed that the particle size of drug loaded PLGA nanoparticles were greater than blank nanoparticles.

The zeta potential for drug loaded optimized nanoparticles was -31.9 ± 3.06 mV. The zeta potential of PLGA nanoparticles were shown in figure 1.39 and 1.40.

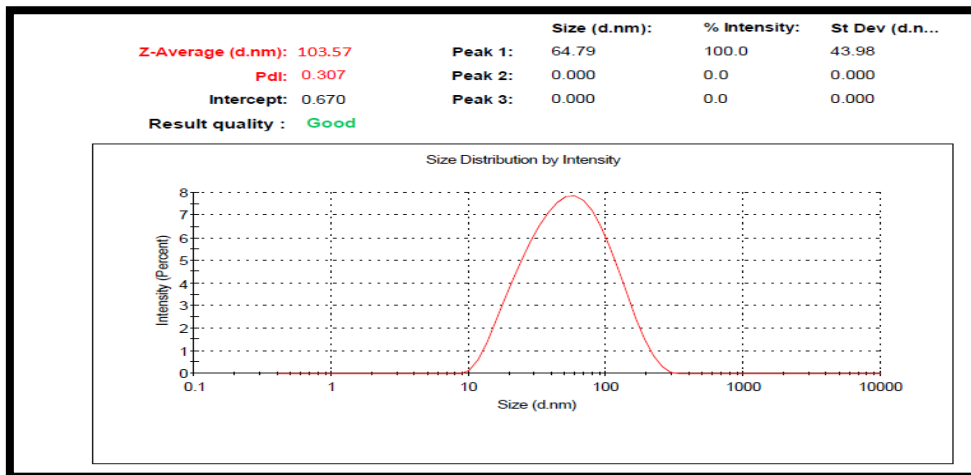


Figure 1.39: Mean particle size of PLGA BM nanoparticle

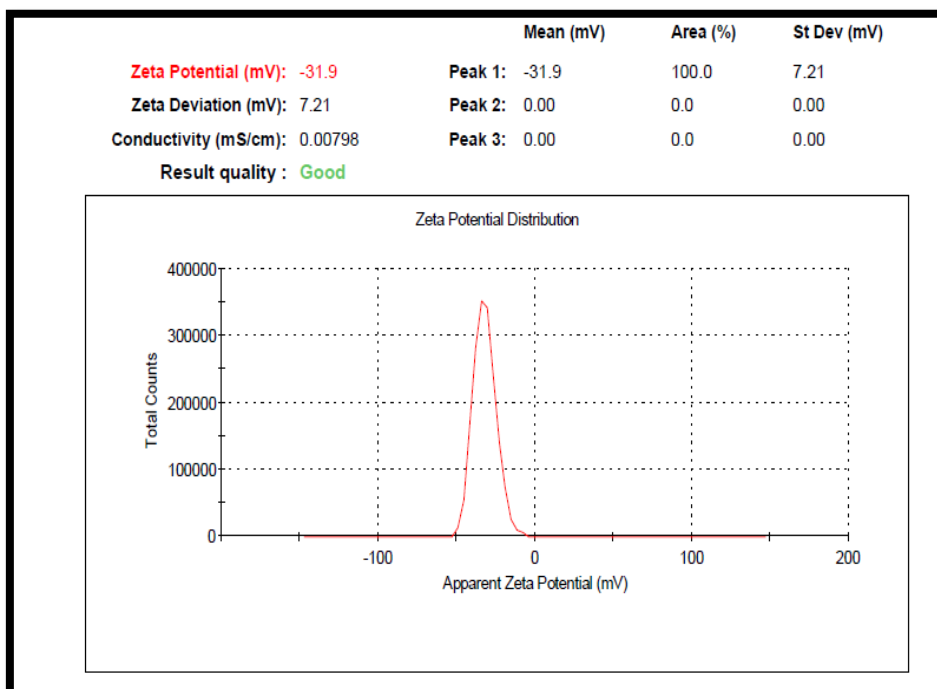


Figure 1.40: Zeta potential of PLGA BM nanoparticles

6.7.1 Results of BM Loaded PLGA Nanoparticle Through Transmission Electron Microscopy

TEM scan displays the development of sphere-shaped nanoparticle. TEM graph also discloses that the particles have a relatively uniform size. The particles were segregated with each other. The dimension of the nanoparticle detected in the graphs were in better arrangement by the information attained from Malvern particle size analyzer. The TEM scan image are characterized in figure 1.41.

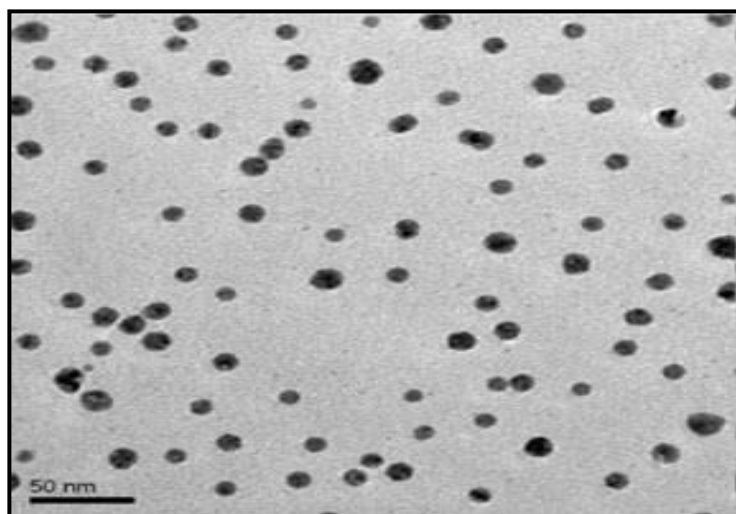


Figure 1.41: TEM image of BM loaded PLGA nanoparticle

6.7.2 Results of Differential Scanning Calorimetry of BM-PLGA Nanoparticle

The differential scanning calorimetry studies of pure Bendamustine, PLGA and bendamustine PLGA nanoparticles shown in fig. no 1.42 DSC thermogram of BM-PLGA nanoparticle. The thermogram of BM were already discussed. The PLGA polymer established a characteristic peak at 45.43°C indicating towards glass transition temperature. The differential scanning calorimetry thermogram of BM-PLGA nanoparticle displayed that polymer is stable up to 250°C with no crystalline material due to nonappearance of sharp peak of bendamustine.

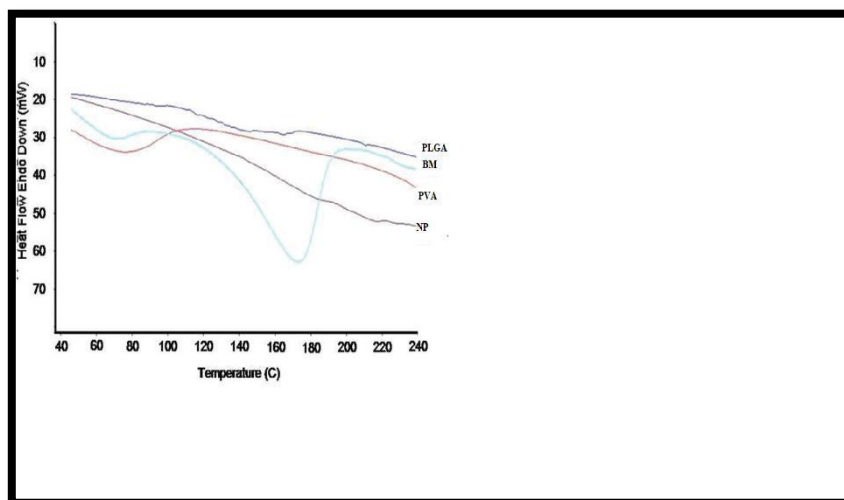


Figure 1.42: DSC thermogram of BM-PLGA nanoparticle

6.7.3 Result of X- ray Diffraction Studies of BM- PLGA Nanoparticle

An x - ray diffraction study of Bendamustine has already studied in prior formulation. In PLGA nanoparticles distorted peak of BM was detected, representing that the pure drug is mixed with

PVA and which does not exist in free form and comparative reduction in the XRD studies. This is due to the variation or decreases in the excellence of crystals of BM and it enhances the change in crystalline form of the drug in amorphous form that helps in solubility enhancement. X-ray diffractogram of pure drug BM, PLGA, PVA and nanoparticle is shown in figure 1.43.

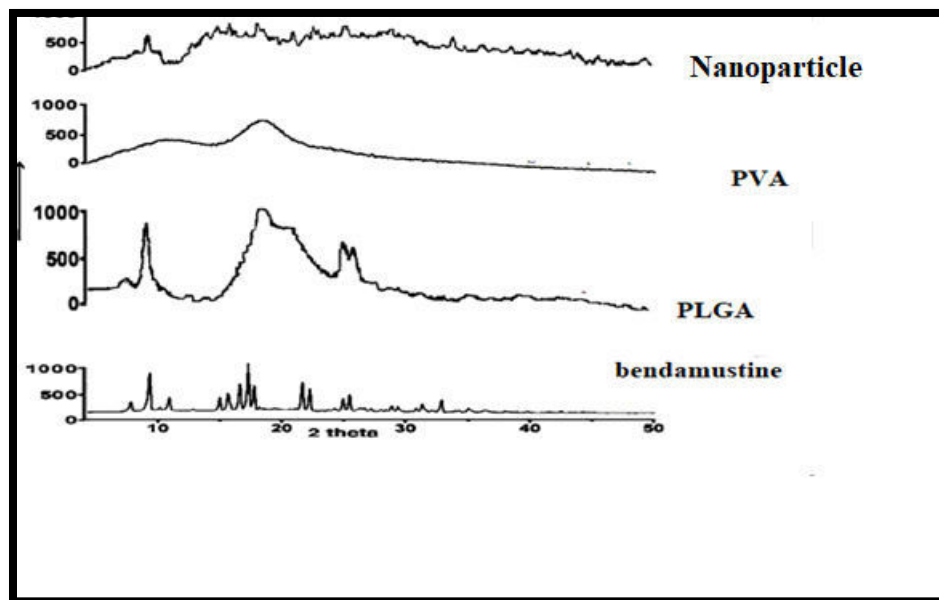


Figure 1.43: X-ray diffraction study of BM- PLGA nanoparticle

6.7.4 Results of In-Vitro drug release of BM Suspension and BM Loaded PLGA Nanoparticles

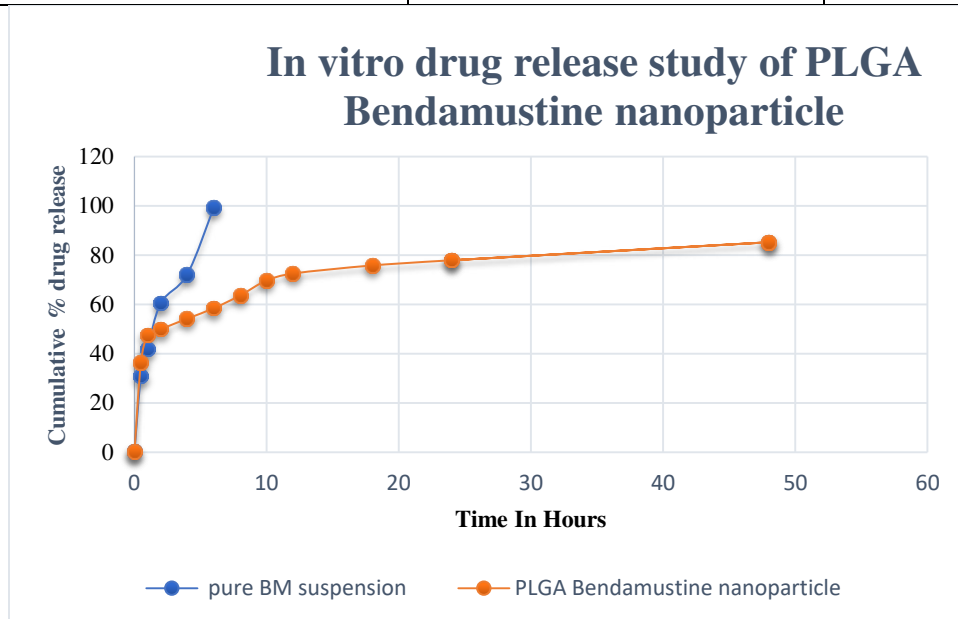
The results of in-vitro drug release of BM suspension and BM loaded PLGA nanoparticles were calculated for 24 hours of duration. The drug release profile was determined in phosphate buffer

At 37°C was given in figure.1.44 and compared with BM pure drug suspension. From the drug release graph, it is sure that pure drug suspension of BM released nearly 98.32% of ± 0.40 of drug towards the end of 6th hours and optimized PLGA nanoparticle released $85.2 \pm 0.24\%$ of drug at its 48th hour. The formulation exhibited a two phase i.e., biphasic release manner with early burst release, and then proceeded by sustained drug release. The preliminary quick release was observed because of drug particles adsorbed in peripheral of nanoparticle surface. All drug molecules dissolved rapidly as they arrive the medium.

Table.1.26: Results of In-Vitro drug release of BM Suspension and BM Loaded PLGA Nanoparticles

Time (hrs)	Cumulative percentage drug release of pure BM suspension	Cumulative percent of drug release of PLGA Bendamustine nanoparticles
0	0	0
0.5	30.9 ± 1.26	36.4 ± 1.13
1	41.8 ± 0.71	47.5 ± 0.20
2	60.5 ± 0.13	49.9 ± 0.59
4	72.1 ± 0.31	54.2 ± 0.05
6	98.2 ± 0.40	58.4 ± 0.28
8	-	63.6 ± 0.18
10	-	69.7 ± 0.19
12	-	72.5 ± 0.04

18	-	75.8 ± 1.03
24	-	77.9 ± 0.02
48	-	85.2 ± 0.24



1.44: Drug release of pattern of BM suspension and BM loaded PLGA nanoparticle

6.7.4.1 Drug Release Kinetics

The optimized formulation of BM-PLGA nanoparticle confirms the first order release pattern in phosphate buffer pH 7.2 as coefficient determination ($R^2 \geq 0.9$). According to the best fit through the maximum R^2 value (0.98) the degree of drug release proponent $n=0.67$ that specifies the pattern of drug release is non-fickian and also followed the standard korsmeyer-peppas model. The drug release kinetics result can be seen in table 1.27 drug release behavior of BM from optimized PLGA nanoparticle.

Table.1.27: Drug release performance of BM from preferred PLGA nanoparticle

Optimized nanoparticle formulation no.	Zero order		First Order		Higuchi model		Korsmeyer-peppas		
	K	R ²	K	R ²	K	R ²	K	n	R ²
Lyophilized formulation of BM-CH	0.0120x10 ⁻¹	0.846	1.3209x10 ⁻³	0.9012	1.902	0.960	5.9492x10 ⁻³	0.674	0.978
Pure BM suspension	0.0189x10 ⁻¹	0.826	1.3101x10 ⁻³	0.9010	1.898	0.940	5.9492x10 ⁻³	0.564	0.965

*K is release constant, R² for coefficient of determination, n is for release exponent

6.8 Formulation and evaluation of dosage form:

6.8.1 Formulation of dry lyophilized powder of Bendamustine loaded Chitosan nanoparticle:

The dry lyophilized powder of chitosan nanoparticle was (NPF.no.4) formulated with mannitol which was used as cryoprotectant. The lyophilized powder (approx. 25 mg) was reconstituted with 10 ml water for injection via shaking. This research showed that no aggregate or clumps were formed during reconstitution with WFI (water for injection).

6.8.2 Evaluation of dry lyophilized powder:

6.8.2.1 Drug Content:

The percentage drug content of lyophilized formulation of BM loaded chitosan nanoparticle was determined by UV-spectroscopic method and was found to be 61.12%.

6.8.2.2 Results of Entrapment Efficiency of prepared Lyophilized Formulation of BM

Observed results suggest that percentage entrapment efficiency reconstituted lyophilized formulation of BM was 64.11%.

6.8.2.3 Results of Particle size, zeta potential of prepared Lyophilized Formulation of BM

The reconstituted lyophilized formulation of BM was found 130.25 ± 3.2 nm with PDI 0.307 and zeta potential of reconstituted lyophilized powder of BM was found -21.3 ± 0.02 mV showed excellent stability.

6.8.2.4 Results of In- vitro drug release studies of prepared Lyophilized Formulation of BM

The in- vitro drug release of prepared lyophilized BM loaded chitosan formulation was significant, shown by graph plotted between cumulative drug release v/s time profile. The percentage of drug release from reconstituted lyophilized powder of BM and the suspension of pure drug BM is given in figure 1.45. Data is shown in table. 1.27.

Table.1.28. Results of In- vitro drug release studies of prepared Lyophilized Formulation of BM

Time (hrs)	Cumulative percentage drug release of pure BM suspension	Cumulative percent of drug release of lyophilized formulation
0	0	0
0.5	30.9 ±1.23	20.6± 0.22
1	41.8 ±0.69	47.6± 0.27
2	60.4± 0.11	49.3± 0.18
4	71.1± 0.31	54.6± 0.21
6	99.1± 0.40	58.4± 0.16
8	-	62.6± 0.16
10	-	70.9± 0.20
12	-	72.7± 0.11
18	-	76.9± 0.29
24	-	78.19± 0.24
48	-	80.3± 0.25

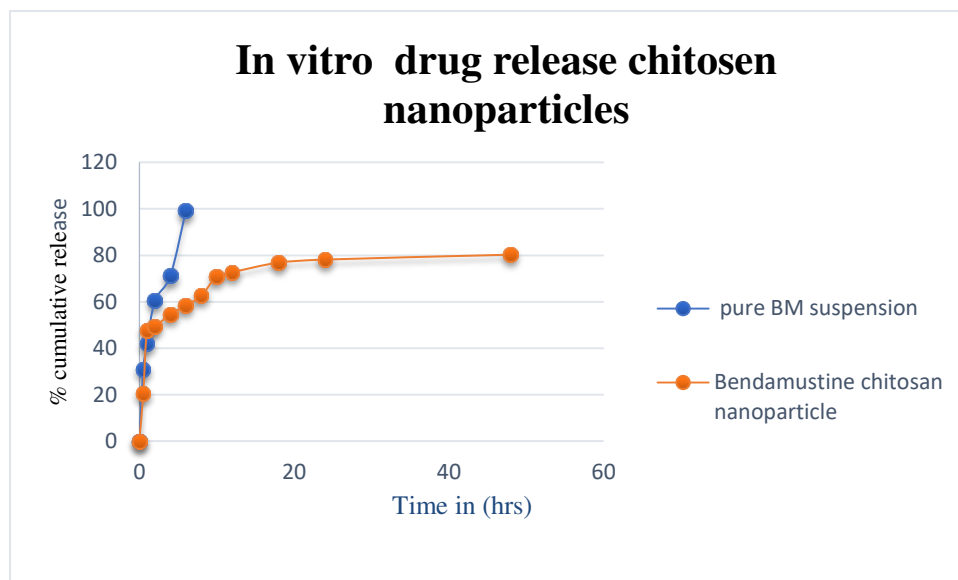


Figure.1.45:Results of In-Vitro drug release of BM Suspension and BM Loaded chitosan Nanoparticles

- **Drug release kinetics of lyophilized formulation of BM-CH**

Based on the results of above graph it has been observed that the lyophilized formulation of BM shown sustained drug release as compared to pure drug suspension. This drug release could be due to the diffusion through polymer matrices. The study specified that pure BM suspension released nearly 99.1% of the pure drug towards the end of 6th hours, whereas 80.3 % release was detected through lyophilized formulation of BM at the end of 48th hours, which displayed the steady release during the whole study. The in vitro drug release profile arisen in biphasic way through a primary eruption (burst) and speedy release stage proceeded by sustained (slower) release stage. The drug release kinetics were studied through estimating the R^2 value. (Shown in table.1.28).

Table.1.29: Drug release behavior of lyophilized BM-CH formulation

Optimized nanoparticle formulation	Zero order		First Order		Higuchi model		Korsmeyer-peppas		
	K	R ²	K	R ²	K	R ²	K	n	R ²
Lyophilized formulation of BM-CH	1.3160x10 ⁻¹	0.8195	1.7463x10 ⁻³	0.945	2.178	0.932	5.868x10 ⁻³	0.78	0.96
Pure drug suspension	1.3060x10 ⁻¹	0.8067	1.7234x10 ⁻³	0.925	2.067	0.912	5.758x10 ⁻³	0.68	0.95

*K is release constant; R² for coefficient of determination, n is for release exponent

The highest value of R² was near about 0.96 for reconstituted lyophilized formulation of BM. That revealed the drug release as of the selected optimized formulation followed the Korsmeyer-Peppas pattern (Table 1.28).

6.8.2.5 Results of In- vitro cellular Cytotoxic study of BM Suspension and BM Loaded chitosan Nanoparticles

The cytotoxic property of pure drug BM loaded chitosan as lyophilized formulation was evaluated by Z-138 cell line. the contact time was 24, 48 and 72 hours MTT assay was used to evaluate the cell viability. The cell viability (IC₅₀) values of pure drug bendamustine and its

lyophilized formulation (NSF-4) was found to be 36.16 ± 0.05 and $18.14 \pm 0.12 \mu\text{m}$ individually next 72 hours contact. The IC_{50} value explains that lyophilized formulation (BM-CH) possesses noteworthy in-vitro anticancer action (antileukemic activity) in comparison with pure drug. No cytotoxic effect was noted when the formulations were exposed to Z-138 cell-line, approved that the formulation is safe.

Table.1.30: The half maximal Inhibitory concentration (IC_{50}) of pure BM suspension also lyophilized formulation of BM-CH on Z-138 cells after 24, 48 and 72 hours.

Cell line	Treatment	$\text{IC}_{50} \mu\text{m}$		
		24 hours	48 hours	72 hours
Z-138	Pure BM suspension	50.6 ± 0.09	48.2 ± 0.12	36.16 ± 0.05
	Lyophilized formulation of BM-CH	46.6 ± 0.21	29.06 ± 1.19	18.13 ± 0.12

The straight contact with drug and cell can cause toxic effects to cell and this might be decreased through incorporation of active drug into the polymeric nanoparticles. All the results reveal that loading of drug into lyophilized formulation powerfully decreased the cellular cytotoxic influence when compared to active drug. The percentage of cell viability at different concentration after 24, 48, and 72 hours are shown from figure.1.46 to 1.48.

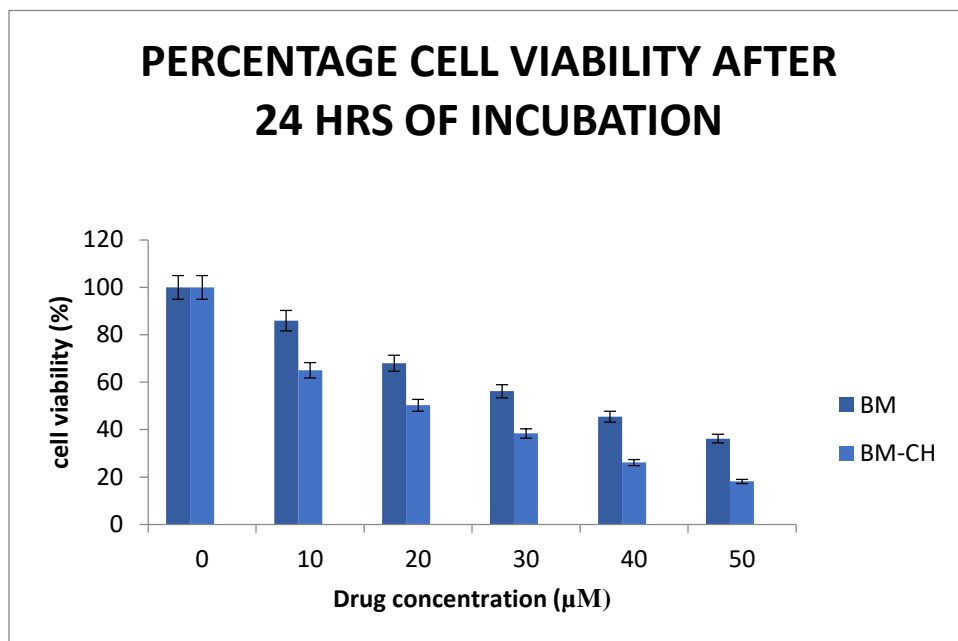


Figure 1.46: Z -138 viability after 24 hours of incubation with pure BM suspension and lyophilized BM loaded chitosan formulation

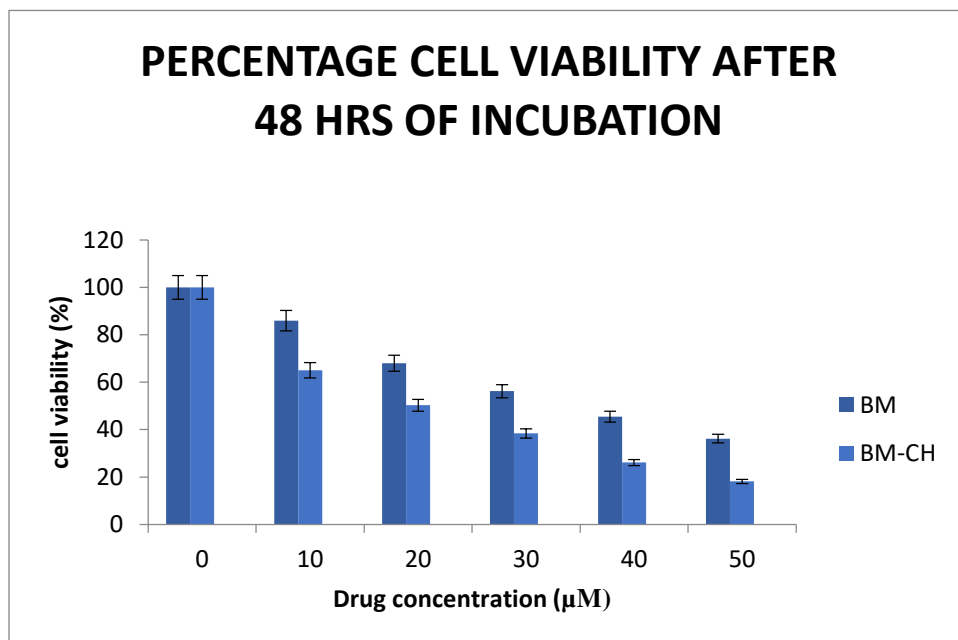


Figure1.47: Z -138 viability after 48 hours of incubation with pure BM suspension and lyophilized BM loaded chitosan formulation

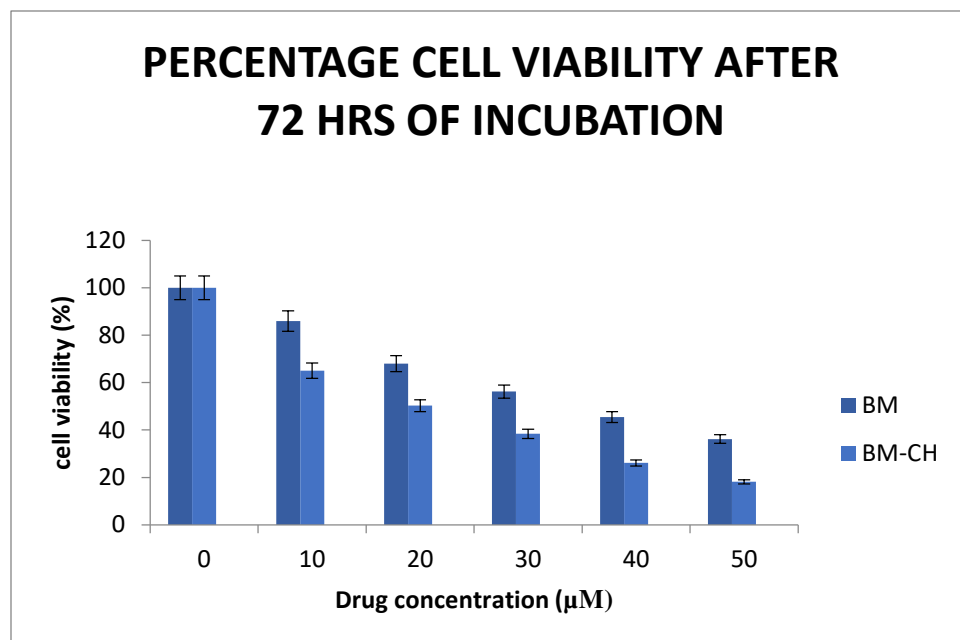


Figure 1.48: Z -138 viability after 72 hours of incubation with pure BM suspension and lyophilized BM loaded chitosan formulation

6.8.3 Stability study:

In stability testing it was observed that the lyophilized powder of BM, degraded about 0.06% of its amount in initial month and 1.03% during 6th month once kept on room temperature ($25^{\circ}\pm 2^{\circ}\text{C}$, $60\pm 5\% \text{RH}$). In the accelerated stability condition ($40^{\circ}\pm 2^{\circ}\text{C}$, $75\pm 5\% \text{RH}$) the lyophilized formulation degraded drug above 1.5% in 1st month and near about 2.11% during 6th months (shown in table 1.30).

Therefore, the lyophilized formulation (lyophilized powder) of BM was considered to be more stable at room temperature when compared to the pure drug suspension and not any noteworthy deviations were observed in particle size, Zeta potential and drug content. The

effect of storage conditions in % residual drug content of BM lyophilized formulations is given in figure 1.49.

Table.1.31: Effect of storage condition on % residual drug content of BM

Formulation code	Room temperature			Accelerated condition		
	% Residual drug content					
	1M	3M	6M	1M	3M	6M
Lyophilized formulation of BM-CH	61.06	61.03	60.03	60.56	60.45	58.45
Pure BM suspension	60.12	60.06	59.06	58.62	58.60	56.62

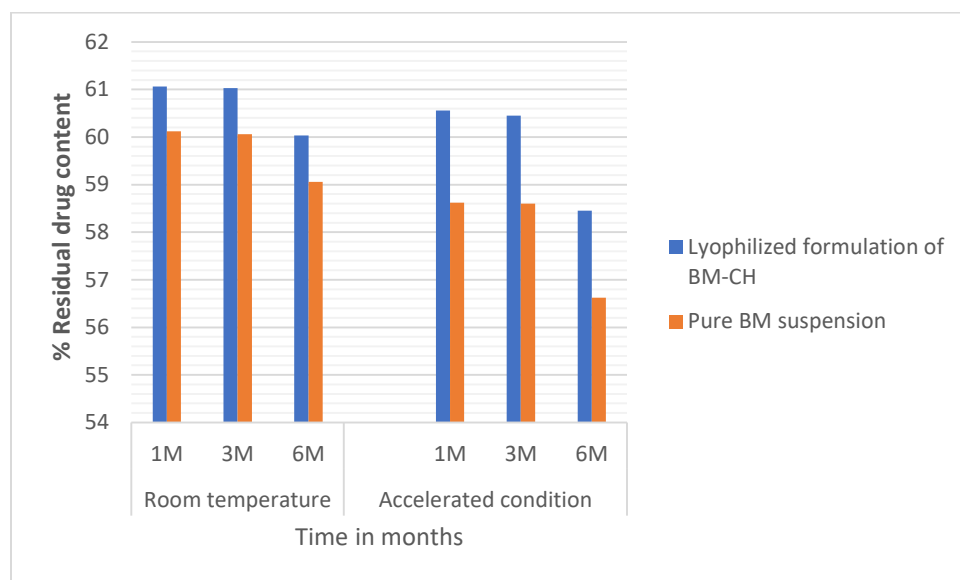


Figure 1.49: Effect of storage conditions on percent residual drug content of pure drug suspension and lyophilized formulation of BM-PLGA

6.9 Formulation of BM loaded PLGA lyophilized powder

The dry lyophilized powder of BM-PLGA nanoparticle was (NPF.no.8) formulated just like chitosan BM loaded lyophilized powder using mannitol as cyroprotectant and WFI

6.9.1 Evaluation of BM-PLGA lyophilized powder:

Percentage drug content: The percentage drug content of lyophilized formulation of BM-PLGA was estimated by UV-spectroscopic method and was found to be 75.28%.

6.9.1.1 Entrapment efficiency:

The percentage entrapment efficiency of reconstituted lyophilized formulation of BM loaded PLGA nanoparticle was found to be 78.16%.

6.9.1.2 Particle size and zeta potential:

The particle size of reconstituted lyophilized formulation of BM was found to be 103.84 ± 0.91 nm with PDI 0.32. Zeta potential was assessed to get evidence about the surface properties of nanoparticles.

6.9.1.3 In vitro drug release:

The in-vitro drug release manner of prepared lyophilized BM-PLGA formulation signified graphically by plotting a graph between percentage cumulative drug release v/s time profile. According to the graph plotted above, it has been observed that the lyophilized formulation of BM- PLGA shown sustained drug release as compared to pure drug suspension also specified that BM suspension released nearly 99.3% of pure drug towards the end of 6 hours whereas 81.59 % drug release was detected through the lyophilized formulation of BM which exhibited sustained release during the entire process of study.

Table 1.32: Cumulative percent of drug release from reconstituted lyophilized powder of BM and the suspension

Time In Hours	Cumulative % drug release of pure BM suspension	Cumulative % drug release (PLGA Bendamustine nanoparticle)
0	0	0
0.5	30.9 ±1.26	36.4 ± 1.13
1	41.8 ±0.71	47.5 ± 0.20
2	60.5 ± 0.13	49.9 ± 0.59
4	72.1± 0.31	54.2 ± 0.05
6	99.2± 0.40	58.4 ± 0.28
8	-	63.6 ± 0.18
10	-	69.7 ± 0.19
12	-	72.5 ± 0.04
18	-	75.8 ± 1.03
24	-	77.9 ± 0.02
48	-	85.2± 0.24

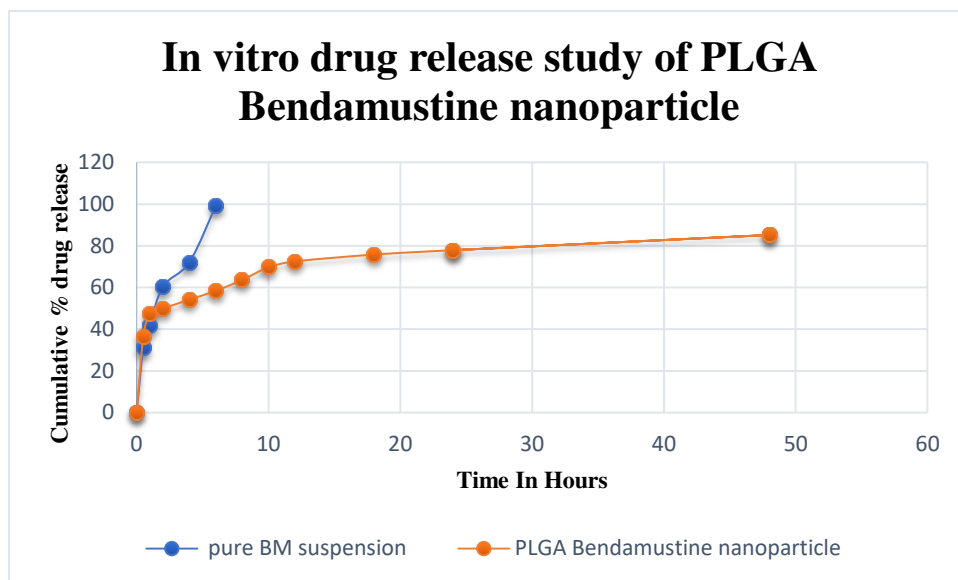


Figure 1.50: Drug release study of pure drug suspension of BM and BM loaded PLGA nanoparticle

6.9.1.4 Drug release kinetics:

According to the bestfit with the maximum correlation coefficient (R^2) value (0.97) and the degree of drug release exponent ($n=0.67$) specifies that the drug release pattern is non-Fickian and followed Korsmeyer-Peppas model. The drug release kinetics of formulation were studied through estimating the R^2 value of different mathematical models. (Shown in table.1.32).

Table1.33: Release kinetics of pure BM suspension and BM-PLGA lyophilized formulation in phosphate buffer.

Optimized formulation no.	Zero order		First Order		Higuchi model		Korsmeyer-peppas		
	K	R ²	K	R ²	K	R ²	K	n	R ²
Lyophilized formulation of BM-CH	0.0120x10 ⁻¹	0.846	1.3209x10 ⁻³	0.9012	1.902	0.960	5.9492x10 ⁻³	0.674	0.978
Pure drug suspension	0.0189x10 ⁻¹	0.826	1.3101x10 ⁻³	0.9010	1.898	0.940	5.9492x10 ⁻³	0.564	0.965

*K is release constant; R² for coefficient of determination, n is for release exponent

6.9.1.5 In-vitro cellular cytotoxic study:

The cytotoxic study of pure BM and BM loaded Poly lactic glycolic acid (PLGA) as lyophilized formulation was evaluated with Z-138 cell line. Subsequent 24,48 and 72 hours of contact. MTT assay performed for cell viability and maximum inhibitory concentration value of formulations were calculated.

The maximum inhibitory concentration values (IC₅₀) of pure drug Bandamustine and its lyophilized formulation (NPF-8) was found to be 36.17 ± 0.05 and 16.13 ± 0.12 μm individually after 72 hours cell contact to drug. The values were given in table.1.33, it explains about the lyophilized formulation (BM-PLGA) possesses noteworthy antileukemic action in comparison to

BM suspension. Not any cellular cytotoxic effect had seen which clear cut approves that the formulation is safe.

Table.1.34: The IC₅₀ value of pure drug suspension also lyophilized formulation of BM-PLGA on Z-138 cells after 24, 48 and 72 hours

Cell line	Treatment	IC50 μm		
		24 hrs	48hrs	72 hrs.
Z-138	Pure BM suspension	50.6 \pm 0.09	48.2 \pm 0.15	36.17 \pm 0.05
	Lyophilized formulation of BM-CH	45.6 \pm 0.21	28.06 \pm 1.19	16.13 \pm 0.12

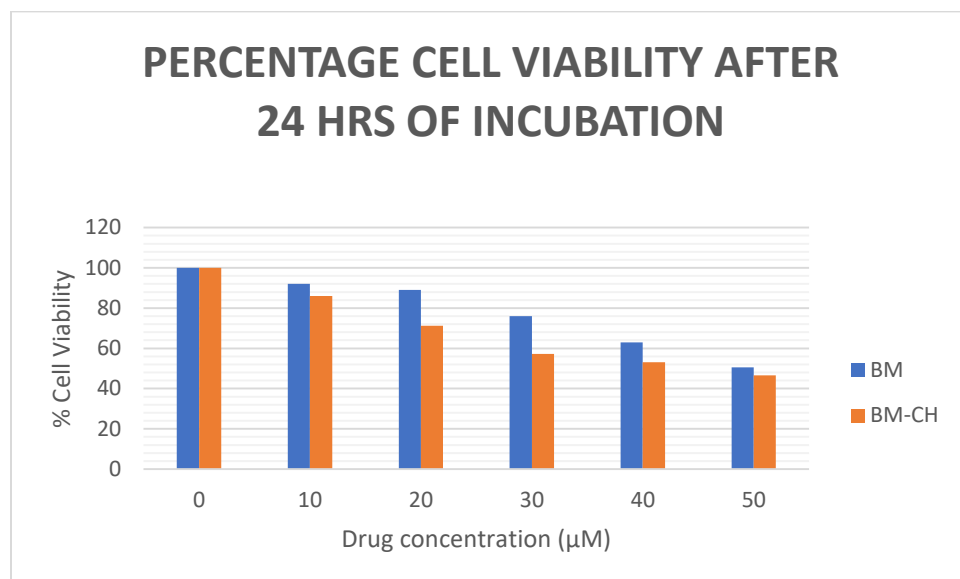


Figure 1.51: Z-138 cells viability after 24 hours incubation with Pure BM suspension and lyophilized formulation of BM-CH

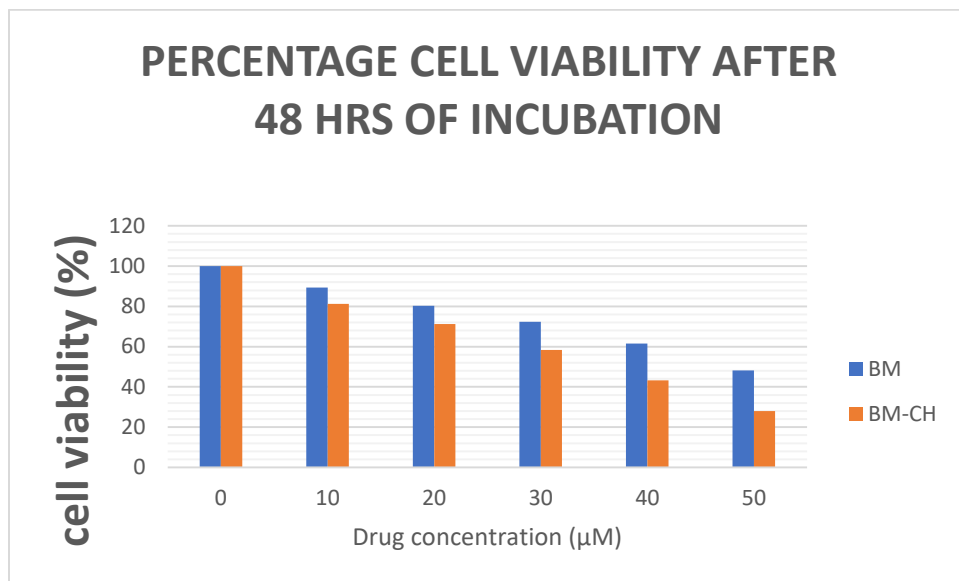


Figure 1.52: Z-138 cells viability after 48 hours incubation with Pure BM suspension and lyophilized formulation of BM-CH

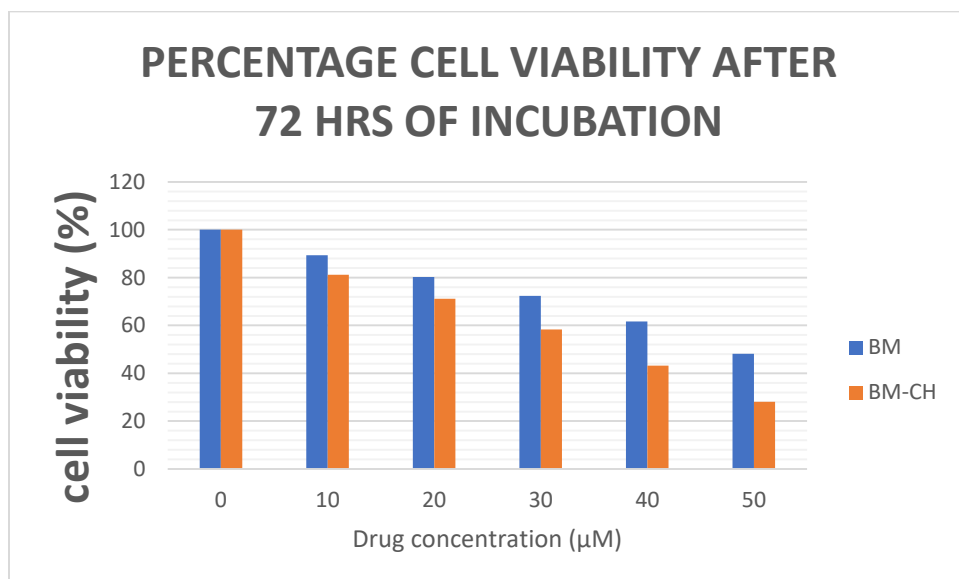


Figure 1.53: Z-138 cells viability after 72 hours incubation with Pure BM suspension and lyophilized formulation of BM-CH

6.9.2 Stability study:

In stability testing it was observed that the lyophilized powder of BM-PLGA degraded nearly 0.03% of active drug amount in initial month and 0.06% in next six months once kept on $25^{\circ}\text{C} \pm 2^{\circ}\text{C}$ room temperature and $60 \pm 5\%$ RH. In the accelerated studies at $40^{\circ}\text{C} \pm 2^{\circ}\text{C}$ and $75 \pm 5\%$ RH the lyophilized formulation degraded around 1.0% drug throughout initial month and near about 1.7% in next 6 months (shown in table.1.34).

Therefore, the lyophilized powder of BM was considered as more stable at room temperature ($25^{\circ}\text{C} \pm 2^{\circ}\text{C}$, $60 \pm 5\%$ RH) as compared to BM suspension and not any noteworthy variations were observed in mean particle size, drug content, and zeta potential. The results were shown in figure 1.54.

Table.1.35: Result of % residual drug content of BM on storage condition

Formulation	Room temperature ($25^{\circ}\text{C} \pm 2^{\circ}\text{C}$, $60 \pm 5\%$ RH)			Accelerated condition ($40^{\circ}\text{C} \pm 2^{\circ}\text{C}$, $75 \pm 5\%$ RH)		
	% Residual drug content					
	1M	3M	6M	1M	3M	6M
Lyophilized formulation of BM-PLGA	75.25	75.20	75.14	74.28	74.25	72.55

Pure BM suspension	60.12	60.06	59.06	58.62	58.60	56.62
--------------------	-------	-------	-------	-------	-------	-------

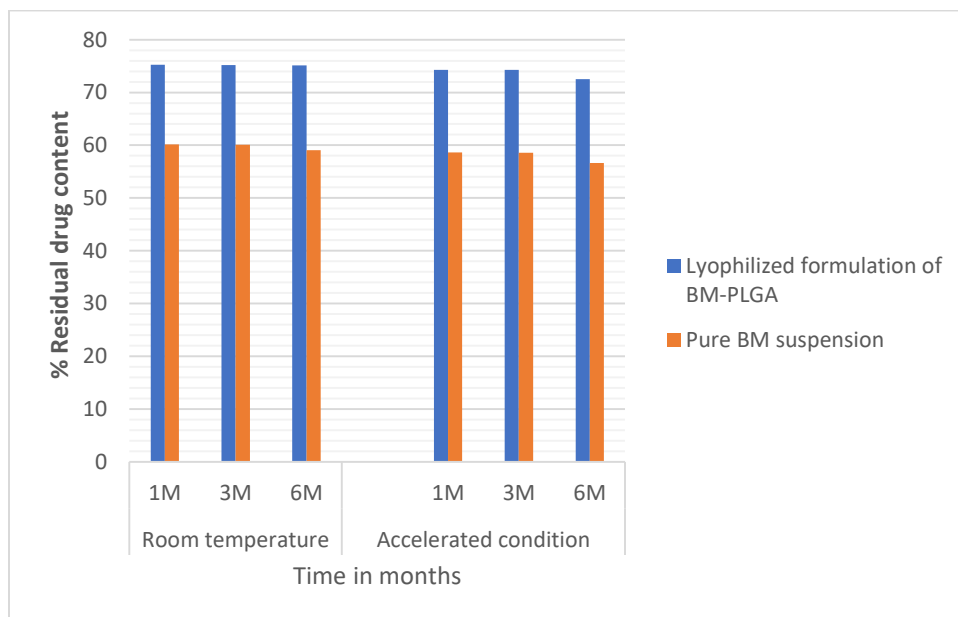


Figure 1.54: Result of % residual drug content of pure drug suspension and lyophilized formulation of BM-PLGA on storage conditions

7.1 General overview

Many current chemotherapeutic and anticancer drugs have low water-solubility and high lipophilicity. For the solubilization of these drugs require high concentration of surfactant and co-solvents which can cause severe side effects. The nanocarrier drug delivery system can be an alternative to overcome this problem. Numerous types of nanocarrier systems are studied broadly for drug delivery of poorly water-soluble anticancer drugs.

In the present research work, bendamustine loaded chitosan and PLGA nanoparticle were prepared, optimized, characterized and finally formulated in desired dosage form. Ionic gelation and solvent diffusion methods were used in the preparation of chitosan and PLGA nanoparticles respectively. Both of nanoparticles were selected for parenteral administration due to its nano size range.

The present research work was classified into three foremost phases. In the first step preparation of both the nanoparticles were done. During the second phase the optimization of chitosan and PLGA nanoparticles was done with the help of preliminary study to select the suitable independent variables and parameters for the preparation of nanoparticle. In preliminary trials suitable range of concentration of polymer, concentration of surfactant and sonication time (independent variable) was determined. These results were again optimized using different factorial design to find out the greatest optimized formulation of nanoparticles. The optimization was completed through Design Expert Software (Version. 10), here total 8 formulations of chitosan and PLGA nanoparticles were prepared and characterized. These nanoparticles were characterized according to their respective particle size and encapsulation efficiency. One of the best nanoparticles (chitosan and PLGA) preparation was selected built on lowest particle size and greatest encapsulation efficiency as dependent variable. An experimental batch of optimized formulation was prepared and the % of bias was determined between predicted and observed responses. The best nanoparticle

Development, Optimization and Evaluation of Nanosized Particles Containing Anticancer Drug

formulations (BM-CH and BM-PLGA) were then evaluated for zeta potential, PDI (polydispersityindex)Transmission electron microscopy (TEM),DSC(Differential scanning calorimetry), X-ray diffraction, percentage yield of drug, drug loading capacity, cumulativerelease of drug and in- vitrodrug release profile.

In the third and last phase both the best optimized preparations (NPF.4 and NPF.8) were formulated into a dry lyophilized powder. These dry lyophilized powder formulations were evaluated for in vitro study, cytotoxic study and stability study.

7.2. Objective of the research

The objective of the current research work is to develop and formulate and optimized the preparation of bendamustine loaded chitosan and PLGA nanoparticles by using two different methods i.e., ionotropic gelation and emulsion solvent diffusion technique, to find out which technique is more suitable and promising for accessing nanoparticle of non-toxic, site specific, better surface properties, acceptable drug release pattern, narrow size distribution and maximum entrapment efficiency.

7.3. Preformulation study

The studies of active drug ingredient and excipients before formulation mainly known as pre-formulation studies. The study is very necessary to evaluate the purity of drug by its melting point, drug- excipient interaction or compatibility studies were determined by FTIR and solubility study.

The melting point of bendamustine was found to be 150°C. Bendamustine was freely soluble in methanol and dimethyl sulfoxide (DSMO). It was sparingly soluble in water. The aqueous solubility of bendamustine was 0.0618mg/ml. The maximum absorbance of drug in methanol was calculated as 329nm. The FTIR spectra of bendamustine displayed characteristic peaks at 3315 cm^{-1} (O-H stretching vibration), 2715.01 cm^{-1} (C-H stretching,

aliphatic), 1502.60 cm^{-1} (N-CH₃ stretching) and 1634.06 cm^{-1} (C=C stretching, aromatic). All these spectra were alike to standard spectra of BM compound. No chemical interaction among drug, excipient and polymer (for ion gelation technique and solvent evaporation technique) were found in compatibility study. The partition coefficient of BM in octanol: water was found to be 4.2 showing that the drug is lipophilic in nature.

7.4. Optimization of chitosan Nanoparticles

Chitosan nanoparticles were prepared by ionic gelation method at room temperature maintained 6 minutes of sonication. For the optimization process, preliminary studies were performed to obtain the variables influencing the development of chitosan nanoparticles. The independent variables examined were, A concentration of chitosan polymer (0.1%-1.0%), B concentration of TPP (Triphosphate) surfactant (0.5%-1.0%) and C sonication time (5-7 min). It was denoted by -1, and +1, analogous to the minimum, and maximum values and the dependent responses were PS (particle size) (Y1) and %EE (entrapment efficiency) (Y2). On the basis of preliminary studies, opalescent nanoparticles were obtained at moderate concentration of chitosan (0.1-0.75% w/v) and surfactant (0.5-1.0 % w/v). This range was optimized once again using factorial Design Expert (Version.10 Stat-Ease Inc., MN) software. Here, response surface methodology was employed using Box-Behnken design, where 8-runs were performed out with 3-factors and 2-levels to optimize and attain the best formulation. Eight batches of chitosan nanoparticle were prepared and characterized (NPF-4). The outcomes of the test for dependent variables were given significant result ($p < 0.05$). (NSF-4) nanoparticle formulation no.4 was having the particle size and entrapment efficiency $130.27 \pm 3.4\text{ nm}$ $64.11 \pm 3.1\%$ respectively, that signified good relation with the predicted values. The composition of formulation attained 0.4% (w/v) polymer concentration, 0.75% (w/v) surfactant concentration and 6 minutes of sonication time. The observed response variables were obtained significant for the dependent variables presented by the

value of R^2 and results of ANOVA.

7.5. Characterization of nanoparticles

- The optimized nanoparticle formulation was having the zeta potential of -21.3 ± 0.02 mV with poly dispersity index 0.245. The drug content and drug loading efficiency were found to be 61.12% and $22\% \pm 0.14$ respectively.
- The TEM image of the optimized formulation [NPS-4] assured that the nanoparticles were non-aggregated, almost spherical in shape containing a narrow size distribution. TEM image was in a proper arrangement and the graph obtained from particle size analyser.
- The BM and chitosan displayed an endothermic peak at 155°C and 102°C respectively as data obtained from DSC thermogram, showing its melting point. The thermal decomposition of BM occurs at maximum temperature 400°C because a broad peak was obtained. The chemical interaction between drug and polymer was not found.
- The pure drug BM displayed sharp diffraction peak in x-ray diffractogram at 2θ of 3.3, 11.2, 12.0, 16.6, 7.8, 13.6, 15.4, 23.1 and 32.0° . The graph showed the crystalline structure of chitosan. The structure was completely demolished because of the cross linkage with TPP during the preparation of nanoparticle. The two peaks were disappeared slowly with the pattern which shows that it is amorphous in nature.
- In-vitro drug release was calculated in phosphate buffer pH 7.4 using Franz diffusion cell. It was detected that almost 99.3% of pure drug suspension was released at the end of 6th hour but chitosan nanoparticle was released 80.30% of drug at the end of 48th hours, showed a steady and sustained drug release during completeduration of study. The release pattern of CH-NPs was in two phasic ways, with a primary eruption followed by fast release phase and then attained sustained release. In primary phase, a burst of

nanoparticle and then drug release of 35 % was observed at the initial 30 minutes due to the drug desorption. The R^2 (coefficient of determination) value of optimized formulation was greater than 0.9 suggesting its first order release. Model confirmed that chitosan nanoparticle presented a non-fickian (anomalous) transport mechanism for the drug release, here the value of R^2 was calculated as 0.96 and $n = 0.78$.

7.6. Formulation and evaluation of dosage form

Drug molecules are delivered to sites of action within the body with the help of dosage form. In the present study, the best optimized formulation (NPF-4) chitosan nanoparticle was formulated as dry lyophilized powder and evaluated. As bendamustine suffers hydrolysis, so it is formulated as lyophilized powder. The dry lyophilized powder of BM-CH nanoparticle was successfully prepared with mannitol as cyro-protectant. The lyophilized powder (approx. 25 mg) was reconstituted with 10 ml water for injection with shaking.

The percentage drug content of lyophilized formulation of BM-CH was assessed by UV-spectroscopic method and was found to be 61.10% as well as the percentage entrapment efficiency of reconstituted lyophilized formulation of BM was found to be 64.09%. After the lyophilization process the particle size of reconstituted lyophilized formulation was found to be 130.20 ± 3.2 nm with very minute change the PDI 0.24. The zeta potential of BM loaded chitosan lyophilized formulation was found to be -21.3 ± 0.02 mV, which specifies that the formulation is in good stability condition

- **In-vitro drug release mechanism**

In-vitro drug release of pure drug suspension was almost 99.4% at the end of 6th hrs though 80.16 % drug release was detected from BM-CH lyophilized nanoparticles, which presented steady and sustained release throughout the whole duration of test.

The value of R^2 was found to be greater than 0.9 suggesting that the drug release

pattern was first order. Model fitting confirmed asnon-fickian (anomalous transport)patternfor drug release, here the R^2 was calculated as 0.98 and $n = 0.68$. The value of n was found to be within limit i.e. (0.5-1.0) for Korsmeyer-Peppas model.

- **Cellular cytotoxicity**

The cellular cytotoxicity/in-vitro anticancer activity of pure drug (BM) and lyophilized formulation of BM was calculatedwitha cell line named Z-138. Next 72 hours contact with drug, cellularviabilityand IC_{50} values of the formulation was calculated by MTT assay.The IC_{50} values of pure drug bendamustine and its lyophilized formulation (NPF-4)was found to be 36.16 ± 0.05 and $18.13 \pm 0.12 \mu\text{M}$ respectively after 72 hours exposure. Results explainedthat the lyophilized formulation havinga noteworthyin-vitroantileukemic activity,when compared with pure drug suspension.

- **Stability study**

In stability testingit was observed that the lyophilized powder of BM degradedabout0.06% of its content in theinitial month and 1% in 6months when stored at $25 \pm 2^\circ\text{C}$, $60 \pm \% \text{RH}$. In the accelerated stability study ($40 \pm 2^\circ\text{C}$, $75 \pm 5 \% \text{RH}$)thelyophilized formulation degradedhigher than 1.5% drug during the1st month and near about2% in the period ofsix months.Therefore,the lyophilized powder of BM was consideredasmore stable on $25 \pm 2^\circ\text{C}$, $60 \pm \% \text{RH}$ (room temperature)conditions when compared with thedrug suspension and no noteworthy changes were observed in meanparticlesize, zeta potential and drug content.The effectof storage conditions in % residual drug content of BM formulations is 61.06% in 1se month and 60.03% in the end of six months at the room temperature condition.

7.7. Optimization of PLGA nanoparticles

PLGA nanoparticles were prepared by emulsion solvent diffusion technique at room temperature maintained 6 minutes of sonication. For the optimization process, preliminary studies were performed to obtain the variables influencing the development of PLGA nanoparticles. The independent variables examined were, A concentration of PLGA polymer (1.0%-4.0%), B concentration of PVA (Polyvinyl alcohol) surfactant (1.0%-5.0%) and C sonication time (5-7 min). It was denoted by -1, and +1, analogous to the minimum and maximum values and the dependent variables were PS (particle size) denoted as Y1 and (%EE) (entrapment efficiency) as Y2. On the basis of preliminary studies, opalescent nanoparticles were obtained at moderate concentration of PLGA (0.5-3.0% w/v) and surfactant (1.0-4.0 % w/v). This range was optimized once again using factorial Design Expert (Version.10 Stat-Ease Inc., MN) software. Here response surface methodology was employed using Box-Behnken design, where 8-runs were performed out with 3-factors and 2-levels to optimize and attain the best formulation with lowest particle size and highest entrapment efficiency. Total 8 batches of PLGA nanoparticle were prepared and characterized. The outcomes of the response are significant ($p < 0.05$). The optimized formulation (NPF-8) was having the particle size and entrapment efficiency of $103.5 \pm 0.04 \text{ nm}$ and $78 \pm 4.16\%$ respectively. It signified good relation with the predicted values. The selected formulation (NPF-8) was in the composition of 1.55% (w/v) polymer concentration % (w/v) surfactant concentration and 6 minutes of sonication time. The observed response variables were obtained significant for the dependent variables presented by the value of R^2 and results of ANOVA.

7.8. Characterization of PLGA nanoparticles

- The nanoparticles were having the zeta potential of -31.9 ± 3.07 mV with poly dispersity index 0.307. The % yield and drug loading efficiency were found to be 80.20% and $28\% \pm 0.14$ respectively.
- The TEM images of the optimized formulation (NPS-8) specifies that the nanoparticles were non-aggregated and almost in spherical shape with the narrow size of distribution. TEM images were shown the diameter of each particle in a good arrangement obtained with the help of particle size analyser.
- BM and PLGA (polymer) displayed an endothermic peak at 155°C and 102°C respectively showing its melting point in the DSC thermogram. The thermogram of BM were already discussed. The PLGA polymer established a characteristic peak at 45.43°C indicating towards glass transition temperature. No separate peak of its melting point was observed due to the amorphous nature of PLGA. The polymer is thermally stable upto 250°C . The optimized nanoparticle had not shown any drug material which is crystalline, due to absence of sharp peak of bendamustine.
- In X-ray diffraction study of PLGA nanoparticles the distorted peak of BM was detected, showing that the drug is mixed with PVA and does not exist in free form and comparative reduction in the diffraction intensities was observed in the nanoparticles. This might be because of the decrease in the superiority of crystals of BM and this result enhances the change of crystalline drug into amorphous nature helpful in enhancement of solubility.
- In-vitro release of pure drug suspension was calculated nearly 99.1% of the drug at the end of 6th hrs, though 85.20 % release was observed from PLGA nanoparticles of optimized formulation, which showed good results. Model fitting of PLGA nanoparticle showed non-fickian mechanism for the release of drug where the R^2 was found to be 0.98 and $n = 0.67$.

7.9. Formulation and evaluation of PLGA nanoparticles

A formulation of desired dosage form is required for targeted drug delivery. In the present study, the best optimized formulation (NPF-8) BM-PLGA nanoparticle was formulated as dry lyophilized powder and evaluated. As bendamustine suffers hydrolysis, so it is formulated as lyophilized powder. The dry lyophilized powder of BM-PLGA nanoparticle was successfully prepared with mannitol as cyroprotectant. The lyophilized powder (approx. 25 mg) was reconstituted with 10 ml water for injection via shaking.

- The percentage drug content of lyophilized formulation of BM (PLGA polymer) was assessed by UV-spectroscopic method and was found to be 75.28% as well as the percentage entrapment efficiency of reconstituted lyophilized formulation of BM was found to be 78.13%. The particle size of reconstituted lyophilized formulation of BM was found to be 103.57 ± 3.2 nm with PDI 0.307. Zeta potential was estimated to get information about the surface properties of nanoparticles. The zeta potential of BM loaded chitosan lyophilized formulation was found to be -31.9 ± 3.07 , which specifies that the formulation is in good stability condition.
- In the in-vitro study, it was observed that pure drug suspension released almost 99.2% of the drug at the end of 6th hrs while 85.20 % release was observed from PLGA nanoparticles. The R^2 (coefficient of determination) value of BM from optimized formulation in phosphate buffer was > 0.9 signifying first order release pattern. Model fitting confirmed that PLGA nanoparticle showed anomalous transport (non-fickian) mechanism for the release of drug, where the R^2 was found to be 0.98 and $n = 0.67$. The value of n was found to be within limit i.e. (0.5-1.0) for Korsmeyer-Peppas model.

- The cellular cytotoxicity/*in-vitro* anticancer activity of pure drug (BM) and lyophilized formulation of BM was calculated using Z-138 cell line. The IC₅₀ values of pure drug BM and its lyophilized formulation (NPF-8) was found to be 36.16 ± 0.05 and $16.13 \pm 0.15\mu\text{M}$ respectively after 72 hours exposure. Results explained that the lyophilized formulation having significant *in-vitro* antileukemic activities compared to pure drug suspension.
- In stability testing of lyophilized powder of BM-PLGA, it was observed that the formulation degraded almost 0.03% of drug content in first month and 0.09% in 6 months when stored at room temperature ($25 \pm 2^\circ\text{C}$, $60 \pm 5\% \text{RH}$). In the accelerated condition ($40 \pm 2^\circ\text{C}$, $75 \pm 5\% \text{RH}$) the lyophilized formulation lost more than 1.0% drug during first month and near about 1.5% in 6 months. Thus, the prepared formulation (lyophilized powder) of BM was found to be more stable at room temperature conditions as compared to pure drug suspension and no noteworthy changes were observed in particle size, zeta potential and drug content. The effect of storage conditions in % residual drug content of BM formulations in the 1st month was 75.25 and 75.14% during the end of 6th months at room temperature.

7.10. Conclusion:

From this research work it was concluded that, both the techniques (ionic gelation and solvent diffusion) were useful in the preparation and development of BM nanoparticles but, the solvent diffusion technique is more suitable and promising method to get nanoparticles.

1. Patra JK, Das G, Fraceto LF *et al.* Nano based drug delivery systems: recent developments and future prospects. *J Nanobiotechnol.*(2018); 16: 71.
2. Martinho N, Damgé C, Reis CP. Recent advances in drug delivery systems. *J Biomater Nanobiotechnol.* 2011; 2:510.
3. Jahangirian H, Lemraski EG, Webster TJ, Rafiee-Moghaddam R, Abdollahi Y. A review of drug delivery systems based on nanotechnology and green chemistry: green nanomedicine. *Int J Nanomed.* 2017; 12:2957.
4. Haba Y, Kojima C, Harada A, Ura T, Horinaka H, Kono K. Preparation of poly (ethylene glycol)-modified poly (amido amine) dendrimers encapsulating gold nanoparticles and their heat-generating ability. *Langmuir.* 2007; 23:5243–6.
5. De Villiers MM, Aramwit P, Kwon GS. *Nanotechnology in drug delivery.* New York: Springer; 2008.
6. Mirza AZ, Siddiqui FA. Nanomedicine and drug delivery: a mini review. *Int Nano Lett.* 2014; 4:94.
7. Kabanov AV, Lemieux P, Vinogradov S, Alakhov V. Pluronic block copolymers: novel functional molecules for gene therapy. *Adv Drug Deliv Rev.* 2002; 54:223–33.
8. Krauel K, Pitaksuteepong T, Davies NM, Rades T. Entrapment of bioactive molecules in poly (alkylcyanoacrylate) nanoparticles. *Am J Drug Deliv.* 2004; 2:251–9.
9. Mahajan HS, Patil SB, Gattani SG, Kuchekar BS. Targeted drug delivery systems. *Pharma Times.* 2007;39(2).
10. Rani K, Paliwal SA. Review on targeted drug delivery: its entire focus on advanced therapeutics and diagnostics. *Sch J App Med Sci.* 2014; 2(1C):328–331.

11. Bhardwaj A, Kumar L. Colloidal drug delivery systems: a future prospective for treatment of tuberculosis. *Am J PharmTech Res.* 2011; 1(3):102–123.
12. Arora S, Lamba HS, Tiwari R. Dermal delivery of drugs using different vesicular carriers. *Asian J Pharm.* 2012; 6:237. doi: 10.4103/0973-8398.107558.
13. Priya K, Kumar V, Damini VK, et al. Somes: a review on composition, formulation methods and evaluations of different types of “somes” drug delivery system. *Int J App Pharm.* 2020; 12(6):7–18.
14. Gattani YS. Floating Multiparticulate drug delivery systems: an overview. *Int J Pharma Bio Sci.* 2010;6(2):35–40.
15. Ravinder K, Sukhvir K. Role of polymers in drug delivery. *J Drug Deliv Ther.* 2014;4(3):32–36.
16. Haijiao L, Jingkang W, Ting W, Jian Z, Ying B, Hongxun H. Recent progress on nanostructures for drug delivery applications. *J Nanomater.* 2016; 2–9.
17. Yousaf A, Ali A, Sadiq A, Shafida A, Umar F. Macromolecules as targeted drugs delivery vehicles: an overview. *Des Monomers Polym.* 2019;22(1):91–97. doi: 10.1080/15685551.2019.1591681.
18. Rav S, Maina SS, Malviya R, Kushwah MG, Khan MG, Yezdani U. Novel approach of targeted drug delivery system and its application. *ARC J Public Health Commun Med.* 2019;4(4):1–4.
19. Kumar A, Nautiyal U, Kaur C, Goel V, Piarchand N. Targeted drug delivery system: current and novel approach. *Int J Pharm Med Res.* 2017; 5(2):448–454.
20. Wakaskar RR (2017) Types of Nanocarriers–Formulation Method and Applications. *J Bioequiv Availab* 9:e77.

21. Kumar A, Nautiyal U, Kaur C, Goel V, Piarchand N. Targeted drug delivery system: current and novel approach. *Int J Pharm Med Res.* 2017; 5(2):448–454.
22. Yoo J, Park C, Yi G, Lee D, Koo H. Active targeting strategies using biological ligands for nanoparticle drug delivery systems. *Cancers.* 2019; 11:640. doi: 10.3390/cancers11050640.
23. Rani K, Paliwal SA. Review on targeted drug delivery: its entire focus on advanced therapeutics and diagnostics. *Sch J App Med Sci.* 2014; 2(1C):328–331.
24. Bhargav E, Madhuri N, Ramesh K, Manne A, Ravi V. Targeted drug delivery - a review. *World J Pharm Pharm Sci.* 2013;3(1):150–169.
25. Mills JK, Needham D. Targeted drug delivery. *Exp Opin Ther Patents.* 1999; 9(11):1499–1513. doi: 10.1517/13543776.9.11.1499.
26. Devarajan PV, Jain S, Editors. *Targeted Drug Delivery: Concepts and Design.* New York Dordrecht London: Springer Cham Heidelberg; 2015.
27. Manish G, Vimukta S. Targeted drug delivery system: a review. *Res J Chem Sci.* 2011; 1(2):135–138.
28. Thakur A, Roy A, Chatterjee S, Chakraborty P, Bhattacharya K, Mahata PP. Recent trends in targeted drug delivery. *SMGroup.* 2015.
29. Kivılcım O, Hakan E, Sema Ç. Novel advances in targeted drug delivery. *J Drug Target.* 2017. doi: 10.1080/1061186X.2017.1401076
30. Scott R, Crabbe D, Krynska B, Ansari R, Kiani M. Aiming for the heart: targeted delivery of drugs to diseased cardiac tissue. *Expert Opin Drug Deliv.* 2008; 5(4):459–470. doi: 10.1517/17425247.5.4.459

31. Idayu IM, Suguna S, Nurul A. Designing polymeric nanoparticles for targeted drug delivery system. *Nanomedicine*. 2015; 288–311.
32. Dagogo-Jack I, Shaw AT. Tumour heterogeneity and resistance to cancer therapies. *Nat Rev Clin Oncol*. 2018; 15(2):81–94. doi: 10.1038/nrclinonc.2017.166.
33. Viet CT, Schmidt BL. Understanding oral cancer in the genome era. *Head & neck*. 2010;32(9):1246–68.
34. R.L. Siegel, K.D. Miller, A. Jemal, Cancer statistics 2016, *CA Cancer J Clin*, 66 (2016), pp. 7-30.
35. Lodish H., Berk A., Zipursky S. L., Matsudaira P., Baltimore D., Darnell J. *Molecular Cell Biology*. 4th. New York, NY, USA: W. H. Freeman; 2000. Tumor cells and the onset of cancer.
36. Reymond N., D'Água B. B., Ridley A. J. Crossing the endothelial barrier during metastasis. *Nature Reviews Cancer*. 2013; 13(12):858–870. doi: 10.1038/nrc3628.
37. Rundhaug JE. Matrix metalloproteinases, angiogenesis, and cancer: commentary re: A. C. Lockhart et al., Reduction of wound angiogenesis in patients treated with BMS-275291, a broad spectrum matrix metalloproteinase inhibitor. *Clinical Cancer Research*. 2003;9(2):551–554.
38. Nishida N., Yano H., Nishida T., Kamura T., Kojiro M. Angiogenesis in cancer. *Vascular Health and Risk Management*. 2006; 2(3):213–219. doi: 10.2147/vhrm.2006.2.3.213.
39. Murphy K, Travers P, Walport M. *Janeway's Immunobiology*. 7th. New York, NY, USA: Garland Science Taylor and Francis Group; 2008. Principles of innate and adaptive immunity; pp. 1–38.

40. Dinarello C. A. Historical review of cytokines. *European Journal of Immunology*. 2007; 37(supplement 1):S34–S45. doi: 10.1002/eji.200737772.
41. Wills-Karp M. Complement activation pathways: a bridge between innate and adaptive immune responses in asthma. *Proceedings of the American Thoracic Society*. 2007; 4(3):247–251. doi: 10.1513/pats.200704-046aw.
42. Sun JC, Lanier LL. Natural killer cells remember: an evolutionary bridge between innate and adaptive immunity? *European Journal of Immunology*. 2009; 39(8):2059–2064. doi: 10.1002/eji.200939435.
43. Murphy K., Travers P., Walport M. *Janeway's Immunobiology*. 7th. New York, NY, USA: Garland Science/Taylor and Francis Group; 2008. Structural variation in immunoglobulin constant regions; pp. 143–213.
44. Koretzky G. A. Multiple roles of CD4 and CD8 in T cell activation. *Journal of Immunology*. 2010; 185(5):2643–2644. doi: 10.4049/jimmunol.1090076.
45. Luckheeram RV, Zhou R, Verma AD, Xia B. CD4 +T cells: differentiation and functions. *Clinical and Developmental Immunology*. 2012; 12. doi: 10.1155/2012/925135.925135.
46. Podojil JR, Miller SD. Molecular mechanisms of T-cell receptor and costimulatory molecule ligation/blockade in autoimmune disease therapy. *Immunological Reviews*. 2009; 229(1):337–355. doi: 10.1111/j.1600-065X.2009.00773.x.
47. Janeway C. A., Jr., Travers P., Walport M., *Immunobiology: The Immune System in Health and Disease*. 5th. New York, NY, USA: Garland Science; 2001. B-cell activation by armed helper T cells.

48. Schroeder HW, Jr, Cavacini L. Structure and function of immunoglobulins. *Journal of Allergy and Clinical Immunology*. 2010; 125(2):S41–S52.
49. Terabe M, Berzofsky JA. The role of NKT cells in tumor immunity. *Advances in Cancer Research*. 2008; 101:277–348. doi: 10.1016/s0065-230x(08)00408-9.
50. Siegel RL, Miller KD, Wagle NS, Jemal A. Cancer statistics, 2023. *CA: A Cancer Journal for Clinicians* 2023; 73(1):17-48. Last accessed February 21, 2023.s
51. Jan AB. Treatment of Chronic Lymphocytic Leukemia. *The new England journal of medicine* 2020; 383:460-473, DOI: 10.1056/NEJMra1908213.
52. Bhutani M, Vora A, Kumar L, Kochupillai V. Lympho-hemopoietic malignancies in India. *Med Oncol*. 2002; 19(3):141-50. doi: 10.1385/MO:19:3:141. PMID: 12482124.
53. Yang J, Jia C, Yang J. Designing nanioparticle-based drug delivery system for precision medicine. *Int J Med Sci* 2021; 18(13):2943-2949. doi:10.7150/ijms.60874
54. Singh A, Garg G, Sharma PK. Nanosphere: A novel approach for targeted drug delivery. Volume 5, Issue 3, November – December 2010; Article-015. ISSN 0976 – 044X. b/,
55. Hwang D, Ramsey JD, Kabanov AV. Polymeric micelles for the delivery of poorly soluble drugs: From nano formulation to clinical approval. *Adv Drug Deliv Rev*. 2020; 156:80-118. doi: 10.1016/j.addr.2020.09.009. Epub 2020 Sep 24.
56. Maiti A, Bhattacharyya S. Review: Quantum Dots and Application in Medical Science. *International Journal of Chemistry and Chemical Engineering*. ISSN 2248-9924 Volume 3, Number 2 (2013), pp. 37-42.
57. Min KH , Park K, Kim Y, Bae SM, Lee S, *et al.* hydrophobically modified glycol chitosan nanoparticles-encapsulated camptothecin enhance the drug stability and tumor

- targeting in cancer therapy, *Journal of Controlled Release, Volume 127, Issue 3, 8 May 2008, Pages 208-218.*
58. Park JH, Gurusamy S, Kim K, Targeted delivery of low molecular drugs using chitosan and its derivatives, *Advanced Drug Delivery Reviews, Volume 62, Issue 1, 31 January 2010, Pages 28-41.*
59. Wang J, Zong J, Zhao D. In situ formation of chitosan-cyclodextrin nanospheres for drug delivery. *Colloids and Surfaces B: Biointerfaces* 2011; 87: 198– 202.
60. Nanda R , Sasmal A, Nayak PL. Preparation and characterization of chitosan polylactide composites blended with Cloisite 30B for control release of the drug paclitaxel, Original Research Article *Carbohydrate Polymers, Volume 83, Issue 2, 10 January 2011, Pages 988-994.*
61. Nam J, Park S, Kim T, Jang J, Choi C, *et al.* formulated Encapsulation of paclitaxel into lauric acid-O-carboxymethyl chitosan-transferrin micelles for hydrophobic drug delivery and site-specific targeted delivery, *International Journal of Pharmaceutics, Volume 457, Issue 1, 30 November 2013, Pages 124-135.*
62. Feng C, Sun G, Wang Z, Cheng X, Park H, *et al.* Transport mechanism of doxorubicin loaded chitosan based nanogels across intestinal epithelium, *European Journal of Pharmaceutics and Biopharmaceutics, Volume 87, Issue 1, May 2014, Pages 197-207*
63. Lucio D , Zornoza A. Influence of chitosan and carboxymethyl chitosan on the polymorphism and solubilisation of diflunisal, *International Journal of Pharmaceutics, Volume 467, Issues 1–2, 5 June 2014, Pages 19-26.*
64. Khan I, Gothwal A, Sharma AK, Qayum A, Singh SK, Gupta U. Biodegradable nano-architectural PEGylated approach for the improved stability and anticancer efficacy of
- Development, Optimization And Evaluation of Nanosized Particles Containing Anticancer Drug

- bendamustine. *Int J Biol Macromol.* 2016; 92:1242-1251.
doi:10.1016/j.ijbiomac.2016.08.004
65. Gidwani B, Vyas A. Formulation, characterization and evaluation of cyclodextrin-complexed bendamustine-encapsulated PLGA nanospheres for sustained delivery in cancer treatment. *Pharm Dev Technol.* 2016;21(2):161-171.
doi:10.3109/10837450.2014.979945
66. Franiak-Pietryga I, Ziółkowska E, Ziemba B, et al. Glycodendrimer PPI as a Potential Drug in Chronic Lymphocytic Leukaemia. The Influence of Glycodendrimer on Apoptosis in In Vitro B-CLL Cells Defined by Microarrays. *Anticancer Agents Med Chem.* 2017;17(1):102-114.
67. Bhandari J, Mishra H, Mishra PK, Wimmer R, Ahmad FJ, Talegaonkar S. Cellulose nanofiber aerogel as a promising biomaterial for customized oral drug delivery. *Int J Nanomedicine.* 2017;12:2021-2031. Published 2017 Mar 14. doi:10.2147/IJN.S124318
68. Taylor J, Xiao W, Abdel-Wahab O. Diagnosis and classification of hematologic malignancies on the basis of genetics. *Blood.* 2017 Jul 27;130(4):410-423. doi:10.1182/blood-2017-02-734541. Epub 2017 Jun 9.
69. Vinhas R, Mendes R, Fernandes AR, Baptista PV. Nanoparticles-Emerging Potential for Managing Leukemia and Lymphoma. *Front Bioeng Biotechnol.* 2017 Dec 18; 5:79. doi:10.3389/fbioe.2017.00079.
70. Hallek M, Shanafelt TD, Eichhorst B. Chronic lymphocytic leukaemia. *Lancet.* 2018;391(10129):1524-1537. doi:10.1016/S0140-6736(18)30422-7
71. Thomas SC, Madaan T, Iqbal Z, Talegaonkar S. Box-Behnken Design of Experiment Assisted Development and Optimization of Bendamustine HCl loaded Hydroxyapatite
- Development, Optimization And Evaluation of Nanosized Particles Containing Anticancer Drug

- Nanoparticles. *Curr Drug Deliv.* 2018;15(9):1230-1244.
doi:10.2174/1567201815666180620123347
72. Ziembra B, Sikorska H, Jander M, et al. Anti-Tumour Activity of Glycodendrimer Nanoparticles in a Subcutaneous MEC-1 Xenograft Model of Human Chronic Lymphocytic Leukemia. *Anticancer Agents Med Chem.* 2020;20(3):325-334.
doi:10.2174/1871520619666191019093558
73. Franiak-Pietryga I, Ziembra B, Sikorska H, et al. Maltotriose-modified poly(propylene imine) Glycodendrimers as a potential novel platform in the treatment of chronic lymphocytic Leukemia. A proof-of-concept pilot study in the animal model of CLL. *Toxicol Appl Pharmacol.* 2020; 403:115139. doi:10.1016/j.taap.2020.115139.
74. Shakeran Z, Keyhanfar M, Varshosaz J, Sutherland DS. Biodegradable nanocarriers based on chitosan-modified mesoporous silica nanoparticles for delivery of methotrexate for application in breast cancer treatment. *Mater Sci Eng C Mater Biol Appl.* 2021;118:111526. doi:10.1016/j.msec.2020.111526
75. Cavalcante RS, Ishikawa U, Silva ES, et al. STAT3/NF- κ B signalling disruption in M2 tumour-associated macrophages is a major target of PLGA nanocarriers/PD-L1 antibody immunomodulatory therapy in breast cancer. *Br J Pharmacol.* 2021;178(11):2284-2304.
doi:10.1111/bph.15373
76. Li L, Yang M, Li R, Hu J, Yu L, Qian X. iRGD Co-Administration with Paclitaxel-Loaded PLGA Nanoparticles Enhance Targeting and Antitumor Effect in Colorectal Cancer Treatment. *Anticancer Agents Med Chem.* 2021;21(7):910-918.
doi:10.2174/1871520620666200721134919.

77. Ghilardi G, Chong EA, Svoboda J, et al. Bendamustine is safe and effective for lymphodepletion before tisagenlecleucel in patients with refractory or relapsed large B-cell lymphomas. *Ann Oncol.* 2022;33(9):916-928. doi:10.1016/j.annonc.2022.05.521
78. Ghaz-Jahanian MA, Abbaspour-Aghdam F, Anarjan N, Berenjian A, Jafarizadeh-Malmiri H. Application of chitosan-based nanocarriers in tumor-targeted drug delivery. *Mol Biotechnol.* 2015; 57(3):201-218. doi:10.1007/s12033-014-9816-3
79. Resen AK, Atiroğlu A, Atiroğlu V, et al. Effectiveness of 5-Fluorouracil and gemcitabine hydrochloride loaded iron-based chitosan-coated MIL-100 composite as an advanced, biocompatible, pH-sensitive and smart drug delivery system on breast cancer therapy. *Int J Biol Macromol.* 2022; 198:175-186. doi:10.1016/j.ijbiomac.2021.12.130
80. Priya S, Batra U, R N S, Sharma S, Chaurasiya A, Singhvi G. Polysaccharide-based nanofibers for pharmaceutical and biomedical applications: A review. *Int J Biol Macromol.* 2022; 218:209-224. doi:10.1016/j.ijbiomac.2022.07.118.
81. Rinaldi F, Forte J, Pontecorvi G, et al. pH-responsive oleic acid based nanocarriers: Melanoma treatment strategies. *Int J Pharm.* 2022; 613:121391. doi:10.1016/j.ijpharm.2021.121391.
82. Zhang N, Li J, Gao W, et al. Co-Delivery of Doxorubicin and Anti-PD-L1 Peptide in Lipid/PLGA Nanocomplexes for the Chemo-Immunotherapy of Cancer. *Mol Pharm.* 2022; 19(9):3439-3449. doi:10.1021/acs.molpharmaceut.2c00611
83. Xiong W, Guo Z, Zeng B, et al. Dacarbazine-Loaded Targeted Polymeric Nanoparticles for Enhancing Malignant Melanoma Therapy. *Front Bioeng Biotechnol.* 2022;10:847901. Published 2022 Feb 17. doi:10.3389/fbioe.2022.847901

84. Singh A, Thotakura N, Kumar R, et al. PLGA-soya lecithin based micelles for enhanced delivery of methotrexate: Cellular uptake, cytotoxic and pharmacokinetic evidences. *Int J Biol Macromol*. 2017; 95:750-756. doi:10.1016/j.ijbiomac.2016.11.111
85. Dennie TW, Kolesar JM. Bendamustine for the treatment of chronic lymphocytic leukemia and rituximab-refractory, indolent B-cell non-Hodgkin lymphoma. *Clin Ther*. 2009; 31 Pt 2:2290-2311. doi:10.1016/j.clinthera.2009.11.031
86. Lalic H, Aurer I, Batinic D, Visnjic D, Smoljo T, Babic A. Bendamustine: A review of pharmacology, clinical use and immunological effects (Review). *Oncol Rep*. 2022; 47(6):114. doi:10.3892/or.2022.8325
87. Darwish M, Bond M, Hellriegel E, Robertson P Jr, Chovan JP. Pharmacokinetic and pharmacodynamic profile of bendamustine and its metabolites. *Cancer Chemother Pharmacol*. 2015; 75(6):1143-1154. doi:10.1007/s00280-015-2727-6
88. Bogeljic Patekar M, Milunovic V, Misura Jakobac K, et al. Bendamustine: an old drug in the new era for patients with non-hodgkin lymphomas and chronic lymphocytic leukemia. *Acta Clin Croat*. 2018; 57(3):542-553. doi:10.20471/acc.2018.57.03.18
89. Elieh-Ali-Komi D, Hamblin MR. Chitin and Chitosan: Production and Application of Versatile Biomedical Nanomaterials. *Int J Adv Res (Indore)*. 2016; 4(3):411-427.
90. Cheung RC, Ng TB, Wong JH, Chan WY. Chitosan: An Update on Potential Biomedical and Pharmaceutical Applications. *Mar Drugs*. 2015; 13(8):5156-5186. Published 2015 Aug 14. doi:10.3390/md13085156
91. Yang W, Fu J, Wang T, He N. Chitosan/sodium tripolyphosphate nanoparticles: preparation, characterization and application as drug carrier. *J Biomed Nanotechnol*. 2009; 5(5):591-595. doi:10.1166/jbn.2009.1067

92. Cortes H, Hernandez-Parra H, Bernal-Chavez SA, et al. Non-Ionic Surfactants for Stabilization of Polymeric Nanoparticles for Biomedical Uses. *Materials (Basel)*. 2021;14(12):3197. Published 2021 Jun 10. doi:10.3390/ma14123197
93. Hassan CM, Trakampan P, Peppas NA. Water Solubility Characteristics of Poly (vinyl alcohol) and Gels Prepared by Freezing/Thawing Processes. In: Amjad, Z. (eds) (2002) Water Soluble Polymers. Springer, Boston, MA. https://doi.org/10.1007/0-306-46915-4_3
94. Allaudin PMS, Kunchithapatham J. A review on preformulation studies of drugs. *International Journal of Pharmaceutical Research and development* 2012; 4 (05): 64-74.
95. Gupta KR, Pounikar AR, Umekar MJ. Drug Excipient Compatibility Testing Protocols and Characterization: A Review. *Asian Journal of Chemical Sciences*, (2019)6(3), 1–22. <https://doi.org/10.9734/ajocs/2019/v6i319000>.
96. Bao QY, Liu AY, Ma Y, et al. The effect of oil-water partition coefficient on the distribution and cellular uptake of liposome-encapsulated gold nanoparticles. *Colloids Surf B Biointerfaces*. 2016; 146:475–481. doi:10.1016/j.colsurfb.2016.06.046
97. Samy M, Abd El-Alim SH, Rabia AEG, Amin A, Ayoub MMH. Formulation, characterization and in vitro release study of 5-fluorouracil loaded chitosan nanoparticles. *Int J Biol Macromol*. 2020; 156:783-791. doi:10.1016/j.ijbiomac.2020.04.112.
98. Bhawana, Basniwal, R. K., Buttar, H. S., Jain, V. K., & Jain, N.. Curcumin nanoparticles: preparation, characterization, and antimicrobial study. *Journal of agricultural and food chemistry*. 2011; 59(5), 2056–2061. <https://doi.org/10.1021/jf104402t>

99. Zhang LL, Ma FF, Kuang YF, Cheng S, Long YF, Xiao QG. Highly sensitive detection of bovine serum albumin based on the aggregation of triangular silver nanoplates. *Spectrochim Acta A Mol Biomol Spectrosc.* 2016;154:98-102. doi:10.1016/j.saa.2015.10.019
- Loquercio A, Castell-Perez E, Gomes C, Moreira RG. Preparation of Chitosan-Alginate Nanoparticles for Trans-cinnamaldehyde Entrapment. *J Food Sci.* 2015;80(10):N2305-N2315. doi:10.1111/1750-3841.12997.
100. Xie F, Cheng Z, Cheng H, Yu P. Simultaneous determination of bendamustine and its active metabolite, gamma-hydroxy-bendamustine in human plasma and urine using HPLC-fluorescence detector: application to a pharmacokinetic study in Chinese cancer patients. *J Chromatogr B Analyt Technol Biomed Life Sci.* 2014;960:98-104. doi:10.1016/j.jchromb.2014.04.027
101. Calvo NL, Maggio RM, Kaufman TS. A dynamic thermal ATR-FTIR/chemometric approach to the analysis of polymorphic interconversions. Cimetidine as a model drug. *J Pharm Biomed Anal.* 2014;92:90-97. doi:10.1016/j.jpba.2013.12.036
102. Chadha R, Bhandari S. Drug-excipient compatibility screening--role of thermoanalytical and spectroscopic techniques. *J Pharm Biomed Anal.* 2014;87:82-97. doi:10.1016/j.jpba.2013.06.016
103. Bharate SS, Kumar V, Vishwakarma RA. Determining Partition Coefficient (Log P), Distribution Coefficient (Log D) and Ionization Constant (pKa) in Early Drug Discovery. *Comb Chem High Throughput Screen.* 2016;19(6):461-469. doi:10.2174/1386207319666160502123917
104. Tiwari S, Kumar V, Randhawa S, Verma SK. Preparation and characterization of extracellular vesicles. *Am J Reprod Immunol.* 2021;85(2):e13367. doi:10.1111/aji.13367

105. Matalqah SM, Aiedeh K, Mhaidat NM, Alzoubi KH, Bustanji Y, Hamad I. Chitosan Nanoparticles as a Novel Drug Delivery System: A Review Article. *Curr Drug Targets*. 2020;21(15):1613-1624. doi:10.2174/1389450121666200711172536
106. Cohen-Sela E, Chorny M, Koroukhov N, Danenberg HD, Golomb G. A new double emulsion solvent diffusion technique for encapsulating hydrophilic molecules in PLGA nanoparticles. *J Control Release*. 2009;133(2):90-95. doi:10.1016/j.jconrel.2008.09.073
107. Abdelwahed W, Degobert G, Stainmesse S, Fessi H. Freeze-drying of nanoparticles: formulation, process and storage considerations. *Adv Drug Deliv Rev*. 2006;58(15):1688-1713. doi:10.1016/j.addr.2006.09.017
108. Soliman NM, Shakeel F, Haq N, et al. Development and Optimization of Ciprofloxacin HCl-Loaded Chitosan Nanoparticles Using Box-Behnken Experimental Design. *Molecules*. 2022;27(14):4468. Published 2022 Jul 13. doi:10.3390/molecules27144468
109. Amin MK, Boateng JS. Comparison and process optimization of PLGA, chitosan and silica nanoparticles for potential oral vaccine delivery. *Ther Deliv*. 2019; 10(8):493-514. doi:10.4155/tde-2019-0038
110. Suzuki M, Takebe G, Takagi T, Tsukada H. Characterization of Novel Paclitaxel Nanoparticles Prepared by Laser Irradiation. *Chem Pharm Bull (Tokyo)*. 2022;70(4):269-276. doi:10.1248/cpb.c21-00994
111. Sharma AN, Upadhyay PK, Dewangan HK. Development, evaluation, pharmacokinetic and biodistribution estimation of resveratrol-loaded solid lipid nanoparticles for prostate cancer targeting. *J Microencapsul*. 2022; 39(6):563-574. doi:10.1080/02652048.2022.2135785

112. Hashad RA, Ishak RA, Fahmy S, Mansour S, Geneidi AS. Chitosan-tripolyphosphate nanoparticles: Optimization of formulation parameters for improving process yield at a novel pH using artificial neural networks. *Int J Biol Macromol.* 2016;86:50-58. doi:10.1016/j.ijbiomac.2016.01.042
113. Sharma H, Kumar K, Choudhary C, Mishra PK, Vaidya B. Development and characterization of metal oxide nanoparticles for the delivery of anticancer drug. *Artif Cells Nanomed Biotechnol.* 2016; 44(2):672-679. doi:10.3109/21691401.2014.978980
114. Malatesta M. Transmission Electron Microscopy as a Powerful Tool to Investigate the Interaction of Nanoparticles with Subcellular Structures. *Int J Mol Sci.* 2021;22(23):12789. Published 2021 Nov 26. doi:10.3390/ijms222312789
115. Wei X, Patil Y, Ohana P, et al. Characterization of Pegylated Liposomal Mitomycin C Lipid-Based Prodrug (Prometil) by High Sensitivity Differential Scanning Calorimetry and Cryogenic Transmission Electron Microscopy. *Mol Pharm.* 2017;14(12):4339-4345. doi:10.1021/acs.molpharmaceut.6b00865
116. Forien JB, Uzuhashi J, Ohkubo T, et al. X-ray diffraction and in situ pressurization of dentine apatite reveals nanocrystal modulus stiffening upon carbonate removal. *Acta Biomater.* 2021; 120:91-103. doi:10.1016/j.actbio.2020.09.004
117. Eshrati Yeganeh F, Eshrati Yeganeh A, Fatemizadeh M, Farasati Far B, Quazi S, Safdar M. In vitro cytotoxicity and anti-cancer drug release behavior of methionine-coated magnetite nanoparticles as carriers. *Med Oncol.* 2022;39(12):252. Published 2022 Oct 12. doi:10.1007/s12032-022-01838-1

118. Stiepel RT, Pena ES, Ehrenzeller SA, et al. A predictive mechanistic model of drug release from surface eroding polymeric nanoparticles. *J Control Release*. 2022;351:883-895. doi:10.1016/j.jconrel.2022.09.067
119. Dupeyrón D, Kawakami M, Rieumont J, Carvalho JC. Formulation and Characterization of Anthocyanins-Loaded Nanoparticles. *Curr Drug Deliv*. 2017;14(1):54-64. doi:10.2174/1567201813666160915102151
120. Al-Nakashli R, Raveendran R, Khine YY, et al. Drug-Loading Content Influences Cellular Uptake of Polymer-Coated Nanocellulose. *Mol Pharm*. 2023;20(4):2017-2028. doi:10.1021/acs.molpharmaceut.2c00997
121. Khan RU, Khan M, Sohail A, et al. Efficacy of pentamidine-loaded chitosan nanoparticles as a novel drug delivery system for *Leishmania tropica*. *Trop Biomed*. 2022;39(4):511-517. doi:10.47665/tb.39.4.003
122. Jain AK, Thareja S. In vitro and in vivo characterization of pharmaceutical nanocarriers used for drug delivery. *Artif Cells Nanomed Biotechnol*. 2019;47(1):524-539. doi:10.1080/21691401.2018.1561457
123. Samy M, Abd El-Alim SH, Rabia AEG, Amin A, Ayoub MMH. Formulation, characterization and in vitro release study of 5-fluorouracil loaded chitosan nanoparticles. *Int J Biol Macromol*. 2020;156:783-791. doi:10.1016/j.ijbiomac.2020.04.112
124. Poy D, Akbarzadeh A, Ebrahimi Shahmabadi H, et al. Preparation, characterization, and cytotoxic effects of liposomal nanoparticles containing cisplatin: an in vitro study. *Chem Biol Drug Des*. 2016;88(4):568-573. doi:10.1111/cbdd.12786

125. Kumar P, Nagarajan A, Uchil PD. Analysis of Cell Viability by the MTT Assay. *Cold Spring Harb Protoc.* 2018;2018(6):10.1101/pdb.prot095505. Published 2018 Jun 1. doi:10.1101/pdb.prot095505
126. Bag A, Ghorai PK. Development of Quantum Chemical Method to Calculate Half Maximal Inhibitory Concentration (IC₅₀). *Mol Inform.* 2016; 35(5):199-206. doi:10.1002/minf.201501004
127. Mi XJ, Park HR, Dhandapani S, Lee S, Kim YJ. Biologically synthesis of gold nanoparticles using *Cirsium japonicum* var. *maackii* extract and the study of anti-cancer properties on AGS gastric cancer cells. *Int J Biol Sci.* 2022; 18(15):5809-5826. Published 2022 Sep 21. doi:10.7150/ijbs.77734

List of Publications

List of Publications:

1. Pandey P, Dwivedi J, Shukla SS. Preparation, Optimization and Characterization of Bendamustine Loaded PLGA Nanoparticle. *Bio Gecko*; 2023, 12(3):2828-45. DOI : <http://biogecko.co.nz/2023.v12.i03.pp2828-2845> .
2. Pandey P, Dwivedi J, Shukla SS. Targeted Approaches through Nanocarriers In Leukemia: A Review. *African Journal of Biological Sciences*; 2024, 6(2):1525-1532. doi: 10.33472/AFJBS.6.Si2.2024.1525-1532.

List of Poster Presented in Conferences

List of Poster Presented in Conferences

1. Poster Presented In International Conference On “ Drug Discovery, Design And Delivery Approaches” Organised By Guru Nanak College Of Pharmaceutical Sciences, Dehradun, Uttrakhand, Dated 26/11/2022.
2. Poster Presented In International Conference On “Antimicrobial Resistance And Gut Microbiome: Rationalizing Prescriptions In Clinical Practice” Organised By Metro College Of Health Sciences & Research, Greater Noida, Uttar Pradesh, Dated 03-04 March 2023.